國立臺灣大學工學院土木工程學系

碩士論文

Department of Civil Engineering

College of Engineering

Master Thesis

以排隊理論及隨機顆粒軌跡模型模擬隨機泥砂傳輸下之泥沙傳輸率及濃度變化

Application of Queueing Theory and Stochastic Particle Tracking Model to Simulating Stochastic Sediment Transport: Concentrations and Transport Rates

洪毓茹

Yu-Ju Hung

指導教授：蔡宛珊 博士

Advisor: Christina W. Tsai, Ph.D.

中華民國 104 年 7 月

July, 2015

誌謝

洪毓茹 謹誌于

國立台灣大學土木工程學研究所

民國一百零肆年捌月

中文摘要

泥砂傳輸在傳統上通常使用定律模型進模擬。然而其間歇性(intermittent)與其隨機(stochastic)的特性使泥砂傳輸更為適合以離散隨機的方法進行描述。本研究運用排隊理論(queueing theory) 以離散隨機的方式設計出一隨機模型的框架，此框架可以用來模擬泥砂顆粒在水中隨機的進入控制體積的行為。泥砂顆粒、控制體積、泥砂傳輸的機制(包含懸浮、沉澱以及從底床被帶起的機制)分別對應於排隊理論中的顧客、商店以及服務。在本研究中主要以隨機擴散粒子追蹤模型(SD-PTM)以及底床顆粒被帶起為主要的泥砂傳輸機制。排隊理論最大的特點在於可以模擬顧客數量及到顧客達時間的隨機性，將此特性運用到泥砂傳輸，就可以進行泥砂顆粒在水中隨機的進入控制體積的行為模擬，其中泥砂顆粒的隨機進入包含泥砂隨機的到達以及每次到達含有隨機的泥砂顆粒數量。本研究以卜松過程(Poisson process)和二項分布(binominal distribution)分別模擬泥砂的隨機到達(random arrivals)以及每次到達的隨機泥砂數量(random magnitude)。

本研究含有三個不同的泥砂進入機制的模擬，分別是泥砂進入控制體積的時間是固定的，但是每次的量是隨機的(random magnitude, RM)、泥砂每次進入控制體積的量為固定的，但是進入控制體積的時間是隨機的(random arrivals, RA)以及泥砂進入控制體積的時間不固定而且每次的量也是隨機的(random-sized batch arrivals)。模擬結果以系綜統計(ensemble statistics)進行分析，統計的系綜包含泥砂濃度、泥沙傳輸速率的系綜平均(ensemble means)和系綜方差(ensemble variances)。再對三種不同的泥砂進入機制的模擬的結果進行比較，比較的結果顯示在相同的平均泥砂輸入速率下，不同於系綜平均，系綜方差的值可以反映出不同的泥砂進入機制。

關鍵字: 排隊理論、隨機泥砂進入、隨機泥沙傳輸、序率模式、顆粒軌跡模型、顆粒隨機被帶起、卜松過程、二項分布

ABSTRACT

Sediment transport is typically simulated using deterministic models. However, the intermittent and stochastic features of sediment transport make it suitable to be described by discrete random processes. This study attempts to apply queueing theory to develop a stochastic framework that could account for the random-sized batch arrivals of incoming sediment particles into receiving waters. Sediment particles, control volume, mechanics of sediment transport (such as mechanics of suspension, deposition and resuspension) are treated as the customers, service facility and server respectively in queueing theory. In the framework, the stochastic diffusion particle tracking model (SD-PTM) and resuspension of particles are included to simulate the random transport trajectories of suspended particles. The most distinguished characteristic of queueing theory is that customers come to the service facility in a random manner. In analogy to sediment transport, this characteristic is suitable to model the random-sized batch arrival process of sediment particles including the random occurrences and random magnitude of incoming sediment particles. The random occurrences of arrivals are simulated by Poisson process while the number of sediment particles in each arrival can be simulated by a binominal distribution. Simulations of random arrivals and random magnitude are proposed individually to compare with the random-sized batch arrival simulations. Simulation results are a probabilistic description for discrete sediment transport through ensemble statistics (i.e. ensemble means and ensemble variances) of sediment concentrations and transport rates. Results reveal the different mechanisms of incoming particles (RM, RA and BA) will result in differences in the ensemble variances of concentrations and transport rates under the same mean incoming rate of sediment particles.

Keywords: queueing theory, sediment transport, random input, SD-PTM, stochastic method, particle tracking model

CONTENTS

LIST OF FIGURES

LIST OF TABLES

Chapter 1 Introduction

Awareness of management and preservation of global water and soil resources in order to meet the present and future needs for human consumption and ecological balance has increased around the world. These precious resources are mostly affected by sediment transport. After wind erosion, sediment particles such as rocks and soils might be transported by streams and rivers, and might deposit in lakes, reservoirs, estuaries and oceans (Malmon, Dunne, and Reneau, 2003). Moreover, sediment transport plays an important role especially in water resource for human society. For example, the life span of a reservoir will be reduced by the sediments which continuously transport from upstream into the reservoir. To alleviate such problem, some engineering techniques such as drawdown flushing, turbid current venting can be properly applied to extending the life of a reservoir. Consequently, in the last several decades, there has been a tremendous wave of interest in sediment transport.

Although sediment transport is not a new topic in the hydraulics field, it remains challenging to comprehend the mechanics of sediment due to many unknowns that carry different degrees of disturbances in nature. The relation between water and sediment remains unclear, even in a simple boundary channel (Muste, Yu, Fujita, & Ettema, 2009). In order to obtain reasonable predictions on sediment transport rates, scientists have acquired lots of in-situ data and experimental data to develop semi-empirical or empirical formulas. Results from these formulas are deterministic, which might be oversimplified due to assumptions or the uncertainty associated with data and/or model parameters, such as the variations of water depth, the roughness of river bed and the spatially non-uniform turbulent diffusivity (Visser, 1997).

In order to provide an improved solution to the above issue, stochastic methods are

introduced to deal with the uncertainties. The output of a deterministic model is fully determined by parameter values, initial and boundary conditions. In other words, for given values of input variables and model parameters, one will receive the same value of output (or model prediction) from a deterministic model. Different from deterministic models, stochastic models possess some inherent randomness. Outcomes of stochastic models will be an ensemble of realizations even for the same set of input variables and model parameters. In other words, stochastic models can provide the probabilistic distribution of the results instead of a single value of prediction obtained from deterministic models. This probabilistic distribution of the results can be a powerful reference for decision makers in risk management.

The idea of treating sediment transport as a probabilistic problem was first proposed by Hans Albert Einstein in 1950. Based on the long term observations in flume experiments, Einstein applied a stochastic process to sediment transport to delineate bed load transport. In Einstein's perspective, an equilibrium of sediment transport is a balance between deposition and entrainment rates, i.e. the amount of sediment deposited on the bed is equal to the amount of sediment eroded from the bed. Without a doubt, when the number of tests or observations increases, the reliability of such event would rise. That is the feasibility of a stochastic analysis. Einstein's bed load theory takes a large number of sediment particles into consideration, which makes stochastic analysis a perfect method to study bed load transport. Since the first appearance of stochastic modeling proposed by Einstein, many researches have proposed to treat sediment transport as a probability probable.

Stochastic sediment transport models can be classified into two categories. One is that stochastic processes governing the movement of a discrete particle. Based on the fundamental of Wiener Process, scientists can describe the Brownian motion of sediment

particles in turbulent flows (e.g. Batchelor, 1977; Pope, 1994). Dimou and Adam (1993) developed a depth-averaged random walk particle tracking model in order to simulate sediment transport in vertically well-mixed estuaries and coastal waters. Oh and Tsai (2007) proposed a stochastic diffusion particle tracking model (SD-PTM) for transport of suspended sediment particles through an open channel flow. The stochastic diffusion particle tracking model is governed by the stochastic differential equation (SDE) consisting of two terms: mean drift term and a Wiener process representing random turbulence motion, i.e. Brownian motion.

The other kind of stochastic sediment transport approaches is that a sediment particle transports among different defined states with a certain probability. Malmon et al. (2003) defined the channels and floodplains in different reaches as the different “states”. By analyzing the transition probability between river channels and floodplains among reaches, the rates of sediment particles overturn in valleys and map particle residence times could be examined. Tsai et al. (2014) integrated Gambler's ruin problem and multi-state discrete-time Markov chain into sediment transport modeling. The states were defined as the number of sediment particles. Based on the Shields number, a sediment particle in the reservoir might deposit with the probability q or suspend with the probability p=1- q. Then the risk of reaching the maximum state of the sediment carrying capacity can be calculated to facilitate decision making. Ancey et al. (2008) developed a birth-death immigration-emigration Markov process to describe the transport of coarse spherical particles down a steep slope in a turbulent shallow water stream. The “states” were defined as different modes of sediment particle movement, such as entrainment and deposition of sediment particles.

In this study, we combine these two methods together by proposing a stochastic framework which belongs to the latter approach, a sediment particle transports among

different defined states and applying the former stochastic diffusion particle tracking model to simulate the particle motion in the framework. In this study, the stochastic framework is an application of queueing theory. Queueing theory is a well-known mathematical study of waiting lines and the results are often adopted to make business decisions regarding the resources needed to provide service. In the proposed model, by treating sediment particles as customers, the control volume as a store and mechanics of sediment transport as service in analogy to the queueing theory, the concentration, deposition rate and re-suspension rate can be calculated. In the queuing theory, the "state" in the framework is defined as the number of incoming sediment particles. In this stochastic framework, the random arrivals and random magnitude of sediment particles can be simulated at the same time, i.e., random-sized batch arrivals.

Very few applications of queueing theory to simulate sediment transport can be found. Compared to other sediment transport models, the most advantageous feature of this stochastic framework is for the random input of sediment particles. Most of the sediment transport formulas only consider the input in a deterministic manner. In the study, the random input takes both random arrivals and batch number of sediment particles in to consideration. In addition, the proposed framework can accommodate various particle size and transport equation. Combination with appropriate sediment transport equations, the proposed stochastic framework can give a more realistic description of sediment transport when modeling sediment transport in a uncertain manner.

1.1 Motivation and Objective of the Study

Most of the sediment transport simulations apply deterministic transport equations while movement of sediment particles in turbulent flow is essentially uncertain. To better describe the particle movements, more and more stochastic approaches are applied to simulate the random characteristics of sediment transport. However, little research has been done by adopting the random input of incoming sediment particles, therefore the major purpose of the present study is to find an appropriate way to model the random input including random numbers and random arrivals of sediment particles (Figure 1). More specifically, the proposed stochastic framework in company with the stochastic diffusion particle tracking model (SD-PTM) are undertaken in order to quantify the variations of sediment concentrations in some areas of concern. Moreover, suggestions of some theoretical as well as practical implications of the framework and SD-PTM are provided.

1.2 Overview of the Thesis

In this thesis, the first section is the general background information as well as the state of the art of stochastic sediment transport . This is followed by the literature review and theoretical foundations for the development of research. After which are the introduction and simulations of particle arrival processes including random magnitude and random occurrences of sediment particles. The combination of the two random input processes is presented in Chapter 6. Finally, a summary is presented and recommendations are made for future research.

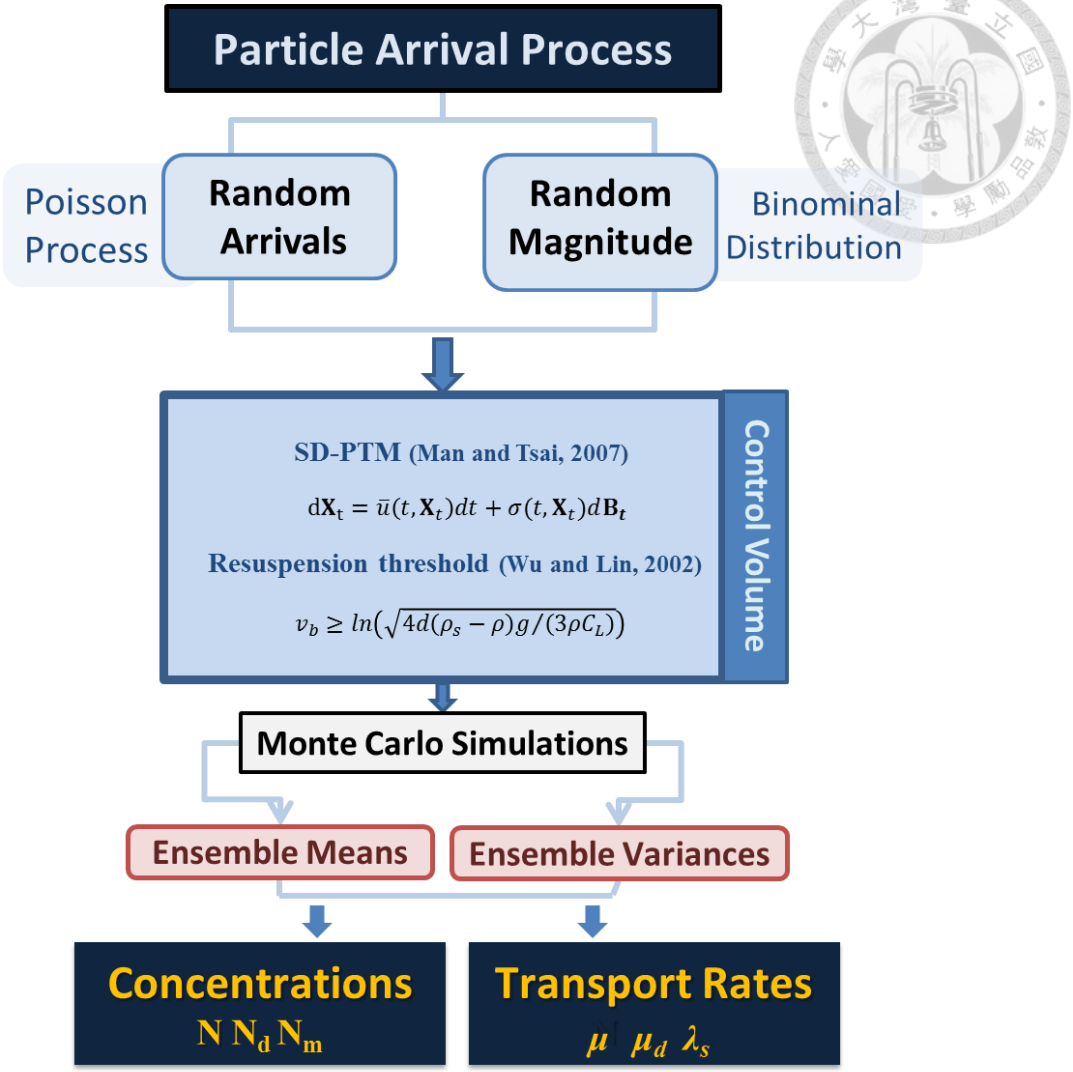

Figure 1. Flow chart

In this study, the application of queueing theory mostly focused on the random input of sediment particles including random magnitude and random arrivals of sediment particles. In the control volume, transport equations of sediment particles included stochastic diffusion particle tracking model (Man and Tsai, 2007) and resuspension process (Wu and Lin, 2002). Then by Monte Carlo simulations, the ensemble means and ensemble variances of particle concentrations and transport rates (depart rates, deposition rates and resuspension rates) can be calculated based on the random particle trajectories in order to describe the stochastic property of sediment transport.

Chapter 2 Literature Review

2.1 Queueing Theory

Queueing theory is a mathematical study of the service system of random queues. The original formula of Queueing theory can be traced back to Agner Krarup Erlang, a telephone exchange engineer in Copenhagen, Denmark. He studied calling pattern of people and tried to develop a formula to figure out how long people have to wait in an exchange phone call. There are at least four main components in queueing theory, customer, service facility, service and queue. A queue is formed when customers arrive at the service facility (store) and are forced to wait in a waiting line due to busy servers serving former customers. On the other hand, if a customer arrives at the service facility while the server is free, he/she will be served immediately. Once a server has finished the service, customers are assumed to leave the service facility. The average number of customers in the service facility (or in the queues) and the average time a customer spends in the service facility (or spends waiting in a queue) often are the most concerned results in queueing theory. The most advantageous property is the flexibility of queueing theory. Customers, service facility, service and the queue could be different representatives and have different assumptions depending on the demands of a problem. For instance, Hanbali and Boxma (2010) assumed that there was an "admission controller" that was put before the store. An admission controller would let the customer in the store with probability **q** or denied the entry of a customer with probability **p**. Then the joint transform of the number of customers served, the number of losses customers during the busy period as well as the length of the busy period was derived. One of the queuing model which might be familiar to the hydraulic field is "fluid queue". In hydraulic field, fluid queue is usually applied to estimate the fluid level in a reservoir and it could also be called by the fluid

model, fluid flow model or stochastic fluid model. The inflow and outflow, which are the arrival and depart rate, respectively, are arbitrary. However, unlike common queue model such as M/M/1 and M/G/1 queue, arrivals in fluid queue is assumed to be continuous rather than discrete. Naden (1987) modeled gravel-bed topography from sediment transport by a simple queue model. In the model, the queue denoted "bedform" and the probability for a discrete sediment particle getting in the queue or not was decided by the mechanics of gravel motion. Sediment particles had a probability **p** to leave a queue. The very particle at the end of the groups would have probability **q** to deposit anywhere. The results of the model presented the bed elevation and displayed at least of two scales of bedforms which are pebble clusters and antidunes. Results in Naden's model showed similar characteristics of field experiments and published flume data (Meland and Norrman, 1966; Francis, 1973; Abbott and Francis, 1977). Naden (1987) also tested the model over a hydrography and found that the behavior of sediment transport activity was extremely variable. Nowadays queueing theory is often adopted to make operation decisions on system optimization problems. Queueing theory is widely used in stochastic service systems such as telecommunications, transportation engineering, computer networks, production, transportation, inventory and other sharing resources.

2.2 Brownian Motion

Brownian motion, named after English botanist Robert Brown, is the random motion of particles in a fluid (a liquid or a gas) resulting from collision among molecules. And a Wiener process has the similar behavior to Brownian motion and at the same time, it is the scaling limit of random walk. That means that if one examines random walk with very small steps (i.e. in a microscopic scale), random walk will approximately become Wiener

process. Wiener process is often used to replace the derivative of Brownian motion, in the result of the characteristic of a Brownian particle that is everywhere continuous but nowhere differentiable proved by Norbert Wiener. For fluid particles, Langevin equation written as a stochastic differential equation is often used to describe the diffusion in inhomogeneous turbulence flows. Pope (1994) treated the increment in the Wiener process as a Gaussian random variable with mean zero and variance *dt* in a stationary homogeneous isotropic turbulent flow with zero mean velocity. For sediment particles in turbulence flows, due to that the movement of sediment particles is stochastic under the influence of turbulence, the stochastic differential equations or stochastic partial differential equations are thought to be suitable to describe the motion. Oh et al. (2010) delineated trajectories of suspended sediment particles using a stochastic diffusion model. The random term due to turbulence was a three-dimensional vector of the Wiener process and the time derivative of the vector was Gaussian white noise. The model was stochastic diffusion particle tracking model, which will be introduced next.

2.3 Stochastic Particle Tracking Model

Evolved from the Langevin equation, the stochastic diffusion particle tracking model (SD-PTM) model is to portray the random trajectories of suspended particles in turbulent flow conditions (Man, 2007; Man and Tsai 2007). Following is the governing equation of sediment particle position $\mathbf{X}_\mathrm{t} = \{X(t), Y(t), Z(t)\}^T$:

$$d\mathbf{X}_\mathrm{t} = \bar{\mathbf{u}}(t, \mathbf{X}_t)dt + \boldsymbol{\sigma}(t, \mathbf{X}_t)d\mathbf{B}_t$$

Where $\bar{\boldsymbol{u}}(t, \boldsymbol{X}_t)$ denotes the drift velocity vector, $\boldsymbol{\sigma}(t, \boldsymbol{X}_t)$ symbolized diffusion coefficient tensor and $d\boldsymbol{B}_t$ is the Wiener process at time *t* in three –dimensional vector form. The first term of the right-hand side of equation interpret the mean drift motion by

the mean drift term $\bar{\mathbf{u}}(t, \mathbf{X}_t)$ which represents the mean particle velocity at $\mathbf{X}_t$ position at time t, where $\mathbf{X}_t = (x(\mathrm{t}), \mathrm{y}(\mathrm{t}), \mathrm{z}(\mathrm{t}))$. Made up of two terms, mean drift flow velocity $\bar{\mathbf{U}}$ and turbulence diffusivity $\mathbf{D}$, the mean drift term can be expressed as follow (Man and Tsai, 2007):

$$\bar{\mathbf{u}}(t, \mathbf{X}_t) = \bar{\mathbf{U}} + \nabla \mathbf{D} = \begin{cases} \bar{U}(t,x,y,z) + \partial D_x/\partial x \\ \bar{V}(t,x,y,z) + \partial D_y/\partial y \\ \bar{W}(t,x,y,z) - w_s + \partial D_z/\partial z \end{cases}$$

where, $\bar{U}, \bar{V}, \bar{W}$ and D_x, D_y, D_z are the mean drift flow velocities and turbulent diffusivities in x, y, z direction respectively. In this study, the suspended sediment particles are assumed to be very fine and follow the fluid while they transport. Therefore particle velocities are assumed to be the same as the flow velocity except for an additional settling velocity $\mathrm{w_s}$ for deposition motion. Based on the assumption that random movement of a particles results from the turbulent flow, the second term of the right-hand side of the govern equation is the random turbulence term, which takes a Brownian motion $d\mathbf{B}_t$ and a diffusion coefficient $\boldsymbol{\sigma}$ into consideration. In this paper, the diffusion coefficient $\boldsymbol{\sigma}$ is presented by a diagonal matrix:

$$\boldsymbol{\sigma}(t, \mathbf{X}_t) = \begin{bmatrix} \sigma_{xx} & 0 & 0 \\ 0 & \sigma_{yy} & 0 \\ 0 & 0 & \sigma_{zz} \end{bmatrix}$$

The relationships between the diffusion coefficients $\boldsymbol{\sigma}$ and the turbulent diffusivities $\mathbf{D}$ were proposed by Man and Tsai (2007).

$$\mathrm{D_i} = \frac{1}{2}\sigma_{ii}^2, \qquad i = x, y, z$$

Recent stochastic particle tracking models focus more on the response of particle trajectories to extreme flow events. The stochastic jump diffusion particle tracking model (SJD-PTM) added a jump term in order to simulation the abrupt change of particle positions under extreme flow events (Oh, 2011). Particles trajectories were addressed in

surface flows in response to a sequence of random occurrences of extreme flow events (Tsai et al., 2014).Oh and Tsai (2010) described the delayed response of sediment particles to extreme flow events as the temporal lag (relaxation lag, i.e. the time lag between the sediment particle and the fluid particle in extreme flows) of particles as a result of the particle inertia effect.

2.4 Pickup Probability

Pickup probability was defined by Einstein (1950) as the probability of the dynamic lift greater than submerged weight of a sediment particle. Based on this concept, Wu and Lin (2002) presented the formulation of the pickup probability for sediment entrainment by assuming the instantaneous velocities were log-normally distributed.

By comparing the lift force and the submerged weight of a particle, one could have the following equation,

$$u_b^2 > \frac{4d}{3C_L}\frac{(\rho_s - \rho)}{\rho}g$$

where the u_b denotes the instantaneous velocity approaching the particle on the bed, d represents the particle diameter, C_L is the lift coefficient, ρ and ρ_s is density of fluid and a sediment particle, respectively.

Different from previous version that treating instantaneous velocities u_b as the random variables of a normal distribution, Wu and Lin (2002) assumed that u_b was lo-normally distributed. Then by taking log on u_b, one could define a new normally distributed random variable $v_b = ln(u_b)$ with mean $\overline{v_b} = ln(5.52u_*)$ and variance $\sigma_v^2 = 0.123$ approximated by the analytical method (Wu and Lin, 2002). Two mathematical approaches, the analytical method and the first-order approximation method, were employed in the deviation of pickup probabilities. Wu and Lin (2002)

indicated that the accuracy of pickup probabilities from two approaches were at the same order of magnitude if the optimal lift coefficient was applied (in this study, C_L= 0.21). After a particle has deposited on the bed, by comparing the threshold $B = ln\left(\sqrt{4d(\rho_s - \rho)g/(3\rho C_L)}\right)$ with v_b, one could decide whether a particle would resuspend or not.

2.5 Experimental Data

Kaftori et al. (1995) found that funnel vortices would dominate the particle motion including deposition and resuspension near the wall structure from experiments. In order to investigate particle motions near the wall in a turbulent boundary layer, Kaftori et al. (1995) conducted 33 experiments in a narrow rectangular flume. In all 33 experiments, 20 of which were with particles. Polystyrene particles were applied for the experiment due to their density (1050 kg/m^3), which was slightly larger than water. The polystyrene particles could settle down and were light enough to respond to the fluid for resuspension. In the experiments, the particles were captured at the outlet from the flume and recirculated and were examined by flow visualization techniques, which was like the setting of random arrivals and random magnitude of incoming sediment particles. Moreover, Kaftori et al. (1995) provided experimental conditions in details (e.g. particle size, water depth, shear velocity, Reynolds number, etc.). In this study, we applied the experimental data of Kaftori et al. (1995) to simulate the regular flow and to compare the particles velocities calculated from the stochastic diffusion particle tracking model (SD-PTM) with the experimental data.

Chapter 3 Theoretical Framework

3.1 Application to Queueing Theory

Queueing systems are denoted by Kendall's notation, which was brought out by Kendall (1953). It has the form ***A/B/c***. **A** specifies the arrival process (e.g. **M** for a Poisson process). **B** denotes the service time distribution (e.g. **M** for exponential distribution). The letter **c** denotes the number of servers. For example, ***M/G/1*** means in a single server system (store) where customers arrive based on Poisson process with rate λ and where the service times are independent and have a distribution function **G** (Takagi, 1991). We could start from a simple demonstrating case, ***M/M/1*** queue. The two *M*s refer to the assumption that both the interarrivals and the service distributions are exponential and the ***1*** to that there is a single server. Suppose the sediment particles arrive at the control volume in accordance with a Poisson process having a rate λ. In other words, the time between successive arrivals are independent exponential random variables having a mean of $1/\lambda$. And in an ***M/M/1*** queue, sediment transport capacity in the control volume is exactly one sediment particle. The sediment transport capacity corresponding to an ***M/M/1*** queue is the number of servers, which is one in this case. The transport process from the beginning to the end of the control volume is defined as a 'service' in an ***M/M/1*** queue. In order to tally with an ***M/M/1*** queue, the successive service times, the transport time, are assumed to be independent exponential random variables having a mean of $1/\mu$. Suppose that after some time, the system becomes steady, then the average number of sediment particles in the system (average concentration) and the average amount of time a sediment particle spends in the system (i.e., mean transport time). In the above-demonstration case, ***M/M/1***, the distribution of sediment transport time is an exponential distribution in the control volume. Unfortunately, the distribution of transport time in

sediment transport is not an exponential distribution. Thus, there are some strategies that aim at solving this problem. The best way, of course, is to find the real distribution of sediment transport time under a given condition. Then it would perfectly fit the queueing process, due to the unrestrained distribution of the service distribution in a general queueing process. The second method is having a proper sediment transport formula to interpret transport of sediment particles well. In the study, the stochastic diffusion particle tracking model (SD-PTM) was applied. As such, not only the distributions, but the uncertain paths of sediment particles in details could be calculated.

Though queueing theory has been widely applied to many other disciplines, its application to sediment transport modeling has remained limited. However, from the stochastic perspective, queueing theory could interpret sediment transport well. For instance, due to the intermittent phenomenon, sediment transport is treated as a random process. Moreover, instead of adopting continuum mechanics, discrete concepts are used to build our model. Randomness and discrete characteristic are two basic concepts in queueing theory (i.e. random number of customers could arrive at the store at any time; and persons are one of the classic examples to explain the discrete concept).

As shown in Table 1, the store is treated as the control volume and customers in queue as sediment particles. Service is a very abstract concept. Service here is very similar to the scene that a server brings a customer into the store from the front door, brings him/her to the back door and then let the customer leave the store. Such process corresponds to a sediment particle getting into the control volume and starting to move (start be served) until it moves out of the control volume in the proposed model. The process between the beginnings (arrive at the store; get into the control volume) and the end (leave the store; depart from the control volume) is defined as services. Hence, in the proposed model, service is defined as the mechanics of sediment transport while server is defined as the

sediment transport itself (i.e. entrainment/ deposition).

Table 1. Application of queueing theory

Queue	Application of queueing theory
Store	Control volume
Customer	Sediment particles
Server	Mechanics of sediment transport

In the study, we apply M/G/k queue. Particles arrive according to Poisson process. The time a particle spends on getting out of the control volume (service time) has a distribution G. The physical meanings of sediment transport are mostly presented on service time. And there are k severs in the control volume. Here we assume $k \to \infty$.

3.1.1 Notation

We consider a two-dimensional water body including different sizes of sediment particles (see Figure 2). The length of the control volume is L. Sediment particles arrive at the control volume according to a Poisson process with a rate λ. The times between arrivals are independent exponential random variables with a mean $1/\lambda$. In the control volume, sediments could deposit at the rate μ_d , re-suspend at the rate λ_s and leave with a depart rate μ.

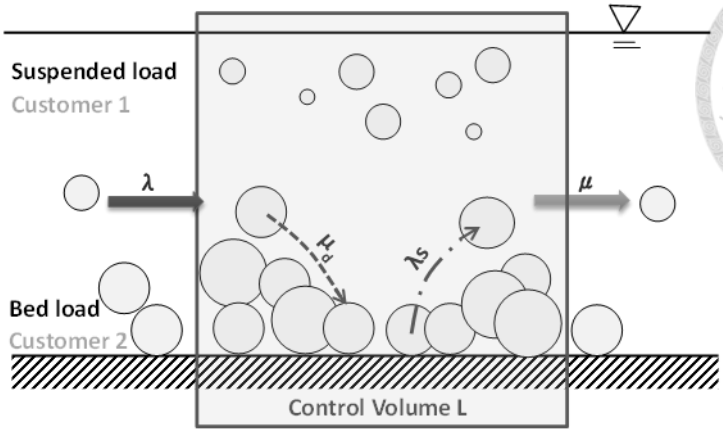

Figure 2. Model illustration.

Sediment particles arrive at a Poisson rate λ. In the control volume, sediments could deposit at the rate μ_d, re-suspend at the rate λs and leave with a depart rate μ.

3.2 Exponential Distribution

An exponential distribution known as a negative exponential distribution, has always provided a good statistical description due to its *Markov property*, "*memoryless*".

Assume there is a continuous random variable T with a distribution function $\boldsymbol{P}\{T \leq x\} = \boldsymbol{F}(x)$ where

$$\boldsymbol{F}(x) = \begin{cases} 1 - \mathrm{e}^{-\mu x} & , x \geq 0 \\ 0 & , x < 0 \end{cases}$$

The probability density function $f(x)$ of this exponential distribution is

$$f(x;\mu) = \frac{d}{dx}\boldsymbol{F}(x) = \begin{cases} \mu e^{-\mu x} & x \geq 0 \\ 0 & x < 0 \end{cases}$$

Then a random variable T has the exponential distribution with mean $\mathbf{E}(T) = \mu^{-1}$ and variance $\mathbf{V}(T) = \mu^{-2}$.

The particularly important feature of an exponential distribution is the "*memoryless*" or a so called "Markovian" property. An example is provided here to prove the no memory property of an exponential distribution. Suppose that there is a time bomb which would explode automatically after a time X distributed according to an exponential distribution:

$$\mathbf{P}[\mathbf{X} < x] = 1 - \mathrm{e}^{-\mu x}, \qquad \infty > \mu > 0$$

The time bomb triggered at time $\mathrm{t} = 0$ would cause an explosion at time $\mathrm{t} = \mathbf{X}$. Before the explosion, at an intermediate time $\mathrm{t} = y$, one might like to know the time remaining before the explosion. Since the bomb does not explode at $\mathrm{t} = y$, we know that $\mathbf{X} > y$ and then we wish to know the distribution of $\mathbf{X} - y$. By calculating

$$\mathbf{P}[\mathbf{X} - y < x | \mathbf{X} > y] = \frac{\mathbf{P}\{y < \mathbf{X}, y + x\}}{\mathbf{P}\{\mathbf{X} > y\}},$$

$$= \frac{1 - e^{-\mu(x+y)} - (1 - e^{-\mu y})}{e^{-\mu y}} = 1 - e^{-\mu y} = \mathbf{P}\{\mathbf{X} < x\}$$

One can discover that $\mathbf{X} - y$ has the same distribution as $\mathbf{X}$. The result means that there is no memory between variables. Moreover, if a continuous positive random variable has the above property, then the distribution of the ransom variable is exponentially distributed.

3.3 Continuous-Time BAMPS

3.3.1 Batch Markovian Arrival Processes (BMAP)

In queueing theory, a Markovian arrival process (MAP) is a mathematical model for the time between each arrival events (Cordeiro & Kharoufeh, 2011). The most well developed MAP is Poisson process where the lengths of inter-arrival times are random variables of an exponential distribution. The batch Markovian arrival process is a generalized MAP, whose arrival events are "batch events." In other words, the Poisson process is a special case of the BMAP by restricting the batch size to unity.

3.3.2 The Continuous-time BMAP

For an irreducible, continuous-time Markovian chain (CTMC) $J \equiv \{J(t),\ \mathrm{t} \geq 0\}$ whose state space $E = \{1,2,\dots,m\}$ where m is a finite, positive integer, the

infinitesimal generator matrix is $\boldsymbol{Q}$. After J enters state $i \in E$, it takes an exponentially distributed amount of time in state i with rate $\lambda_i = -q_{ii}$, where q_{ii} denotes the i th diagonal element of $\boldsymbol{Q}$. There are two kinds of transition ways. One type is for an arrival with "batch" size $k\ (k > 1)$, the process would transit to state $j \in E$ with probability $p_{ij}(k)$, where j might be equal to i. As for the second type, the batch size is 0, and the process would transit to state j with probability $p_{ij}(0)$ where in this case, j ≠ i. For each $i \in E$, the probabilities $p_{ij}(k)$ and $p_{ij}(0)$ must satisfy the following condition,

$$\sum_{k=1}^{\infty}\sum_{j=1}^{m} p_{ij}(k) + \sum_{j\in E\setminus\{i\}} p_{ij}(0) = 1 \qquad (1)$$

And for $k \geq 0$, we could define the matrices $\boldsymbol{D}_k = \left[d_{ij}(k)\right]_{i,j\in E}$ where

$$d_{ij}(0) = \begin{cases} -\lambda_i & j = i \\ \lambda_i p_{ij}(0) & j \neq i \end{cases} \qquad (2)$$

and

$$d_{ij}(k) = \lambda_i p_{ij}(k), \quad j, i \in E, \quad k \geq 1 \qquad (3)$$

The matrix $\boldsymbol{D}_0$ includes the transition rates of J with no arrival while matrices $\boldsymbol{D}_k (k \geq 1)$ involve the transition rates for batch size k. Based on condition (1) and equation (2) and (3), it could be seen that

$$\boldsymbol{Q} = \sum_{k=0}^{\infty} \boldsymbol{D}_k \qquad (1)$$

Let $N(t)$ stands for the total number of arrivals up to time t. The process, $(N, J) \equiv \{N(t), J(t),\ t \geq 0\}$ is defined as a batch Markovian arrival process (BMAP) with state space $\{(n, j),\ n \geq 0,\ j \in E\}$ and infinitesimal generator matrix,

$$\mathbf{Q}^* = \begin{bmatrix} \boldsymbol{D_0} & \boldsymbol{D_1} & \boldsymbol{D_2} & \cdots \\ \mathbf{0} & \boldsymbol{D_0} & \boldsymbol{D_1} & \cdots \\ \mathbf{0} & \mathbf{0} & \boldsymbol{D_0} & \cdots \\ \vdots & \vdots & \vdots & \ddots \end{bmatrix} \qquad (4)$$

A BAMP is described by matrices $\boldsymbol{D_k}$, therefore, $\boldsymbol{D_k}$ is often thought as the representation of a BMAP. In addition, $J(t)$ is the ***phase process*** while $N(t)$ is often called the

counting process in a BMAP. The phase process $J(t)$ in this study was simulated by random variables of a binominal distribution and the counting process $N(t)$ was described by the Poisson process in this study.

3.3.3 Poisson Process

One of the most well-known continuous-time batch Markovian processes is Poisson process, a well-developed continuous-time counting process $\{\mathrm{N(t)}, \mathrm{t} \geq 0\}$. In a continuous-time BMAP, if there is only one state m=1 in the state space *E*, the time between arrivals is exponentially distributed and for each arrival, the batch size is equal to 1, then the counting process$\{\mathrm{N(t)}, \mathrm{t} \geq 0\}$ is a Poisson process. The generator matrix is expressed as

$$\mathbf{Q}^{*} = \begin{bmatrix} -\boldsymbol{\lambda} & \boldsymbol{\lambda} & \mathbf{0} & \cdots \\ \mathbf{0} & -\boldsymbol{\lambda} & \boldsymbol{\lambda} & \cdots \\ \mathbf{0} & \mathbf{0} & -\boldsymbol{\lambda} & \cdots \\ \vdots & \vdots & \vdots & \ddots \end{bmatrix}$$

($D_0 = -\lambda, \mathrm{D}_1 = \lambda,$ and $D_k = 0$ for all $k \geq 2$)

In this study, Poisson process governs the arrivals of sediment particles in this study. $N(t)$ denotes the number of the sediment particles in the control volume up to time t. For $\mathrm{t} = 0$, the number of sediment particles is equal to zero, $\mathrm{N(0)} = 0$; and for each $\mathrm{t} > 0$, the probability distribution of $\mathrm{N(t)}$ is a Poisson distribution with a Poisson rate $\lambda > 0$ which only depends on the length of the time intervals.

In this study, the ***interarrivals*** are defined as time intervals between arrivals of sediment particles. Random variables of interarrivals $(\mathbf{T}_1, \mathbf{T}_2, \mathbf{T}_3, \ldots\ldots)$ are distributed according to an exponential distribution are independent of each other.

$$\mathbf{P}\left[\mathbf{T}_{\mathrm{j}} < x\right] = 1 - e^{-\lambda x}, \qquad \text{for all } j \geq 1$$

For $\mathrm{i} \neq \mathrm{j}$

$$\mathbf{P}\left[\mathbf{I}_{\mathrm{i}} < x \text{ and } \mathbf{I}_{\mathrm{j}} < y\right] = \mathbf{P}[\mathbf{I}_i < x]\mathbf{P}[\mathbf{I}_{\mathrm{j}} < y]$$

3.3.4 Batch Poisson Process

In BMAP, if the batch size is larger than one in the standard Poisson process with rate λ, it is a batch Poison process. For a batch size k, p_k denotes the probability of batch size of an arrival (k≥1) and $\sum_{k\geq 1} p_k = 1$. The generator matrix of a batch Poisson process is presented as follow,

$$\mathbf{Q}^* = \begin{bmatrix} -\boldsymbol{\lambda} & \boldsymbol{p_1\lambda} & \boldsymbol{p_2\lambda} & \boldsymbol{p_3\lambda} & \cdots \\ \mathbf{0} & -\boldsymbol{\lambda} & \boldsymbol{p_1\lambda} & \boldsymbol{p_2\lambda} & \cdots \\ \mathbf{0} & \mathbf{0} & -\boldsymbol{\lambda} & \boldsymbol{p_1\lambda} & \cdots \\ \vdots & \vdots & \vdots & \vdots & \ddots \end{bmatrix}$$

($\mathrm{m} = 1, \mathrm{D}_0 = -\lambda$ and $D_k = \lambda p_k$ for each $k \geq 1$)

Chapter 4 Random Magnitude (RM) Simulated by Binomial Distribution

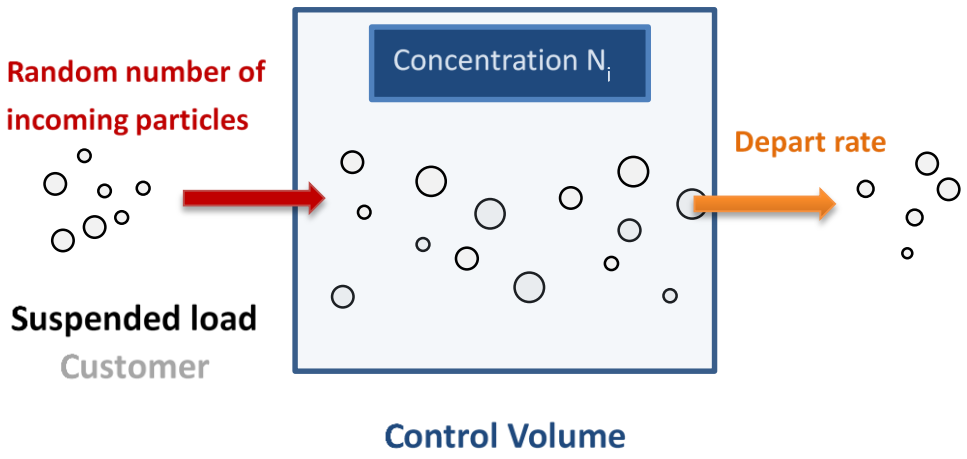

Figure 3. Illustration of random magnitude of incoming particles.

4.1 Introduction

In this section, the number of incoming sediment particles is assumed to be a random variable (Figure 3). The probability distribution of a random variable can be different distributions depending on the characteristic of the incoming events. Herein we apply the binomial distribution as the probability distribution of the random numbers of incoming sediment particles. The main reason for choosing a binomial distribution is for the discrete property of sediment particles. In our study, sediment particles arrive in the control volume in the unit of bead, which is the discrete concept, and therefore the probabilistic distribution must be discrete, such as the binomial distribution. The simulations are intended to compute the solid discharge and the concentration in the control volume. When the system becomes steady, the number of moving particles within the control volume is a constant n. Notice that the "state" here is defined as the number of incoming

sediment particles. In these simulations, we aim to find a special equilibrium situation. A special equilibrium situation means that the number of particles in motion within a control volume tends to be a constant n under certain flow conditions. Theoretically, when the simulation time is sufficiently large, the stationary random process can be achieved (i.e. let $t \to \infty$).

4.2 Assumptions

There are two assumptions in these simulations. The first one is that there are no correlations among sediment particles or between fluid particles and sediment particles. The other assumption is that the probabilistic characteristics of random numbers of incoming sediment particles in a regular flow can be simulated by a binomial distribution.

4.3 Procedure

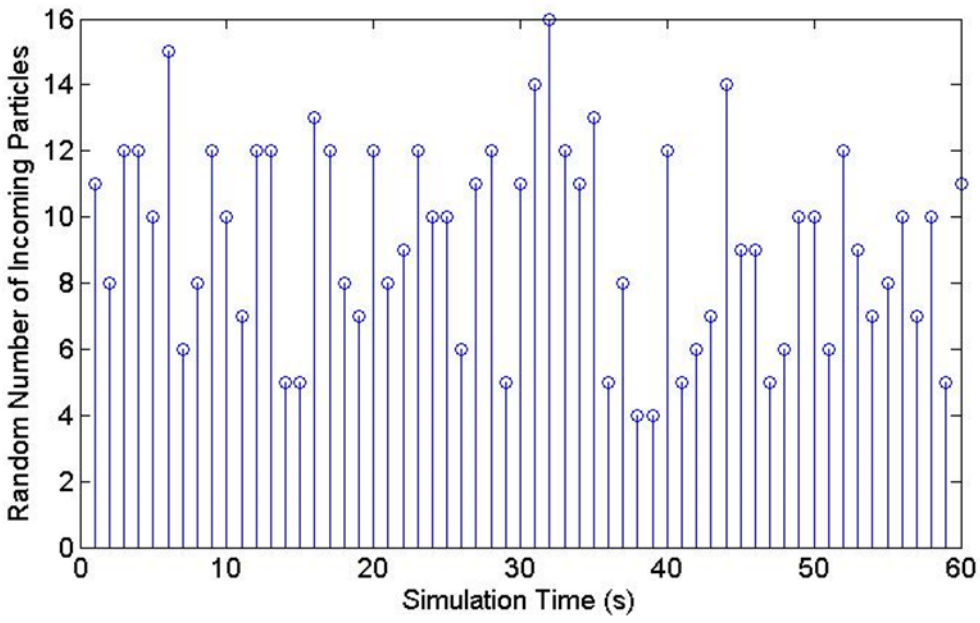

Figure 4. Random number of incoming sediment particles.

(1). Generate a series of random numbers according to the binomial distribution $B(100,0.1)$. Release the suspended particles along with time (Figure 4).

(2). Apply the stochastic particle tracking model (PTM) to simulate particle trajectories.

(3). Calculate the number of moving sediment particles, particle position $X_t \leq$ the length of the control volume (L) and the service time, t_i, that one particle spends on transporting through the control volume.

(4). Repeat (1) to (3) and calculate the ensemble means and variances of sediment concentrations.

4.4 Simulations

4.4.1 Case RM-1D

Introduction

In this 1-D simulation, all particles are suspended load with the same diameter and there are no correlations among particles. The numbers of incoming sediment particles are random variables following a binomial distribution, $B(100,0.1)$. It means that on the average, there will be ten sediment particles arriving at the control volume per second. It must be noted that particles will be released at the same time step, when there are more than one particle released in a time step (Figure 5). Moreover, as shown in Table 2, there are no deposition and re-suspension, only suspension when particles are in motion.

The position of a moving particle can be described by the stochastic diffusion equation (SDE) (Tsai et.al, 2007),

$$d\mathbf{X}_i = \left(\overline{U}_i + \frac{\partial D_i}{\partial x_i}\right) dt + \sqrt{2D_i}\, dB_i$$

Table 2. Comparison table of case RM-1D and queue.

Queue	**Case RM-1D**
Store	Control volume
Customer	Suspended load
Server	Suspension
(Mechanics of sediment transport)	**Governing Equation**: **SD-PTM** Mean drift + Brownian motion $d\mathbf{X}_t = \bar{u}(t, \mathbf{X}_t)dt + \sigma(t, \mathbf{X}_t)d\mathbf{B}_t$

Table 3. Flow conditions and variables. (RM-1D)

Variables	**value**	**Units**
Mean flow velocity, $\bar{\mathbf{U}}$	**0.2**	$\mathbf{m/s}$
Diffusivity, $\boldsymbol{\sigma}$	**0.1**	$\mathbf{m/s^{1/2}}$
Time step, $\boldsymbol{\Delta t}$	**1**	**S**
Simulation time **T**	**60**	**S**
Length of the control volume, **L**	**5**	**M**
Runs	**100000**	

Simulation Results

Table 4 gives the results as expected: the mean velocity of particles is slightly smaller than the mean drift flow velocity. Due to the gravity effect, the time delay of the sediment particles is a normal phenomenon in flow.

Table 4. Results. (RM-1D)

Result	value	Units
Ensemble mean particle velocity	**0.1980**	**m/s**
Depart rate (at steady state)	**10.005**	**bead/sec**

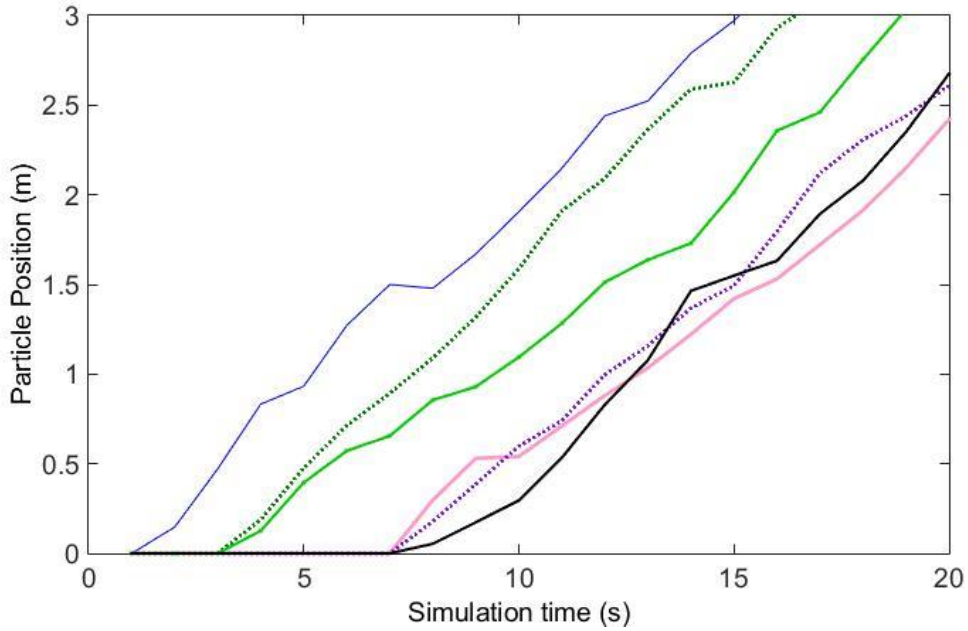

Figure 5. Particle trajectory along time in a 1-D flow. (RM-1D)

Trajectories of some particles along over time are schematized in Figure 5. The lines on Figure 5 represent different paths of individual particles. The fluctuations of the lines can reflect the effect of the turbulence term (i.e. Brownian motion). It should be noted that Figure 5 shows that there are random numbers of particles generated by a binomial distribution, arriving at the control volume in different time steps. It also displays that once more than one sediment particle is produced in a time step, they will be released at exactly the same time step. In addition, the particles will not be affected by each other, since this study assumed that there are no correlations among sediment particles.

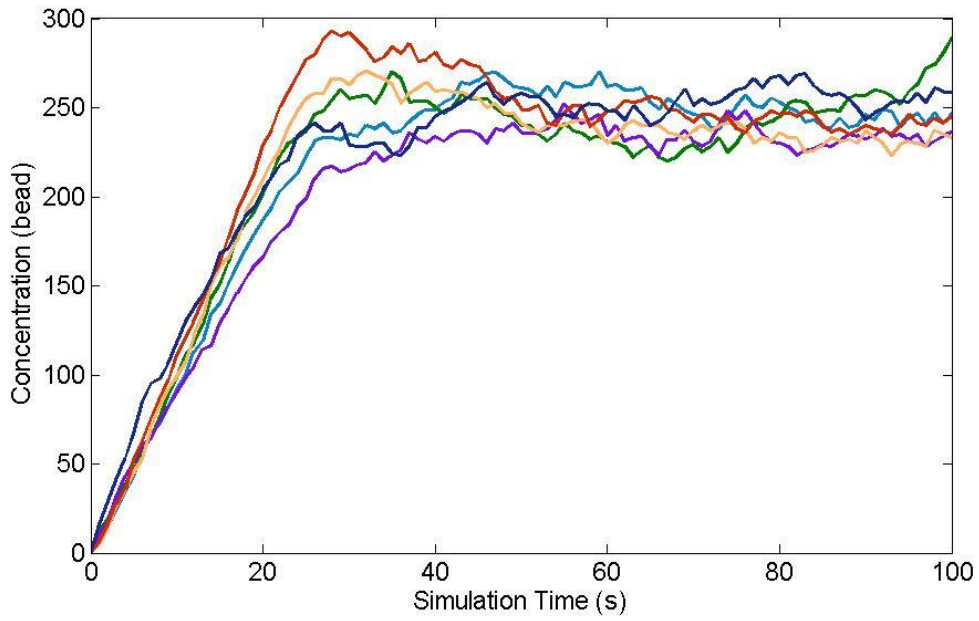

Figure 6. Concentration of some scenarios. (RM-1D)

Figure 6 provides the number of sediment particles in the control volume along with time (bead). The main purpose of Figure 6 is to schematically show the concentration results of scenarios. Each line represents one scenario in Figure 6. Since there are no particles in the control volume before the simulation, Figure 6 shows that the number of particles in the control volume. The particle number increased rapidly at the beginning and then after about 40 seconds, they started to fluctuate between 200 and 300.

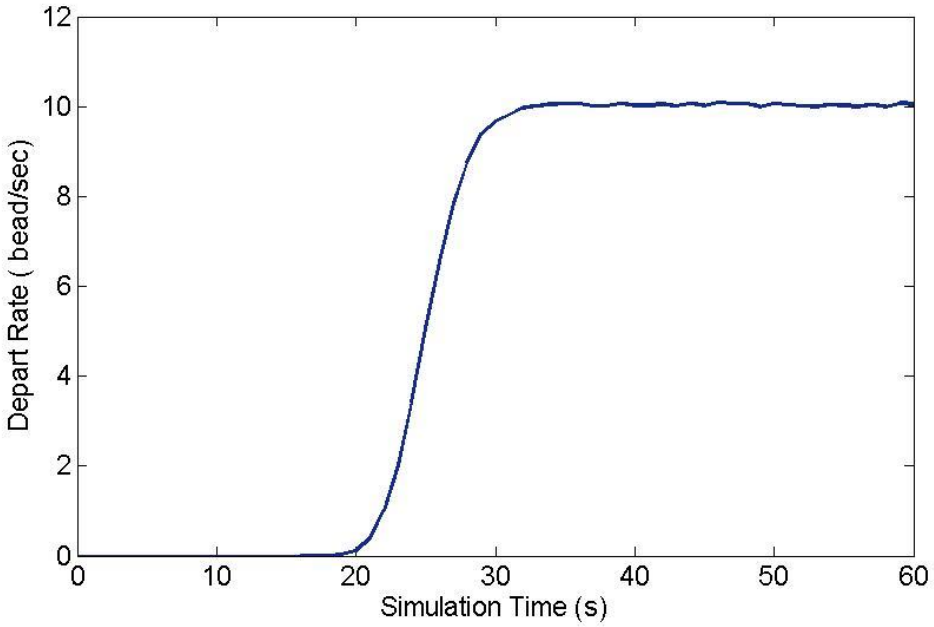

Figure 7. Depart rate of sediment particle. (RM-1D)

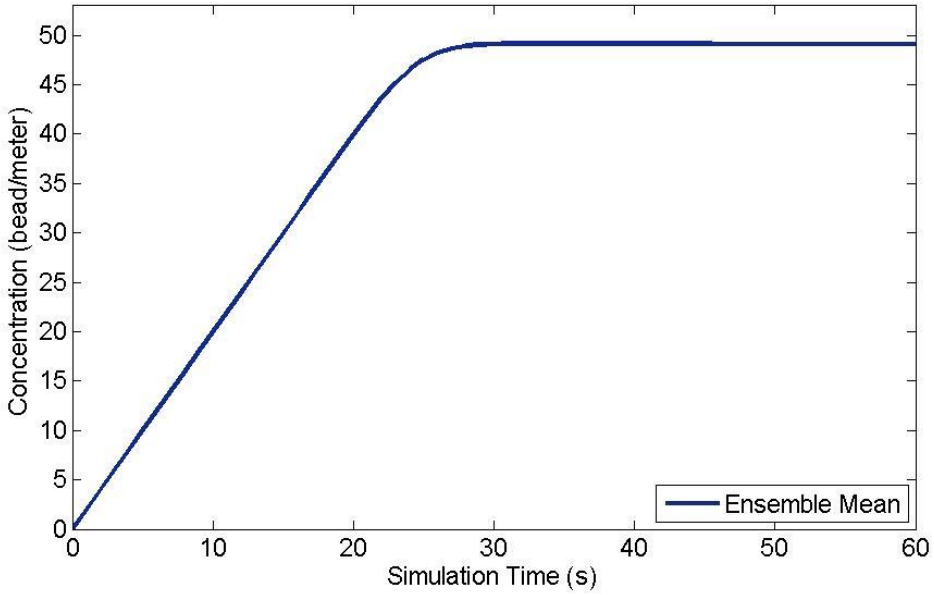

Figure 8. Ensemble mean of concentration. (RM-1D)

Figure 8 presents the ensemble means of concentrations based on 10000 scenarios over time. Contrary to Figure 6, the line in Figure 8 is much smoother. Moreover, it is found that the steady situation was achieved while time is around 30 seconds ($n = 46.735\ \text{beads/meter}$), which can also be proved in Figure 7. Figure 7 revealed the

depart rates of the sediment particles along with time. The beginning rates were zero due to the assumption that initial condition of the control volume was empty. Therefore, sediment particles came into the control volume. Then the depart rate started to grow in S shape and became stable (t = 32 seconds). It is the time that the service/depart rate (μ=9.978 bead/sec) is almost equal to the arrival rate (λ=10 bead/sec), which proved that the system did become steady.

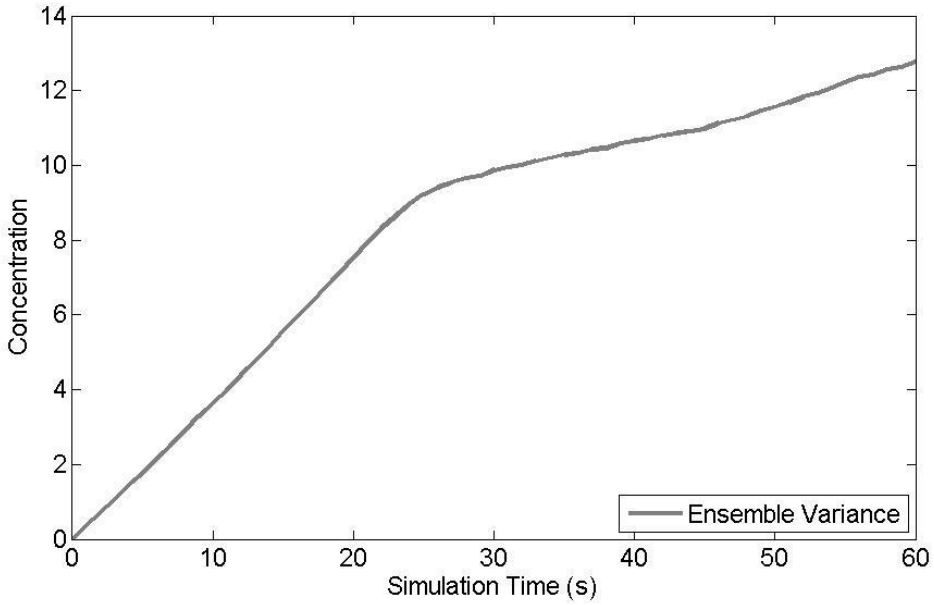

Figure 9. Ensemble variance of concentration. (RM-1D)

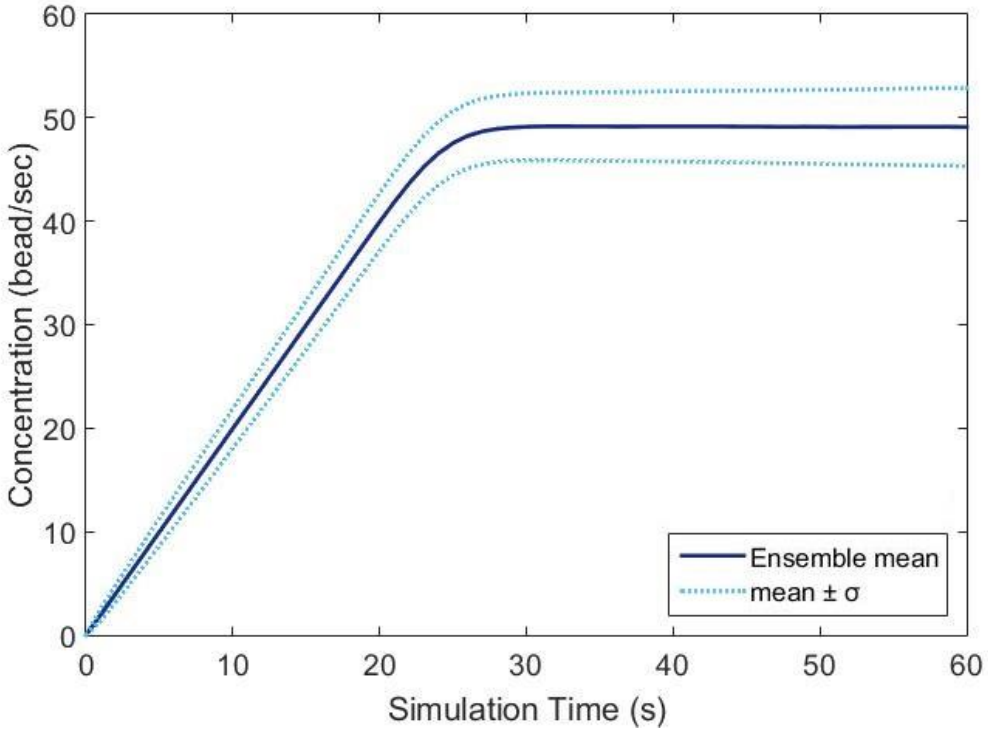

Figure 10. Ensemble variance of concentration **±σ**. (RM-1D)

The ensemble variances of concentrations along with time are shown in Figure 7. In stochastic processes, the ensemble statistical moments such as the ensemble variances are advantageous as opposed to the deterministic process while the ensemble means would be the same as the result of deterministic process. Herein the ensemble mean plus and minus one standard deviation (±σ) is shown in Figure 8 assuming the concentrations are normally distributed. It is clearly that the variations of concentrations were small at the beginning and would grow larger along with time in Figure 10. Whether for standard deviation or variance, they both are measures used to quantify the amount of variation of the results. For this case, the two random variables are the Brownian and the random incoming process and they are independent of each other. Besides, the statistical characteristics of the binomial distribution could tally with the prerequisite of standard deviation. In the binomial distribution $B(n, p)$, if n is large enough, then the distribution

could be treated as a normal distribution $N(np, np(1-p))$ due to an insignificant skewness of the binominal distribution.

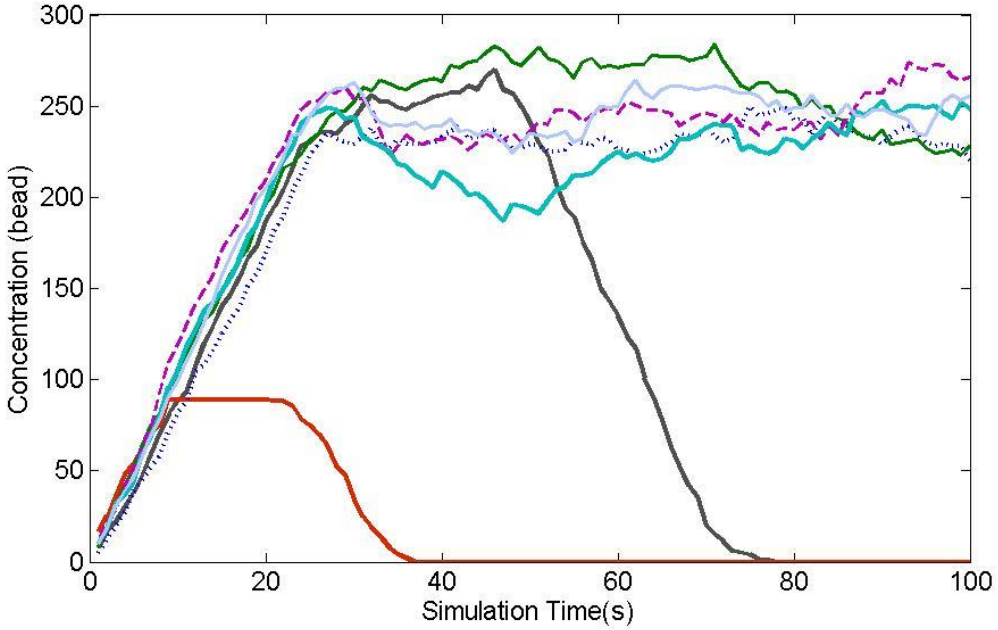

Figure 11. Concentration of some scenarios. (RM-1D)

It is interesting to observe that some scenarios of concentrations (the red line and the dark blue line in Figure 11) behaved differently from other scenarios whose shapes were like the results of ensemble mean in Figure 8. The shapes of these scenarios were similar to bell shapes. One conjecture of this circumstance is that the supply shortage of incoming sediment particles in the latter part of simulations. Therefore, as the simulation time went on, the concentration would drop and return to zero. The frequency of this situation would become higher when there are more scenarios in a simulation. And this is probably the reason why the ensemble variance of concentration in Figure 9 would grow along with simulation time after the system becomes steady.

Segments

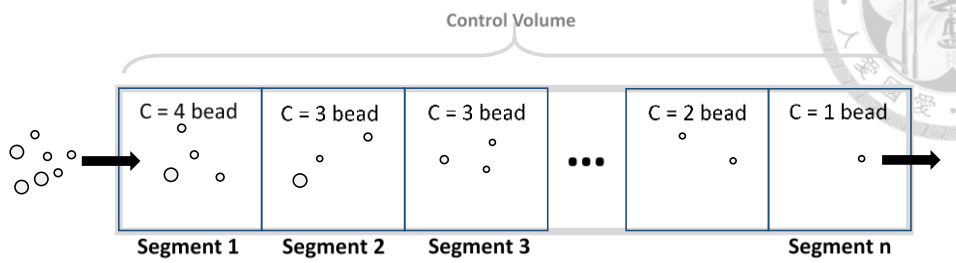

Figure 12. Illustration of segments.

In case RM-1D, the control volume was divided into small segments whose lengths were all equal to one meter (Figure 12). The position of segment is shown in Table 5. The concentration (i.e., number of sediment particles) of each segment can be calculated and compared, as shown in Figure 15. The ensemble means of concentration in different segments are shown in Figure 13. The ensemble means of the first segment seemed to behave differently from other segments in Figure 13. Such difference can be attributed to the larger size of the time step, which was one second in this simulation. For instance, after a particle being released into the control volume, it might take less than one time step transporting through the first segment. That is the reason why the ensemble mean of concentrations in the first segment was less than other segments when the system reached equilibrium. In order to solve the inconsistency and to prove the explanation, the simulation was run again and this time, the time step was equal to 0.1 second. Figure 14 illustrates the ensemble means of concentrations in each segment with the time step =0.1 second. Compare Figure 14 with Figure 13, it could be find that the values of the ensemble means of concentrations in the first segment were almost equal to other segments when the system became steady. Based on the comparison, it is suggested that the size of the time step should be smaller when examining the concentrations in subsequent segments. Otherwise, the values of the concentrations in beginning segments might be

underestimated when the size of the time step is larger. Figure 15 presents the variance of the ensemble means of concentrations between segments. At the beginning of the simulations, there might be particles in the beginning segments but there might be few particles in the subsequent segments, therefore the variance would increase along with the simulation time. Until there were particles in all segments, the variance started to decrease. When the control volume became steady, the variance of the ensemble means of particle concentrations between segments approached zero.

Table 5. Position of Segments.

Segment	**1**	**2**	**3**	**4**	**5**
Position (m) (in x direction)	[0,1)	[1,2)	[2,3)	[3,4)	[4,5)

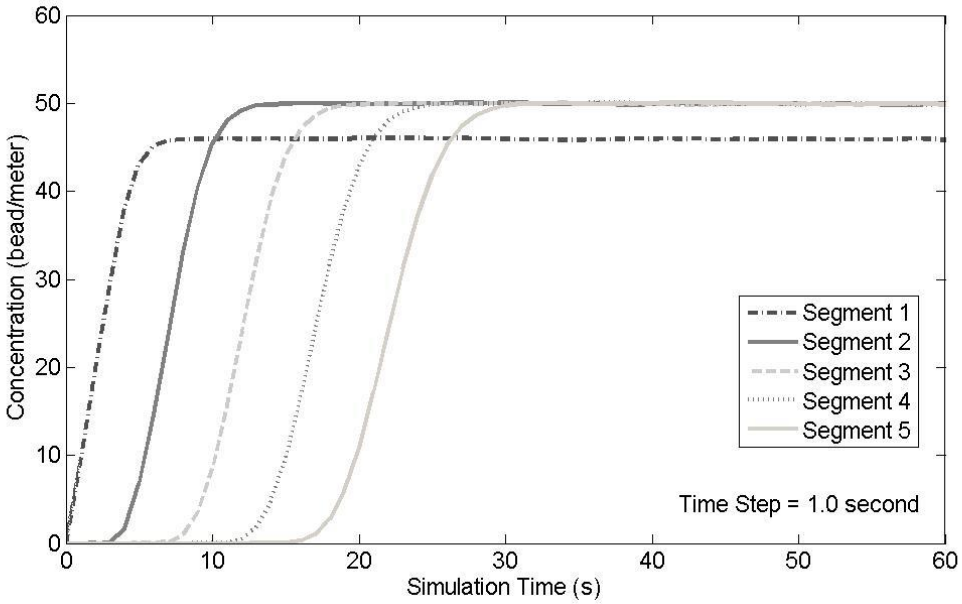

Figure 13. Ensemble mean of concentrations in segments. (dt = 1.0s)

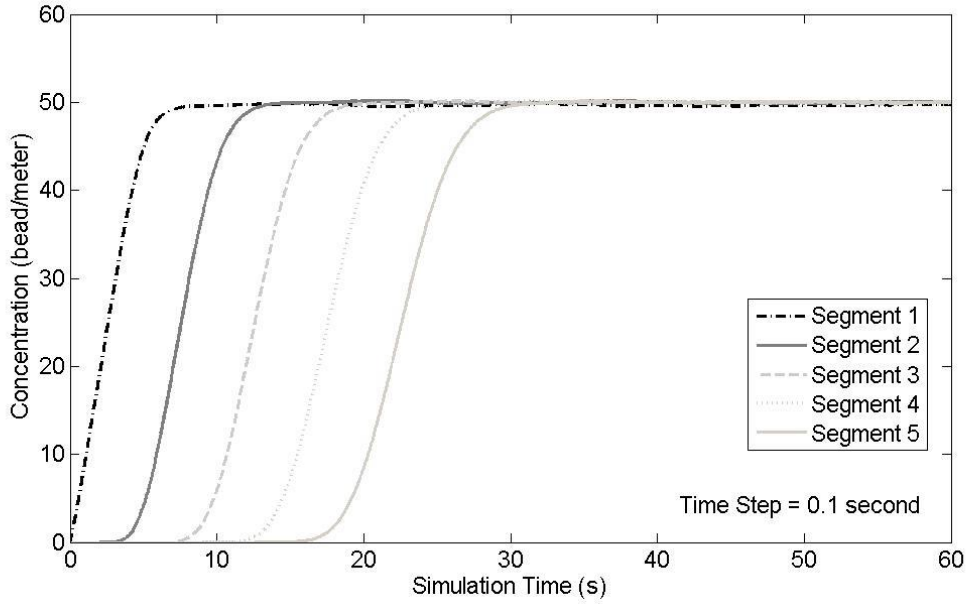

Figure 14. Ensemble mean of concentrations in segments. (dt = 0.1s)

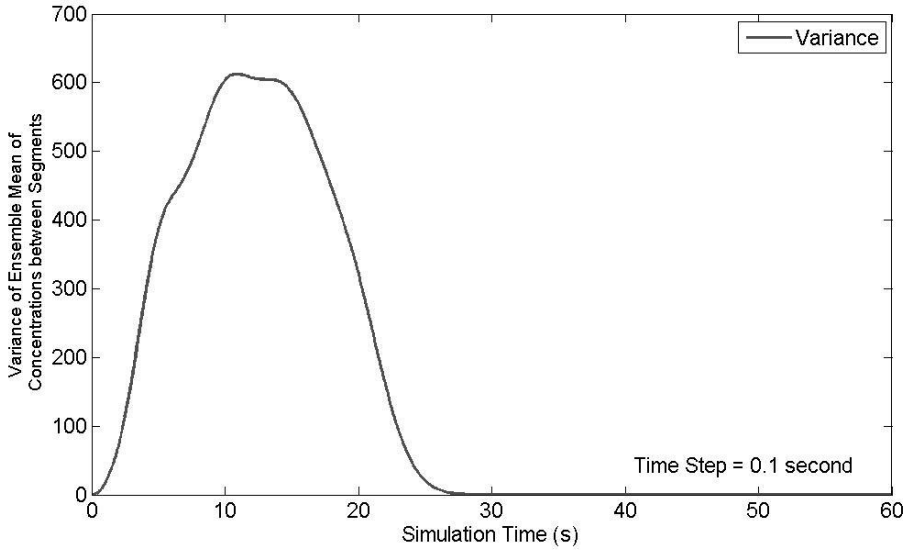

Figure 15. Variance of ensemble means of concentrations between segments.

Different sizes of control volume

The duration that system spends to become steady is proportional to the size of control volume. We compared five cases with different control volume sizes. Each case was based on ten thousands scenarios and the results are listed in Table 6. The first row represents

the ensemble mean times that the system spent to become steady based on ten thousands scenarios in each realization; and the second row is the concentration (bead/meter) when the system reached equilibrium.

Table 6. Comparison of different sizes control volume.

L (m)	**2**	**4**	**6**	**8**	**10**
T_{mean}(s)	11	24	33	44	56
Concentration(bead/meter)	47.92	48.98	49.31	49.47	49.42

The y-axis in Figure 16 is the number of particles in the control volume (beads/meter), which is treated as the concentration of sediment particles in this study. The control volume was empty before sediment particles were released. As a result, the larger the control volume, the smaller the concentration would be at the beginning of each simulation. Thus, Figure 16 shows clearly that the beginning slope of lager-sized particles would be flatter. As such, it would take longer time for the particle transport to become steady. The first row in Table 6 shows that the time duration that a system took to reach equilibrium is proportional to the size of the control volume. Lines in Figure 16 show that the concentrations at an equilibrium state were almost the same. Table 6 enlists more details about the concentration at equilibrium. The larger the size of control volume, the larger the concentration. In addition, it can be found that when the size of control volume is larger than a certain value, the value of concentration in equilibrium reaches asymptotically to a constant (In the study, n = 49.4 bead/meter when the size of the control volume were larger than 6 meters.) However, it should be noted that the steady concentration was smaller in the control volume of two meters, which is also the smallest size in proposed scenarios, shown as solid black line in Figure 16, Figure 17 and Figure 18. It shows that with the given incoming rate (10 beads/sec), if the control volume is

smaller than two meters, it would be harder to find the same steady results as other simulation with larger control volume sizes. In spite of the different value of concentration in equilibrium, the depart rates shown in Figure 18 revealed that the case (L=2) did reach the steady state, as the depart rate was equal to the incoming rate of sediment particles.

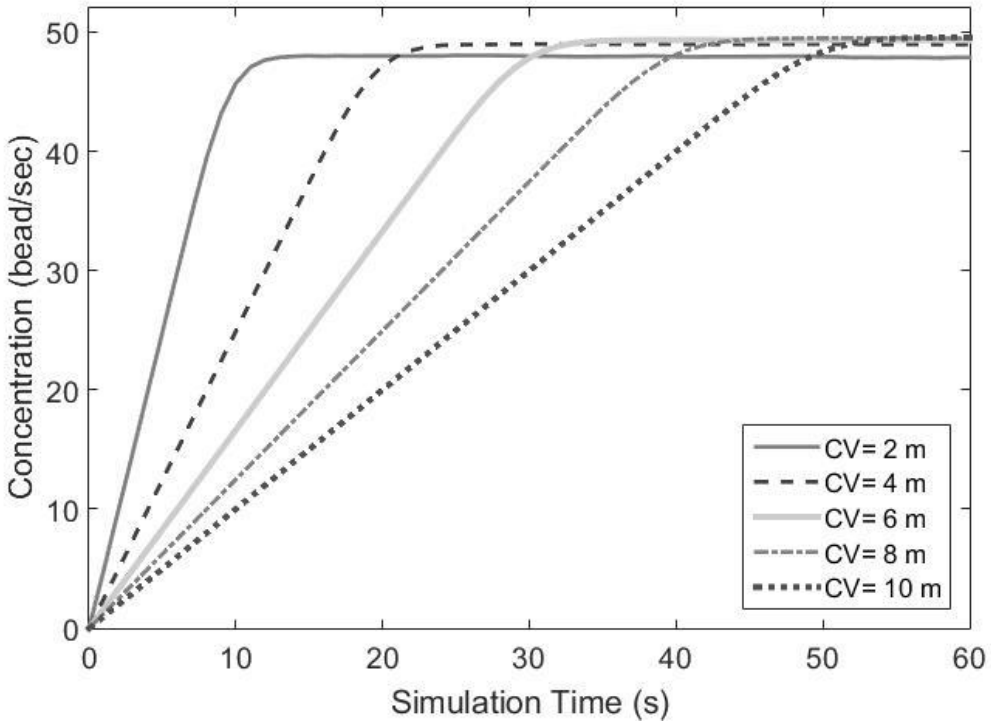

Figure 16. Ensemble means of different sizes of control volumes.

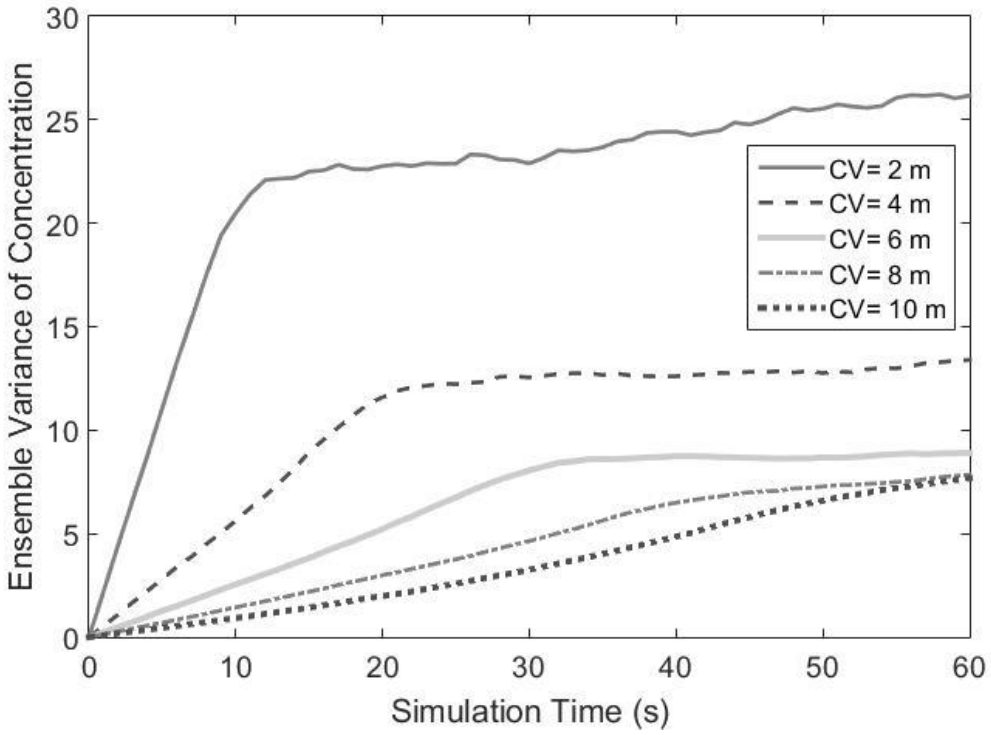

Figure 17. Ensemble variances of concentration of different control volumes sizes.

Figure 17 presents the ensemble variances of concentrations of different control volume sizes. The L in the legend denotes the length of control volume. In Figure 17, ensemble variance highlights differences between lager and smaller sizes of control volume. Ensemble variance of smaller sizes (L= 2, 4 m) was much larger than that of larger sizes of control volume (L= 8, 10 m). And the turning point resulting from the effect when the sediment particles start to leave the control volume, the line became smother and smother as the control volume became larger. The difference of ensemble means between different sizes of concentrations is reduced while the sizes became larger. It can be expected that when the size of control volume becomes infinite, the ensemble variance might be almost a straight line close to zero.

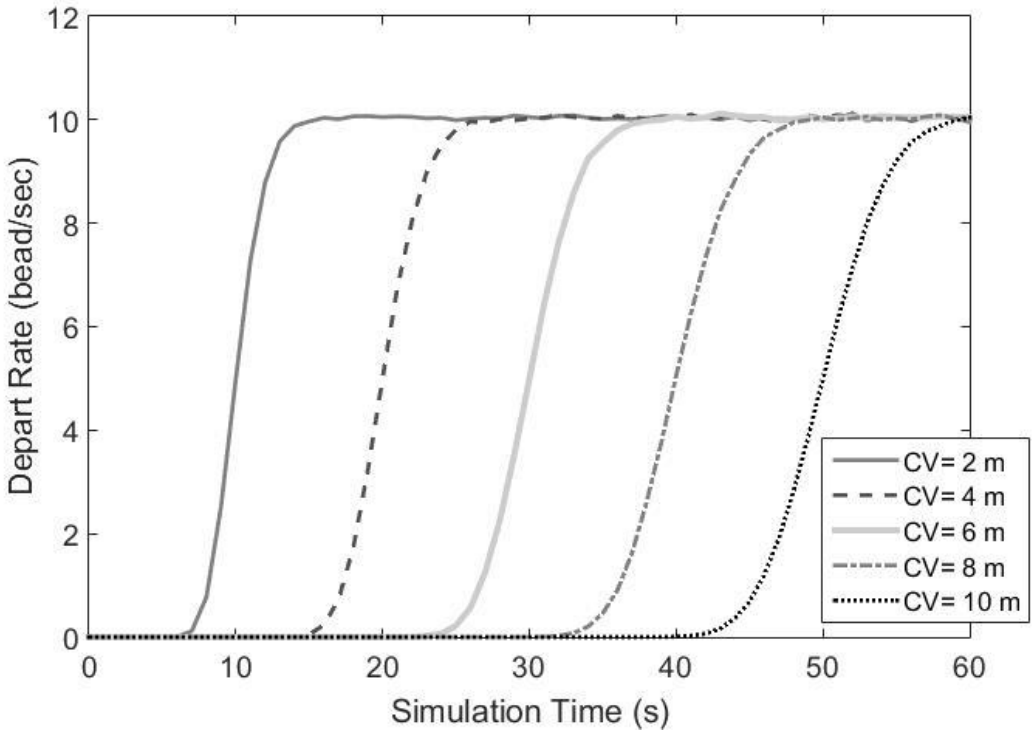

Figure 18. Depart rates of different control volume sizes.

Figure 18 schematizes the depart rates of different control volume sizes along with time. The S curves deliver an important concept that regardless of the control volume size, as soon as the sediment particles start to leave the control volume, the system would rapidly reach the equilibrium in about 20 seconds. And the final depart rates confirmed that the five cases (the length of L = 2, 4, 6, 8, 10 m) all reached an equilibrium, as all final depart rates were equal to the mean incoming rates of sediment particles.

Summary

In case RM-1D, the number of incoming sediment particles is assumed to be a random variable of a binomial distribution $B(100,0.1)$ in flow. The transport equation applied to simulate the sediment transport was stochastic diffusion process which took the Brownian motion (turbulence) into consideration. In this case, the concentrations were represented by the number of sediment particles per meter. Based on 100,000 scenarios, the ensemble means, ensemble variances of particle concentrations and ensemble means of depart rates were calculated. The results proved the system did reach equilibrium in the simulation. We also divided the control volume into small segments. It is suggested that the simulation should apply a smaller time step. Different control volume sizes were also examined in this case. And the results show that the larger sizes of the control volume, the longer time it would take for the system to become steady. Moreover, it is found that when the size of the control volume is larger, the peak of variance of the concentration would be smaller. The RM-1D simulation proved the proposed stochastic framework incorporate with SD-PTM was acceptable to simulate sediment transport in one-dimensional flow.

4.4.2 Case RM-2D (without resuspension)

Introduction

Shown in Table 7, deposition of sediment particles was included in the simulation. All sediments were suspended load with uniform size equal to 250 μm and other flow conditions and variables are listed in Table 8. The flow velocities in this simulation are presented in Figure 19. The flow velocities are calculated based on the logarithmic velocity profile, $\bar{U} = \left(\frac{u_*}{\kappa}\right) ln\left(\frac{z}{z_0}\right)$, where κ is the von Karman constant (0.4), $z_0 = k_s/30$ is the position corresponding to the zero velocity (k_s denoted the effective roughness height).

The equation of shear velocity applied was $u_* = \sqrt{gHS_0}$. In the simulation, the release point of incoming sediment particles was at the half of the flow depth (1m). The random numbers of incoming sediment particles were non-negative integer random variables which generating by a binomial distribution $B(100,0.1)$. That means that incoming rate of sediment particles would be equal to 10 beads per second.

The SD-PTM was applied as the sediment transport equation for sediment particles trajectories in the control volume. The following are the govern equations of particle position in the X and Z direction, respectively.

$$\boldsymbol{X}_{n+1} = \boldsymbol{X}_n + \frac{u_*}{\kappa} \ln\left(\frac{\boldsymbol{Z_n}}{\boldsymbol{Z}_0}\right)$$

$$\boldsymbol{Z}_{n+1} = \boldsymbol{Z}_n + (\overline{W_n} - w_s + \kappa u_* - 2\kappa u_* \boldsymbol{Z_n}/H)\Delta t + \sqrt{2(\kappa u_* \boldsymbol{Z_n}(1 - \boldsymbol{Z_n}/H))}\Delta \boldsymbol{B}_t$$

Table 7. Comparison table of case RM-2D (without resuspension) and queue

Queue	Case RM-2D (without resuspension)
Store	Control volume
Customer	Suspended load
Server	Suspension/**Deposition**
(Mechanics of sediment transport)	**Governing Equation** : **SD-PTM** Mean drift + Brownian motion $\boldsymbol{X}_{n+1} = \boldsymbol{X}_n + u_*/\kappa \ \ln(\boldsymbol{Z_n}/\boldsymbol{Z}_0)$ $\boldsymbol{Z}_{n+1} = \boldsymbol{Z}_n + (\overline{W_n} - w_s + \kappa u_* - 2\kappa u_* \boldsymbol{Z_n}/H)\Delta t + \sqrt{2(\kappa u_* \boldsymbol{Z_n}(1 - \boldsymbol{Z_n}/H))}\Delta \boldsymbol{B}_t$

Table 8. Flow conditions and variables. (RM-2D-without resuspension)

Variables	**value**	**units**
Slope, **S**	**0.02**	**%**
Particle diameter, **D**	**250**	**μm**
Particle density, $\boldsymbol{\rho_p}$	**2500**	**kg m^{-3}**
Flow density, $\boldsymbol{\rho_f}$	**1000**	**kg m^{-3}**
Settling velocity, $\mathbf{w_s}$	**0.1038**	**m/s**
Reference height	**0.000275**	**m**
Length of the control volume, **L**	**2**	**m**

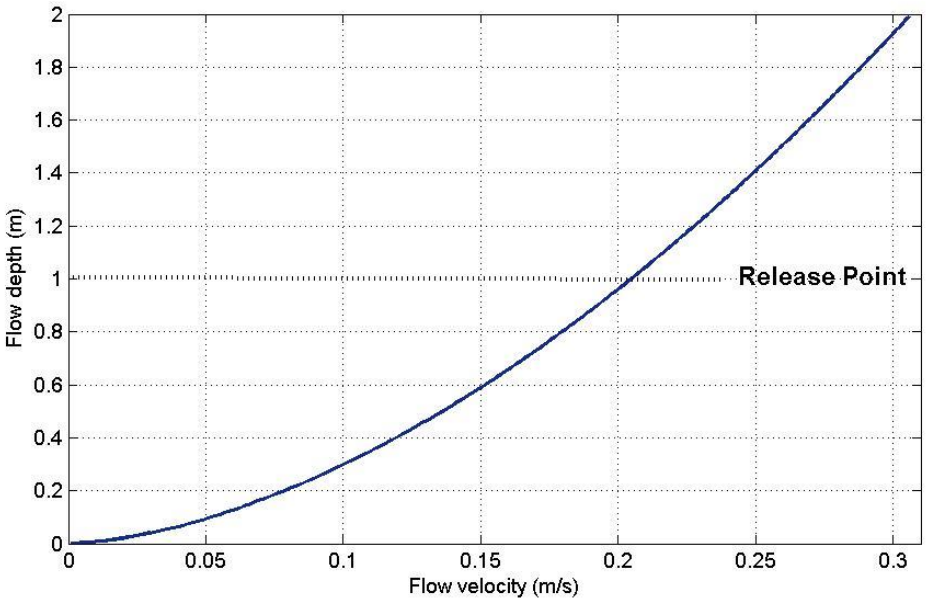

Figure 19. Flow velocity versus flow depth. (RM-2D-without resuspension)

Table 9. Model parameters (RM-2D-without resuspension)

Parameters	**value**	**units**
Time step, Δt	**1**	**s**
Simulation time **T**	**30**	**s**
Runs	**10000**	

Simulation Results

In this case (RM-2D-without resuspension) not only the depart rate but also the deposition rate, shown in Table 10, could be calculated. When the system became steady, the depart rate plus the deposition rate of sediment particles was almost equal to the mean of random arrival rate (10 beads/sec). Comparing with one-dimensional case (RM-1D), the depart rate was a little bit smaller due to deposition of sediment particles.

Table 10. Results. (RM-2D-without resuspension)

Results (after steady)	value	units
Depart rate	**8.7576**	**bead/sec**
Deposition rate	**1.2459**	**bead/sec**
Moving sediment particles	**34.806**	**bead/meter**

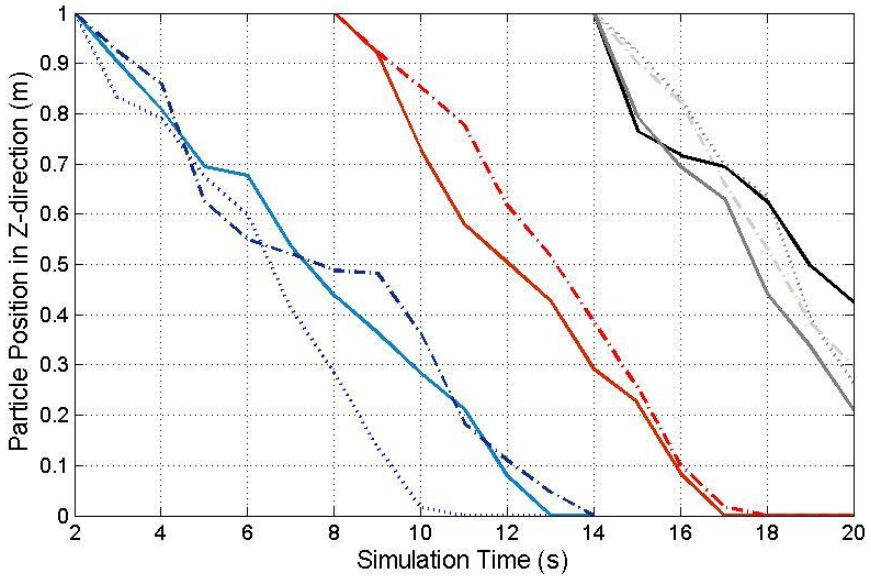

Figure 20. Particle trajectories in Z-direction. (RM-2D-without resuspension)

Figure 20 drew some scenarios of sediment particle trajectories; one line represents one trajectory of a sediment particle in the Z-direction. As illustrated in Figure 20, particle trajectories fluctuated in the Z-direction. The released height was half of the flow depth (Figure 19). Shown in Figure 20, different numbers of sediment particles were released along with the simulation time. The random variables generated by the normal distribution $N(10,2)$ were the random numbers of sediment particles. And if the number was larger than one, then the sediment particles would be released at the same time point, which is at the very beginning of the corresponding time step. Figure 20 shows that some of sediment particles would deposit in the control volume. Then based on 10000 scenarios,

ensemble means and ensemble variances of sediment concentration were calculated from the X-T and Z-T planes.

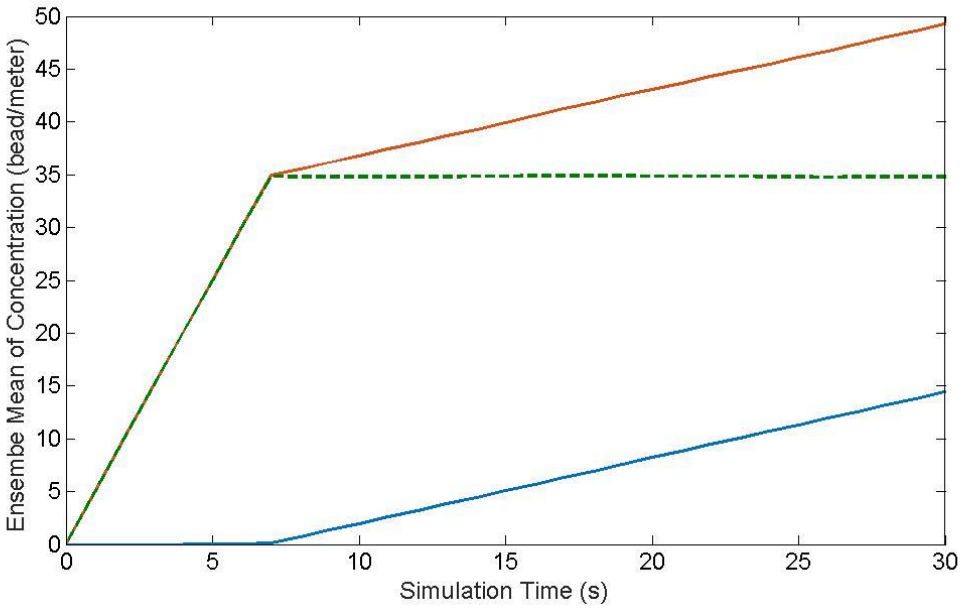

Figure 21. Ensemble mean of concentration (bead/meter). (RM-2D-without resuspension)

By comparing the particle position in X and Z direction, the amount of the sediment concentrations could be calculated. The concentrations were classified into three types: N, N_d, N_m. Despite the motion of sediment particles, N represented by the red line was for the total number of sediment particles in the control volume; N_d represented the number of the deposition sediment particles, shown as the blue line; the last one was the number of sediment particles in motion denoted as N_m, illustrated by the green dash line in Figure 21 and Figure 22. Ensemble means of three kinds of particle concentrations were displayed in Figure 21. Re-suspension of sediment particles was not considered in case RM-2D (without simulation), therefore, the number of the concentrations of deposition sediment particles N_d would increase along with the simulation time. Consequentially, the number of concentration N, the total number of sediment particles

in the control volume, certainly would become lager, too. The green dash line representing the ensemble means of concentrations of moving sediment particles in Figure 21 had the same trend as the concentration N since sediment particles had not started to deposit at the beginning of the simulation time. After the deposition started to affect the numbers of moving particles in the control volume, the increasing trends decreased and the slope became milder. Therefore there would be a turning point in Figure 21. Until the deposition rate became stable, the concentration of deposition particles became stable. In this case, since the time step was one second, the turning angle might be a little bit sharp. The time step was a little bit too large to see the whole picture of the sediment particles motion. It is like the situation that at one time step the sediment particles are all in motion, and at the next step, most of them have already deposited at the bed. If the time step is small enough, we may be able to see much more details about the turning point, i.e., it might become much smoother. However, as mentioned before, the aim of this study is to find an equilibrium situation of the control volume, it might be too time consuming to assume a too small time step. Taking both computational efficiency and the theoretically accuracy into consideration, we adopted time step =1 second in the simulation.

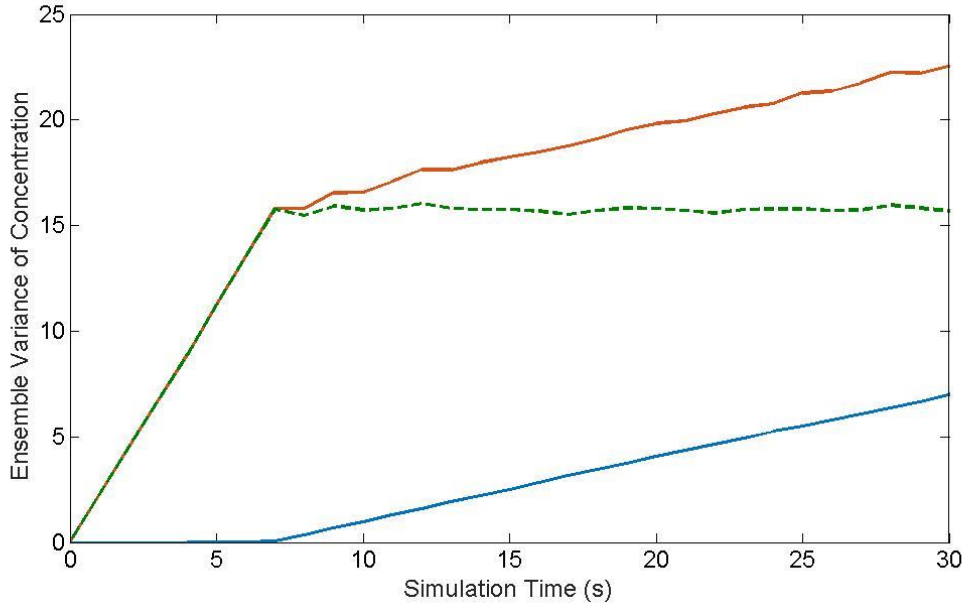

Figure 22. Ensemble variance of concentration. (RM-2D-without resuspension)

The ensemble variances of concentrations are represented in Figure 22. The trends of the ensemble variances of the concentrations are similar with those of the ensemble means in Figure 21. The ensemble variances of N_d were much more stable than N, N_m. This might result from the number of particles. In this simulation, the length of control volume was set to be two meters. Under this condition, the total numbers of sediment particles N were almost twice of the number of deposition particles N_d. In addition, lacking the consideration of the re-suspension process, the numbers of N and N_d would only increase along with simulation time, therefore the variation would be larger along with simulation time.

This could also explain the relatively unstable depart rates when comparing with the deposition rates in the control volume. The number of depart rates was larger than deposition rates; consequently, the fluctuations in Figure 23 would be more conspicuous than those in Figure 24. Depart rates of sediment particle (bead/sec) were shown in Figure 23. Depart rates were calculated by comparing particle position in the X-direction at

present X_n with the previous time step X_{n-1}. While $X_{n-1} \leq L$ and $X_n > L$, then the sediment particle is thought to depart from the control volume at time n (L is the length of the control volume in x direction). We calculate the number of sediment particles which just had departed at each time step (bead/sec). The depart numbers might be affected by the length of control volume at the beginning of the simulation, however, after the system becomes steady, the amount of depart rates should become stable. The same calculation could be applied in the Z-direction for resuspension rates in Figure 24. The steep S curves in Figure 23 and Figure 24 reflected the small size of control volume and the large size of time step. However, these will not influence the equilibrium results.

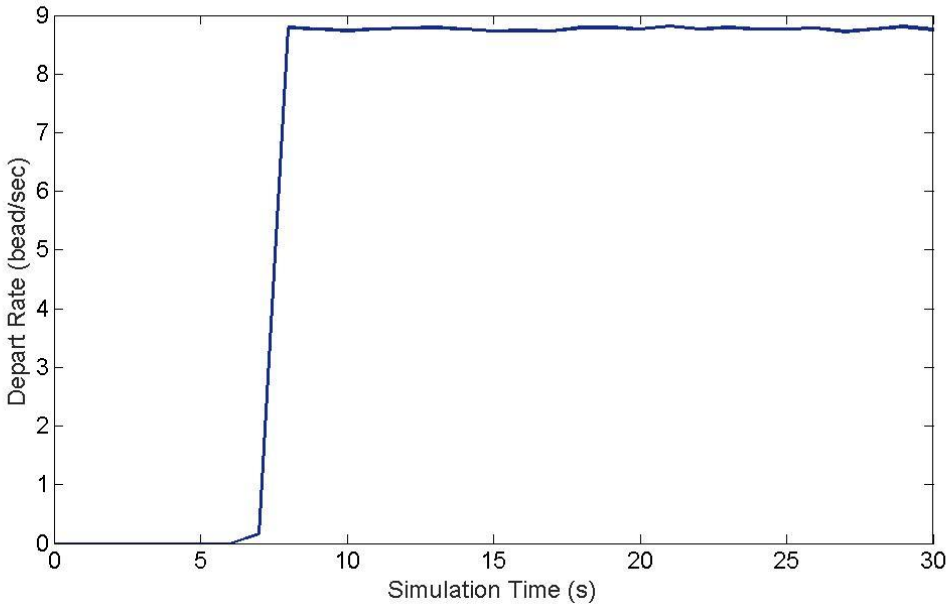

Figure 23. Depart rate of sediment particles. (RM-2D-without resuspension)

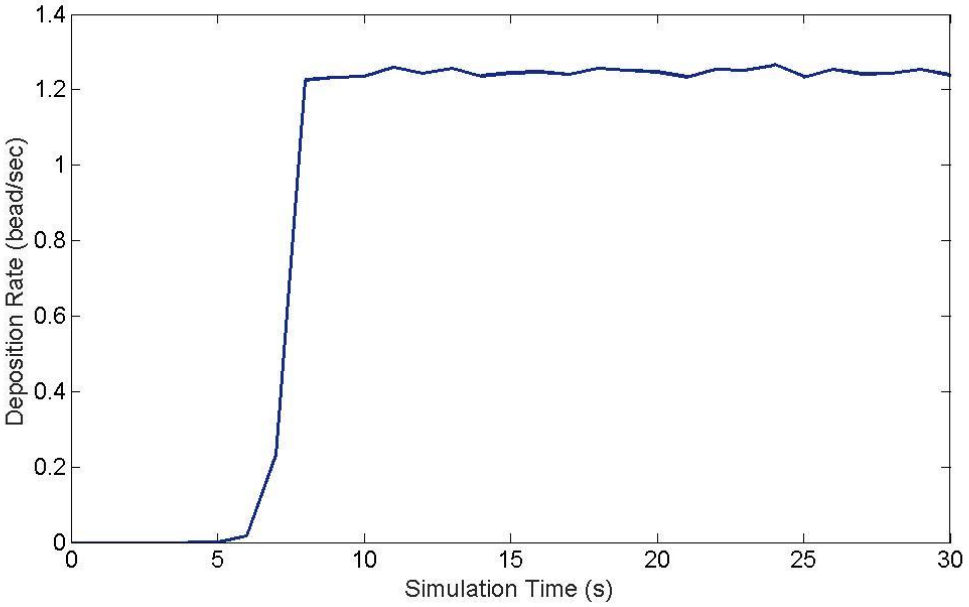

Figure 24. Deposition rate of sediment particles. (RM-2D-without resuspension)

Summary

In case RM-2D (without resuspension), mechanics of sediment transport included the suspension and deposition. In Figure 21 and Figure 22, the ensemble means and ensemble variances of three kinds of concentrations in the control volume were displayed. Table 10 shows that the sum of deposition rate and the depart rate of sediment particles were almost the same as incoming rates, which confirmed that the system did become equilibrium. The concentrations of the moving sediment particles (N_m) stayed the same after the system became steady. In this case, mechanics of sediment transport only included suspension and deposition, as the result, the concentrations of deposition particles would become lager. As a result, despite the system was equilibrium, the total number of the sediment particles and deposition particles in the control volume would become larger along with simulation time.

4.4.3 Case RM-2D

Introduction

The aim of this simulation is to model sediment transport and find the sediment concentrations while the input of incoming sediment particles is random. In this case, sediment particles were uniform size equal to 275 mm with the specific density 1.05, arriving at the control volume with random sizes. The random numbers of particle were generated by a binominal distribution B(100,0.1). After being released at the center of water depth, sediment particles would transport through the control volume based on the stochastic diffusion particles tracking model (SD-PTM). Different from previous case (Case RM-2D-without resuspension), particle motion in this case (Case RM-2D) involved not only suspension and deposition but also resuspension of sediment particles (Table 11). The resuspension process was proposed by Wu and Lin (2002). The instantaneous velocity approaching the particle on the bed was treated as a random variable of a log-normal distribution. After sediment particles deposited on the bed, by comparing the lift force and submerged weight of sediment particles, one could determine whether a sediment particle would resuspend or continue to stay on the bed. In the simulation, the flow conditions were experimental data proposed by Kaftori et al. (1995) and were listed in Table 12. The fluid velocity in the longitudinal direction $\overline{U}$ was approximated by the logarithmic profile and shown in Figure 19. Herein, the total simulation time was one minute; and time step is equal to one second (Table 13).

Table 11. Comparison table of case RM-2D and queue

Queue	**Case RM-2D**
Store	Control volume
Customer	Particles with diameter 2.75mm
Server	Suspension/**Deposition/Resuspension**
(Mechanics of sediment transport)	**Governing Equation** : **1. SD-PTM (Man and Tsai, 2007)** Mean drift + Brownian motion $\boldsymbol{X}_{n+1} = \boldsymbol{X}_n + u_*/\kappa \ \ln(\boldsymbol{Z_n}/\boldsymbol{Z}_0)$ $\boldsymbol{Z}_{n+1} = \boldsymbol{Z}_n + (\overline{W_n} - w_s + \kappa u_* - 2\kappa u_* \boldsymbol{Z_n}/H)\Delta t + \sqrt{2(\kappa u_* \boldsymbol{Z_n}(1 - \boldsymbol{Z_n}/H))}\Delta \boldsymbol{B}_t$ **2. Resuspension threshold (Wu and Lin, 2002)** $v_b \geq ln\left(\sqrt{4d(\rho_s - \rho)g/(3\rho C_L)}\right)$

Table 12. Flow conditions and particle parameters[1]. (RM-2D)

Variables	**value**	**units**
Particle diameter, **D**	**275**	**μm**
Particle density, $\boldsymbol{\rho_p}$	**1050**	**kg m^{-3}**
Flow density, $\boldsymbol{\rho_f}$	**1000**	**kg m^{-3}**
Settling velocity, $\mathbf{w_s}$	**0.0025**	**m/s**
Roughness height	**0.000550**	**m**
Reference height	**0.000275**	**m**
Von Karman constant, **κ**	**0.4**	
Shear velocity, $\mathbf{u_*}$	**0.0086**	**m/s**
Flow height, **H**	**0.0284**	**m**

[1] Particle diameter, particle density, and flow height in Table 2, were experimental data proposed by Kaftori et al. (1995).

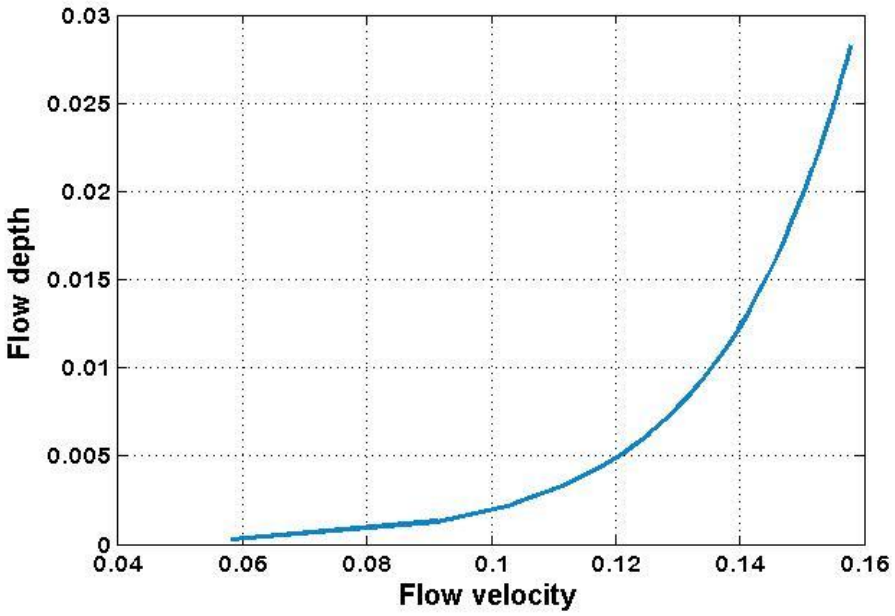

Figure 25. Flow velocity versus flow depth. (RM-2D)

Table 13. Model parameters (RM-2D)

Parameters	**value**	**units**
Time step, Δt	**1**	**s**
Simulation time **T**	**30**	**s**
Control volume size, **L**	**2**	**m**
Runs	**10000**	

Simulation Results

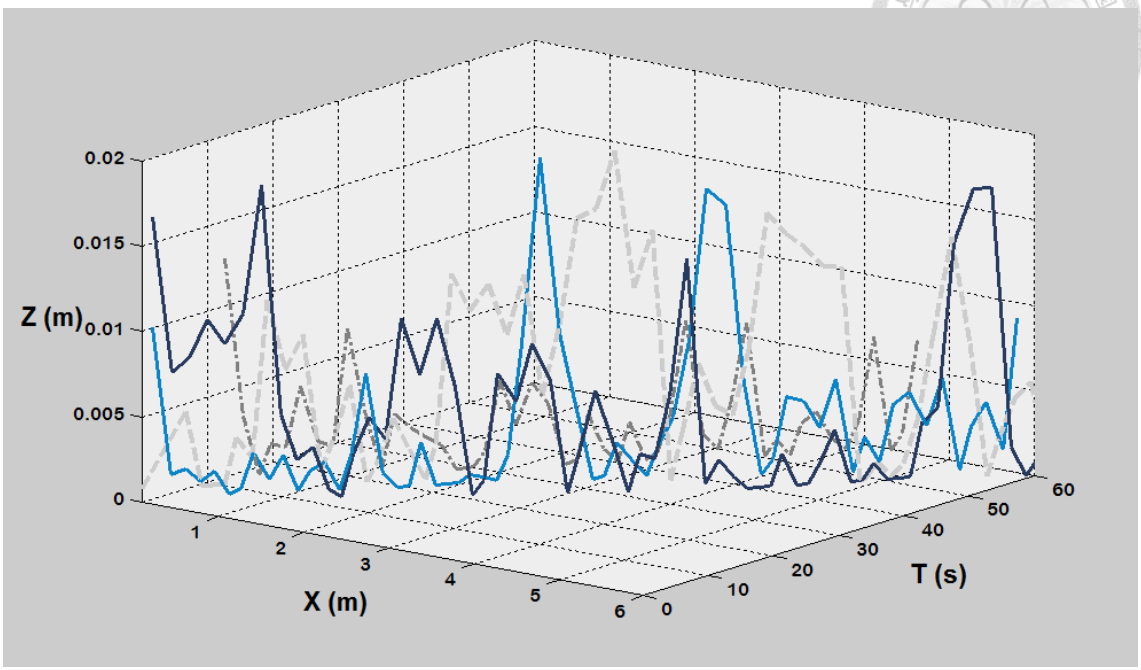

Figure 26. Schematic diagram of some particle trajectories. (RM-2D)

Four particles trajectories $(x(t), z(t))$ in a scenario were drawn in Figure 26 and Figure 27 in order to simply offer an idea about the particle motion in the control volume. Figure 27 offers different views of particles trajectories. X-T plane delivers the idea that particles would arrive at the control volume continuously along with time and the number of particles could be different. Z-T plane shows the particle positions resulting from deposition and the resuspension of sediment particles.

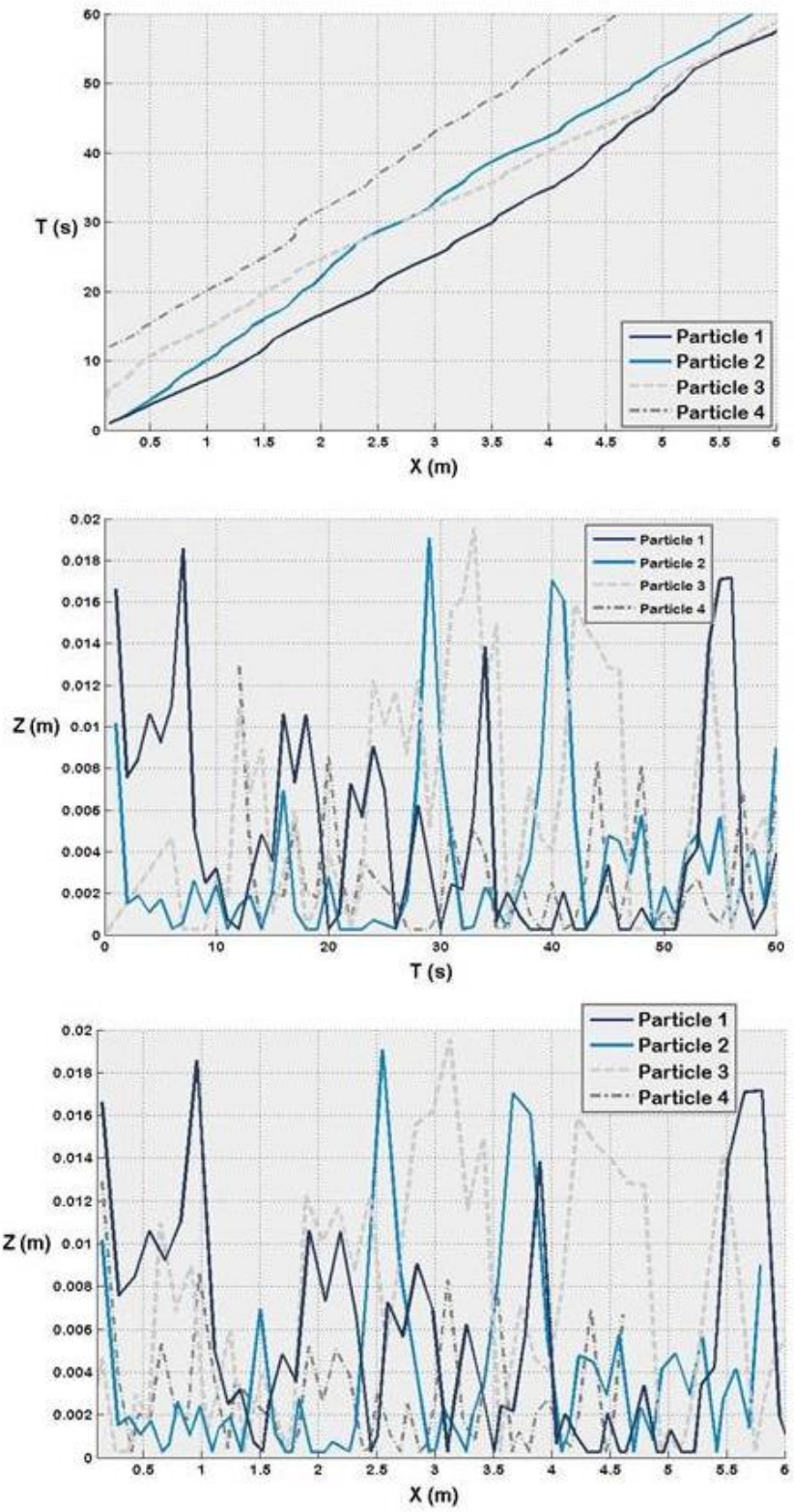

Figure 27. Schematic diagram of some particle trajectories in X-T plane, X-Z plane and Z-T plane respectively. (RM-2D)

Table 14. Results. (RM-2D)

Results (at steady state)	**value**	**units**
Concentration N	**71.800**	**bead/meter**
Concentration N_m	**17.308**	**bead/meter**
Concentration N_d	**89.108**	**bead/meter**
Arrival rate, $\boldsymbol{\lambda}$	**10.001**	**bead/sec**
Depart rate, $\boldsymbol{\mu}$	**9.992**	**bead/sec**
Deposition rate, $\boldsymbol{\mu_d}$	**22.923**	**bead/sec**
Resuspension rate, $\boldsymbol{\lambda_s}$	**21.826**	**bead/sec**

Table 14 presents the results of this simulation including different concentrations in bead per meter and different rates of sediment particles in bead per second at a steady state.

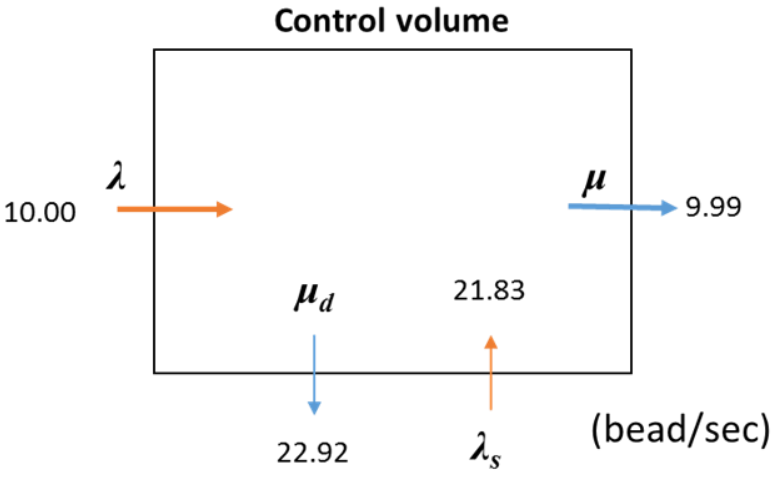

Figure 28. Simulation results. (RM-2D)

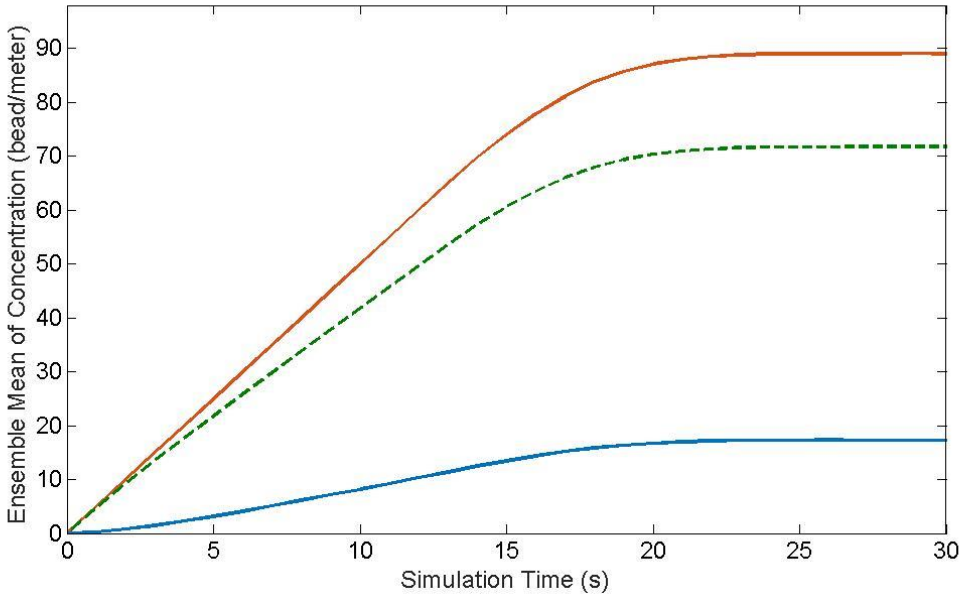

Figure 29. Ensemble mean of concentration (bead/meter). (RM-2D)

Figure 29 illustrated the ensemble means of concentration N, N_d, N_m, which represented the number of total particles, deposition particles and moving particles respectively.

All lines in Figure 29 reached an asymptotic constant, which confirmed the steady state of the system. The equilibrium of the system was a dynamic equilibrium, as shown in Figure 28 for sediment particles would continuously arrive at the control volume along with simulation time. Different from Case RM-2D (without resuspension), the number of deposition particles N_d would become steady due to resuspension of particles. As the result, the total number of sediment particles in the control volume N would become stable. Particle transport would become more uncertain due to resuspension, thus it could be found in Figure 29 that the system took more time to become equilibrium compared with Figure 21. The concentration of moving particles (N_m, green dash line) would become lager than that in Figure 21 when resuspension of particles was taken into consideration. It can be interpreted that the resuspension of sediment particles had a great

impact on the values of particle concentration. One of the reasons to explain why the resuspension process would have such a great impact on the concentration was the size of the particle. Small particles would respond to the flow and resuspend from the bed much more easily, such as the particles in the simulation whose density was slightly heavier than water.

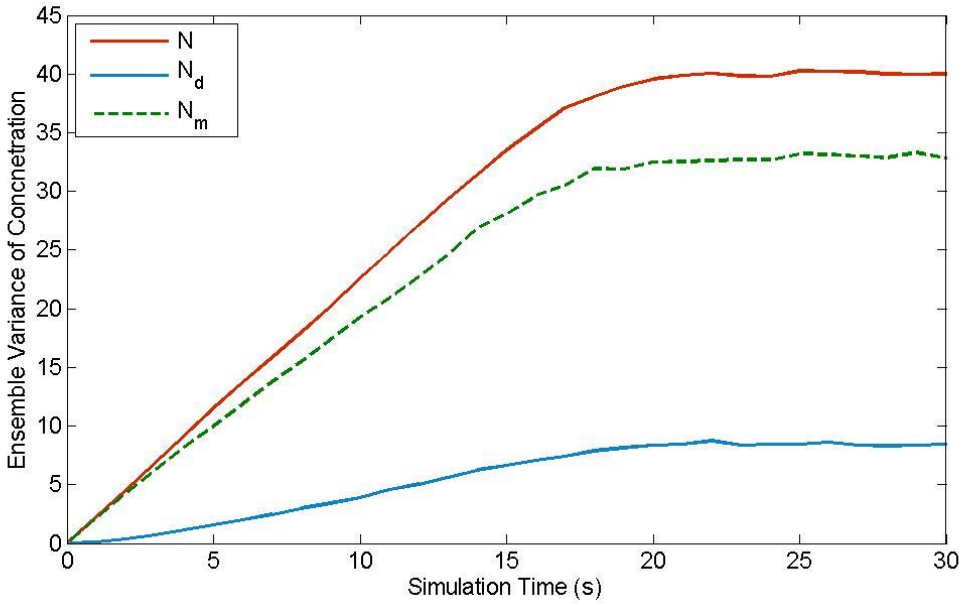

Figure 30. Ensemble variance of concentration. (RM-2D)

Figure 30 shows the ensemble variances of three kinds of concentrations, N, N_d, N_m. The fluctuations of the ensemble variances were caused by the randomness of three random variables (random magnitude of arrivals, Brownian motion and random instantaneous velocity). The values of ensemble variances of N_m in Figure 30 were higher than those in Figure 22 due to the randomness of resuspension.

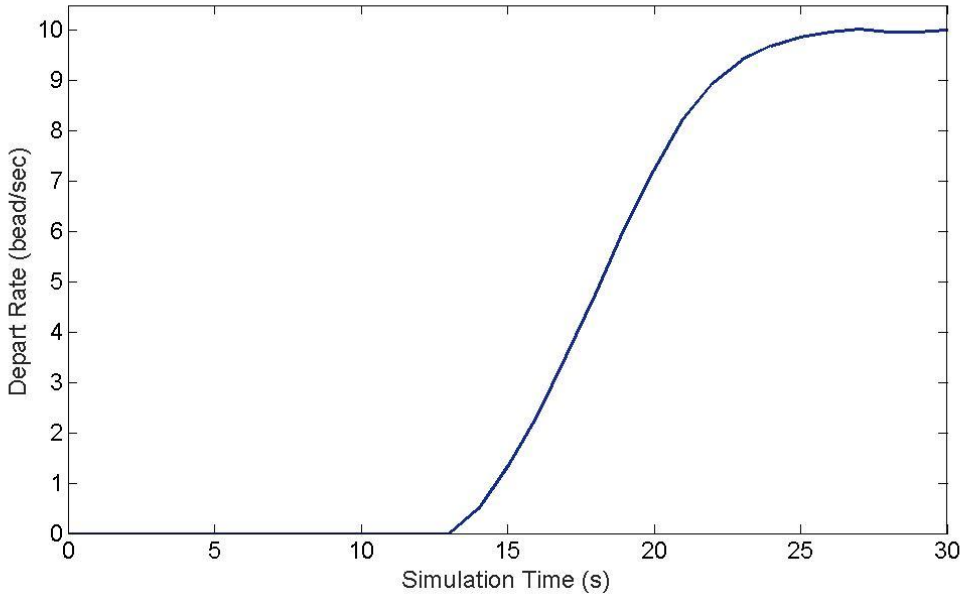

Figure 31. Depart rate of sediment particles (bead/sec). (RM-2D)

Depart rates of sediment particles were shown in Figure 31. While the size of the control volume was the same as the Case RM-2D (without resuspension), the S shape was wider and smoother. It revealed that the system took longer time to reach equilibrium. At the time when system became equilibrium, depart rate was equal to the incoming rate of sediment particles which was 25 seconds in this case. The continuation of the time whose values of depart rate was zero at the beginning of the simulation could represents the ensemble mean time for a sediment particle transporting through the control volume. In this case, the ensemble mean of particle velocity was 0.1538 m/s while in the experiments of Kaftori et al. (1995), particle velocity was 0.143. The larger value might be due to a lack of considering the interaction between sediment particles.

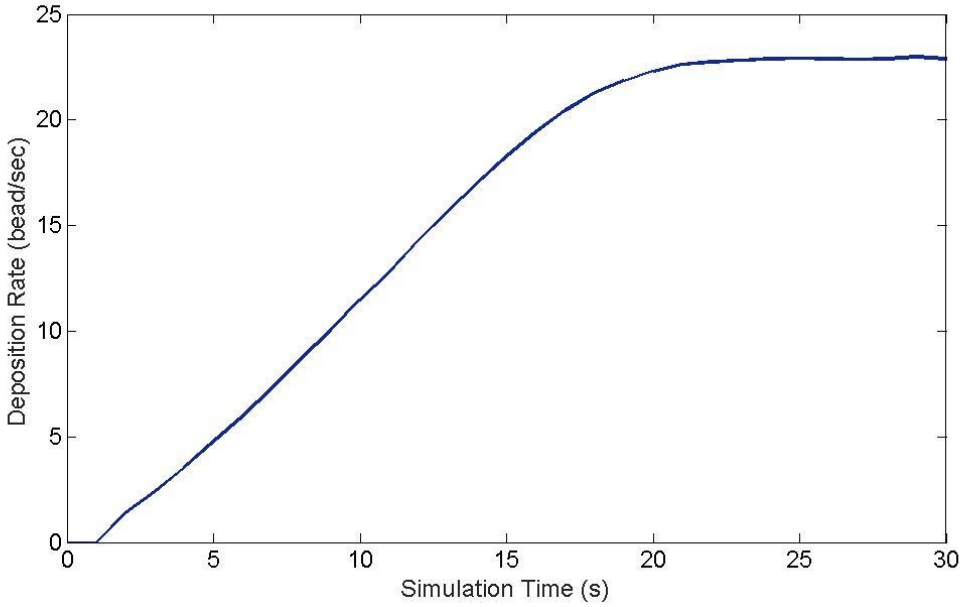

Figure 32. Deposition rate of sediment particles (bead/sec). (RM-2D)

Deposition rate and resuspension rates of sediment particles were illustrated in Figure 32 and Figure 33 respectively. The deposition rates and resuspension rates all become stable when the system became steady. It could be seen more clearly when the graphs of these two rates were put together in Figure 34.

At the beginning of simulation, the values of deposition and resuspension rates were zero for a short time and then increased until reaching a stable value. In other words, at the beginning, sediment particles all transported in the water, after some time, some of them would deposit, which was the time when the resuspension happened. However, Figure 34 shows the values of deposition rate and resuspension were different by one bead. It would be a very unusual situation when the system was in a dynamic equilibrium, the arrival rate and the depart rate were almost the same, the values of concentrations stayed constants, yet the deposition rate was not equal to the resuspension rate. If the values of deposition and resuspension rates were truly different, the number of deposition

particles should have changed. In other words, the values of deposition rate and resuspension rates did not match with the concentration results. The discussions of this question were presented in the next section.

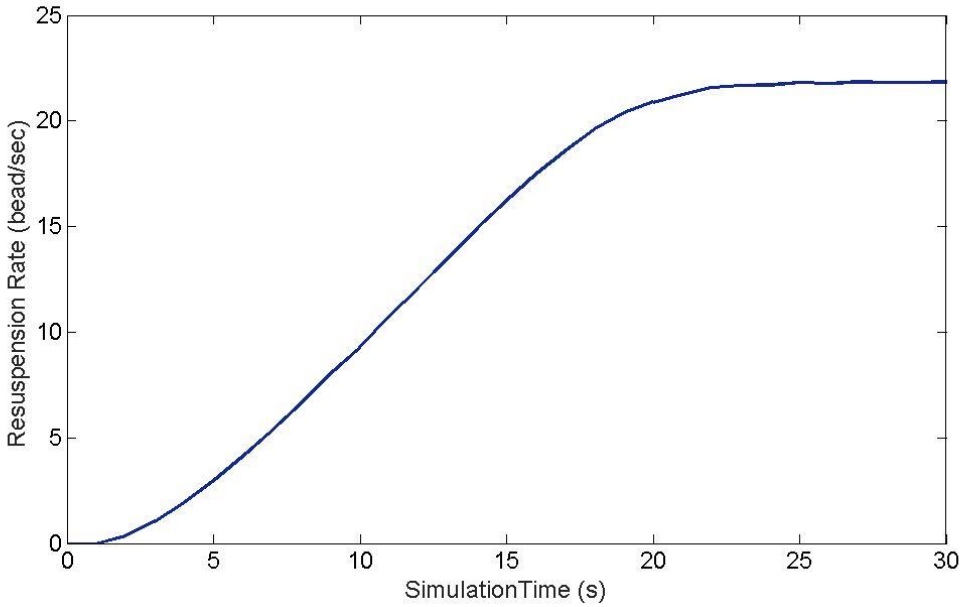

Figure 33. Resuspension rate of sediment particles (bead/sec). (RM-2D)

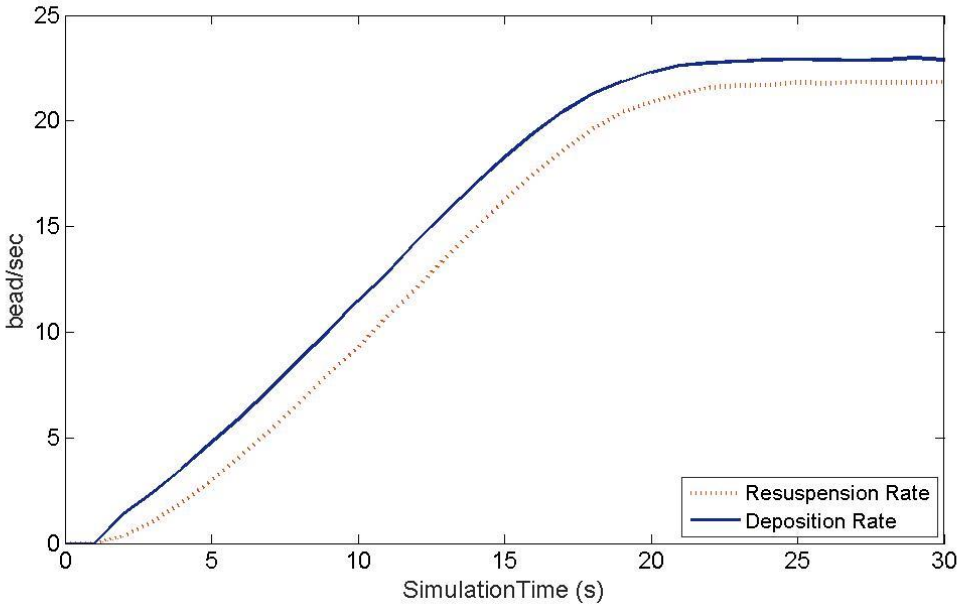

Figure 34. Deposition and resuspension rate of sediment particles (bead/sec). (RM-2D)

Selection of Time Step

The size of the time step plays an important role in this simulation, especially for the SD-PTM. Figure 35 would deliver the idea more clearly. The small grids in Figure 35 denote the timescale equal to 0.05, while the interval time between blue lines is one second. If the time scale is 0.05 second, in the one second labeled in Figure 35, the particle has been through two depositions and two resuspensions. If the time scale is one second, trajectory of the particle shows that it does not deposit nor resuspend. It corresponds to the idea that the smaller the time step, the more the details revealed in the results. Based on this concept, Case RM-2D was simulated again. This time, the size of the time step was selected as 0.1 second. Compared with Figure 34, the trends of deposition and resuspension rates are overlapping with each other in Figure 36. However, the values of deposition rate and resuspension rates of the simulation with time step equal to 0.1 second are much larger than that of simulation with time step equal to 1 second.

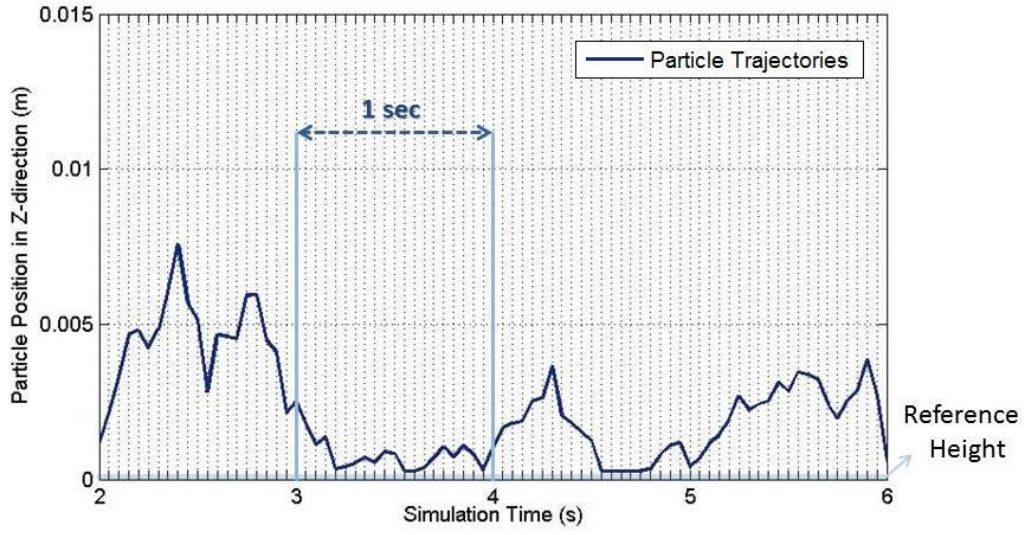

Figure 35. Illustration of the influence of different time steps

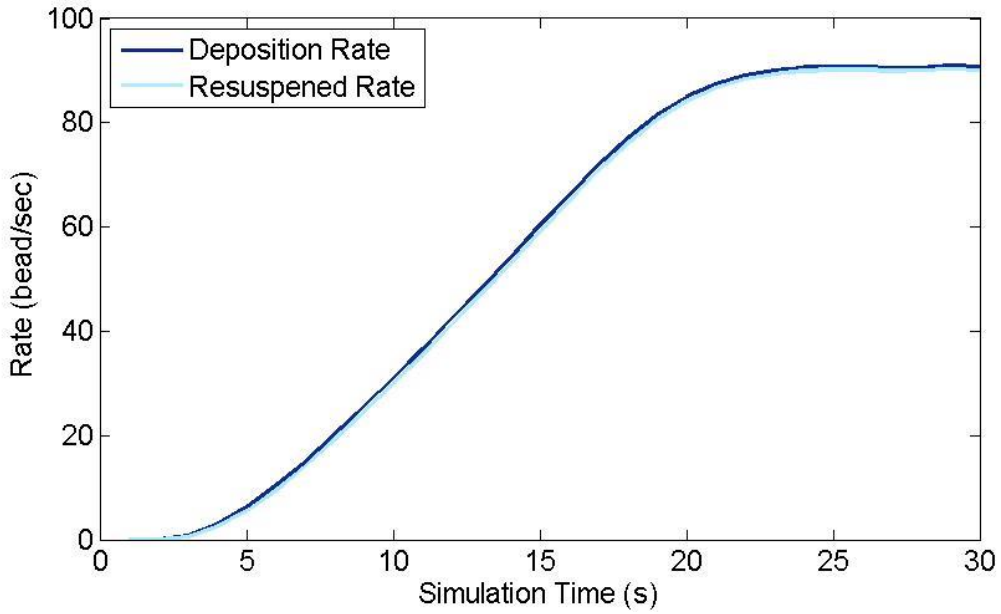

Figure 36. Deposition rate and resuspension rate of sediment particles when time step is equal to 0.1 seconds.

Table 15. Comparison of results of simulations with different time scales.

dt	$\boldsymbol{\mu_d}$ (bead/sec)	$\boldsymbol{\lambda_s}$ (bead/sec)	$\boldsymbol{\mu}$ (bead/sec)	**N** (bead/meter)	$\mathbf{N_d}$ (bead/meter)
0.05	135.18	134.72	10.00	88.94	6.85
0.1	90.68	90.09	10.01	89.54	8.80
1	22.90	21.80	10.00	89.00	17.28

Regarding the deposition number of particles, Table 15 lists the results of simulations with different time steps. $\boldsymbol{\mu}$, $\boldsymbol{\mu_d}$ and $\boldsymbol{\lambda_s}$ denote the depart, deposition and resuspension rates of the sediment particles in the unit of bead per second. N_d and N represent the number of deposition particles and the total particles in the control volume in the unit of bead per meter. The results in Table 15 were means of the equilibrium value. In other words, we calculated the ensemble means of $\boldsymbol{\mu}$, $\boldsymbol{\mu_d}$, $\boldsymbol{\lambda_s}$, N_d and N when the system became steady.

Values in the first and second columns show that the smaller time step, more details about particle movement would show. The fourth column represents the total number of particles in the control volume when the system was steady. The values in the third and fourth column revealed that different time scales would not affect the depart rates and the total amounts of particles in the control volume. However, the last column shows that the number of deposition particles would be different due to the influence of different time scale. It could be found that when the time step was smaller, the number of deposited particles would be smaller. One of the primary reasons is the influence of the turbulence term in SD-PTM ($\Delta B_t = \sqrt{\Delta t} N(0,1)$). If the time step becomes larger, in each time step, the effect of turbulence term, Brownian motion, would be proportionally enlarged. Therefore, if the sizes of the particles are small and the particles transport close to the bed like the simulations, particles would tend to deposit due to the assumption of the deposition that when the particle position in the Z-direction is smaller or equal to the reference height. Compared with them, the value of N_d with a time step equal to one second was lager. Yet, the numbers of deposited particles in Table 15 with the time step equal to 0.1 and 0.05 were at the same order. These results suggest that the timescale should be smaller than one second in our study. In the next simulations, the time step was all determined to be 0.1 second. In sum, choosing an appropriate time scale is an important subject for the simulation, the balance between theoretical accuracy and computational efficiency depends mostly on time scale.

Summary

In the simulation, random number of particles arriving at the control volume along with time. The random variables were generated by the binominal distribution B(100,0.1) with the time step dt = 1 second. Sediment transport equations composed of the stochastic diffusion particle tracking model (Man and Tsai 2007) and particle resuspension (Wu and Lin, 2002) were applied to portray particle trajectories affected by suspension, deposition and resuspension. Resuspension of particles was involved by assuming instantaneous velocity approaching the particle on the bed as a log normally distributed random variables (Wu and Lin, 2002). Consequently, there were three random variables in the RM-2D simulation, the number of incoming sediment particles, turbulence term in SD-PTM and the instantaneous velocities approaching on particles. The flow conditions and particle parameters applied were proposed by Kaftori et al. (1995). The results shows that the depart rate was consistent with the incoming rate. Results also revealed that resuspension played an important role in the concentration of moving sediment particles in the control volume. The number of deposition/resuspension particles and the difference between deposition and resuspension rates resulted from the size of the time step. Use of a smaller time step would reveal more details about particle motions while use of a the larger time step would lead to more significant particle deposition due to the enlarged turbulence term in SD-PTM.

Chapter 5 Random Arrivals (RA) Simulated by Poisson Process

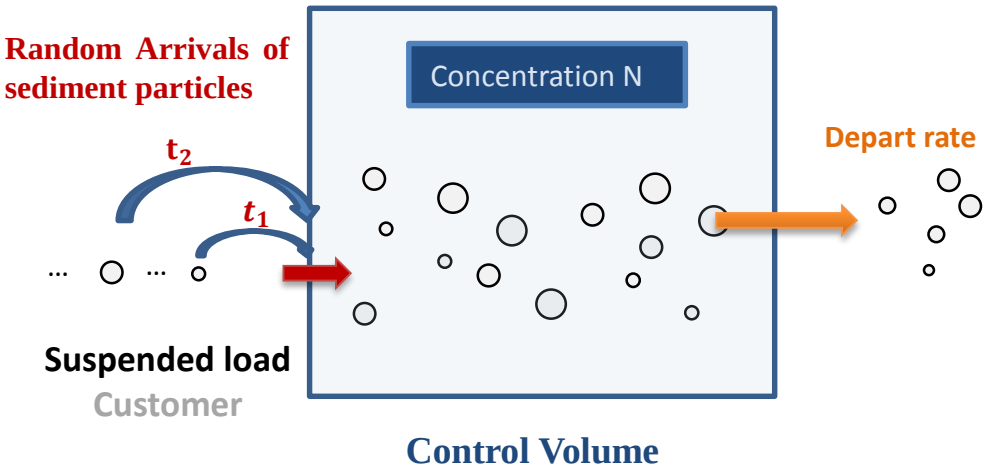

Figure 37. Illustration of random arrivals of incoming sediment particles.

5.1 Introduction

In this section, sediment particles arrive at the control volume in a random manner. The inter-arrival times are assumed to be exponentially distributed random variables. Then the numbers of events which are the arrivals of sediment particles are random variables of a Poisson distribution. In other words, the random arrivals of particles are governed by Poisson process $N(t)$. In the study, $N(t)$ denotes the "state" which is the number of the incoming sediment particles in the control volume at time *t*. In a continuous-time BMAP, if there is only one state m=1 in the state space *E*, the time between arrivals is exponentially distributed and for each arrival, the batch size is equal to 1, then the counting process$\{\mathrm{N(t)}, \mathrm{t} \geq 0\}$ is a Poisson process.

This case is actually the application to the M/G/1 process in queueing theory. In this case, we intend to observe the variation of concentrations and the depart rate of sediment

particles. The concentration in this case is defined as the number of moving sediment particles (beads) in the control volume. In addition, the steady state is defined as the situation where the number of sediment particles in the control volume becomes a constant **n**. Then the condition that the depart rate plus the deposition rate are equal to the incoming rate plus the resuspension rate can be proved. Herein, the depart rate is calculated by comparing the previous particle position and the instant particle position in the X-direction. For instance, if particle position X_n at time $t = n$ is larger than the length of the control volume L, and if particle position at time $t = n - 1$, X_{n-1}, is smaller than L, then it is certain that the particle has just left the control volume at time t_n. The depart rate is the number of sediment particles having left the control volume in the unit of bead per second. The deposition rate is calculated by comparing the present and previous particle position in the Z-direction. When Z_n is equal to Z_0 (reference height) and Z_{n-1} is higher than the reference height, the deposition rate in the unit of bead per second can be calculated. The resuspension rate is calculated based on the opposite condition of the deposition rate ($\mathbf{Z_n > Z_0 \mid Z_{n-1} = Z_0}$).

5.2 Assumptions

There are two assumptions in these simulations. The first one is that there are no correlations among sediment particles or between fluid particles and sediment particles. The other assumption is that the probabilistic characteristics of random arrivals of incoming sediment particles can be simulated by the Poisson process.

5.3 Procedure

(1). Apply Poisson process to generate a series of random numbers of event occurrences. It is noteworthy that each event (arrival) contains one sediment particle.

(2). Apply the stochastic particle tracking model to simulate the particle trajectories.

(3). Calculate the concentrations and transport rates by comparing the particle position according to the criteria listed in Table 16 and Table 17.

(4). Repeat (1) to (3) and calculate the ensemble means and variances.

Table 16. Conditions for concentrations.

Concentration (bead/meter)	Condition
Total number $\mathbf{N}$	$\boldsymbol{X}_{\mathrm{n}} \leq \mathrm{L} \mid \boldsymbol{X}_{\mathrm{n}} > 0$
Deposition $\mathbf{N_d}$	$\boldsymbol{Z}_{\mathrm{n}} = \boldsymbol{Z}_0 \mid \boldsymbol{X}_{\mathrm{n}} \leq \mathrm{L}_{\mathrm{CV}}$ & $\boldsymbol{X}_{\mathrm{n}} > 0$
Moving $\mathbf{N_m}$	$\mathbf{N} - \mathbf{N_d}$

Table 17. Conditions for transport rates.

Transport rates (bead/sec)	Condition
Depart Rate	$\mathbf{X}_{\mathrm{n}} > \mathrm{L} \mid \mathbf{X}_{\mathrm{n-1}} \leq \mathrm{L}$
Deposition Rate	$\mathbf{Z}_{\mathrm{n}} = \mathbf{Z}_0 \mid \mathbf{Z}_{\mathrm{n-1}} > \mathbf{Z}_0$
Resuspension Rate	$\mathbf{Z}_{\mathrm{n}} > \mathbf{Z}_0 \mid \mathbf{Z}_{\mathrm{n-1}} = \mathbf{Z}_0$

5.4 Simulations

5.4.1 RA-2D

Introduction

In the simulation, the objective is to see particle transport patterns when the particles arrive at the control volume randomly. Figure 38 illustrates the random arrivals of sediment particles. The inter-arrival times $\mathrm{t_i}$ are random variables of an exponential distribution with mean $1/\lambda$. In other words, the numbers of events in each time step are

random variables of the Poisson distribution with λ. The setting of this simulation is shown in Table 18. Particles in this simulation would suspend and deposit according to SD-PTM (Man and Tsai, 2007). After depositing on the reference height, whether particles would resuspend or not depends on the threshold proposed by Wu and Lin (2002). In this simulation, the particle parameters and flow conditions are from experimental data proposed by Kaftori et al. (1995) are listed in Table 19. The flow velocities are calculated based on the corresponding logarithmic velocity profile, $\overline{U} = (u_*/\kappa)\, ln(z/z_0)$, as shown in Figure 39. The time step is 0.1 second in this simulation and other model parameters are shown in Table 20. The random arrivals were simulated by Poisson process with a constant rate $\lambda = 10$ beads per second.

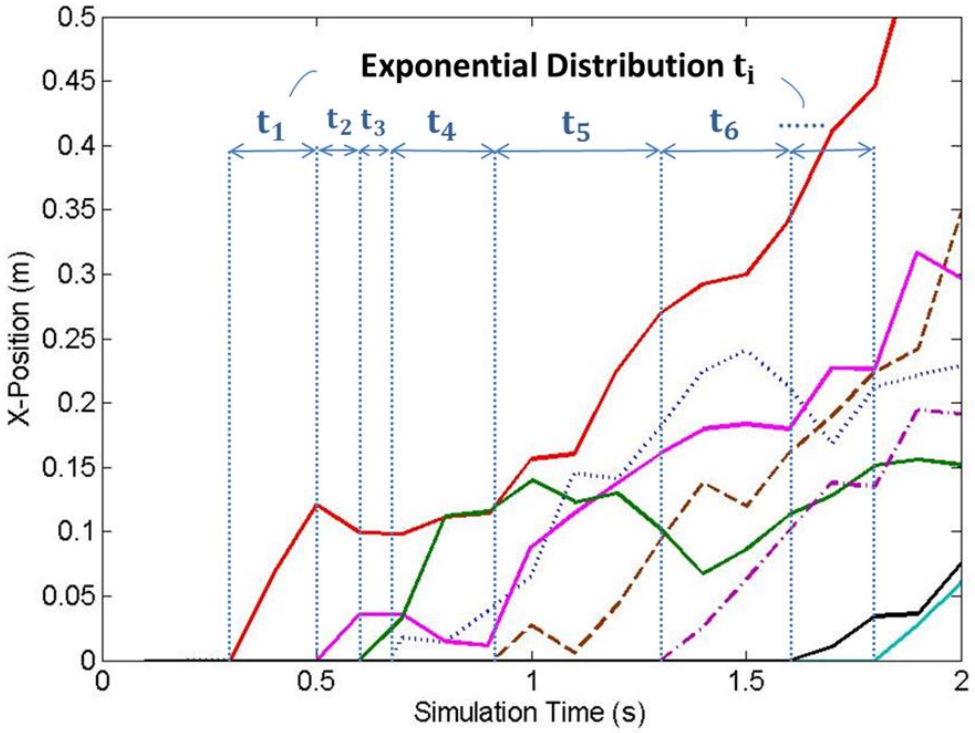

Figure 38. Particle trajectory along time in X-direction. (RA-2D)

Table 18. Comparison table of case RA-2D with queue

Queue	**Case RM-2D-resuspension**
Store	Control volume
Customer	Particles with diameter 2.75 mm
Server	Suspension/**Deposition/Resuspension**
Service (Mechanics of sediment transport)	**Governing Equation** : **1. SD-PTM (Man and Tsai, 2007)** Mean drift + Brownian motion $\boldsymbol{X}_{n+1} = \boldsymbol{X}_n + u_*/\kappa \ \ln(\boldsymbol{Z_n}/\boldsymbol{Z}_0)$ $\boldsymbol{Z}_{n+1} = \boldsymbol{Z}_n + (\overline{W_n} - w_s + \kappa u_* - 2\kappa u_* \boldsymbol{Z_n}/H)\Delta t + \sqrt{2(\kappa u_* \boldsymbol{Z_n}(1 - \boldsymbol{Z_n}/H))}\Delta \boldsymbol{B}_t$ **2. Resuspension threshold (Wu and Lin, 2002)** $v_b \geq ln\left(\sqrt{4d(\rho_s - \rho)g/(3\rho C_L)}\right)$

Table 19. Flow conditions and particle parameters. (RA-2D)

Variables	**value**	**units**
Particle diameter, **D**	**275**	**μm**
Particle density, $\boldsymbol{\rho_p}$	**1050**	**kg m^{-3}**
Flow density, $\boldsymbol{\rho_f}$	**1000**	**kg m^{-3}**
Settling velocity, $\mathbf{w_s}$	**0.0025**	**m/s**
Roughness height	**0.000550**	**m**
Reference height	**0.000275**	**m**
Von Karman constant, **κ**	**0.4**	
Shear velocity, $\mathbf{u_*}$	**0.0086**	**m/s**
Flow height, **H**	**0.0284**	**m**

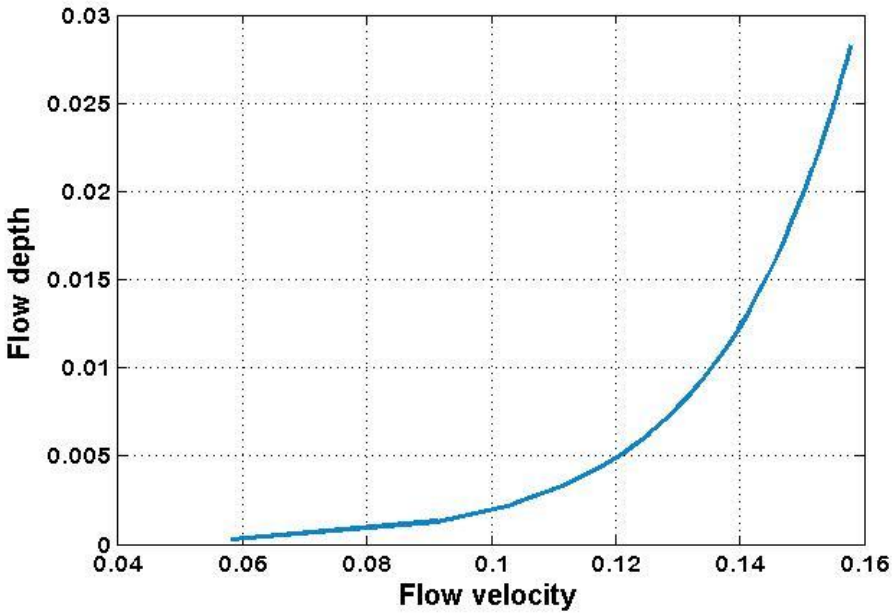

Figure 39. Flow velocity versus flow depth. (RA-2D)

Table 20. Model Parameters (RA-2D)

Parameters	**value**	**units**
Time step, Δt	**0.1**	**s**
Simulation time **T**	**30**	**s**
Control volume size in X-direction	**2**	**m**
Runs	**10000**	

Simulation Results

Table 21 presents simulation results when the system is in equilibrium. Results included different concentrations and different rates in the unit of beads per meter and bead per second respectively.

Table 21. Results. (RA-2D)

Results (at steady state)	**value**	**units**
Concentration N	**89.49**	**bead/meter**
Concentration N_m	**80.68**	**bead/meter**
Concentration N_d	**8.81**	**bead/meter**
Arrival rate, $\boldsymbol{\lambda}$	**10.01**	**bead/sec**
Depart rate, $\boldsymbol{\mu}$	**10.01**	**bead/sec**
Deposition rate, $\boldsymbol{\mu_d}$	**90.73**	**bead/sec**
Resuspension rate, $\boldsymbol{\lambda_s}$	**90.16**	**bead/sec**

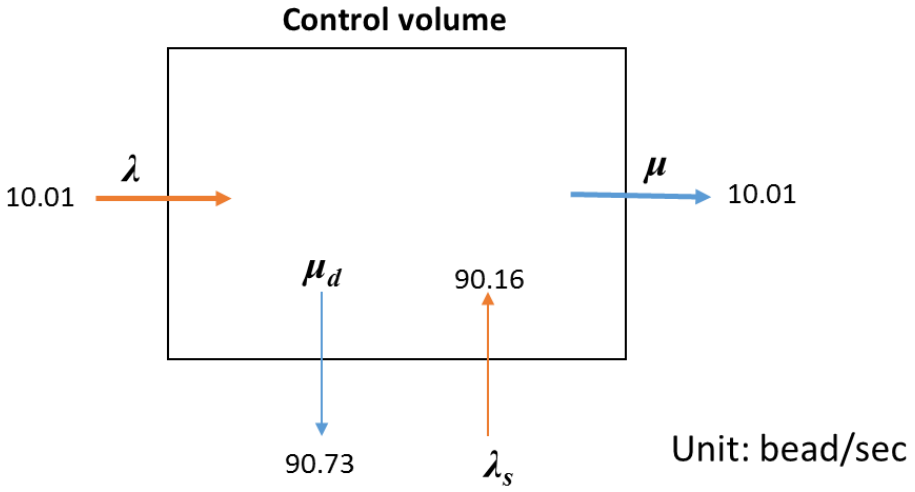

Figure 40. Simulation results. (RA-2D)

Figure 40 schemes the steady results in the system. The arrival and depart rates were the same and inside the control volume the exchange rates of particles were almost equal to each other. Based on Figure 40, the dynamic equilibrium could be confirmed.

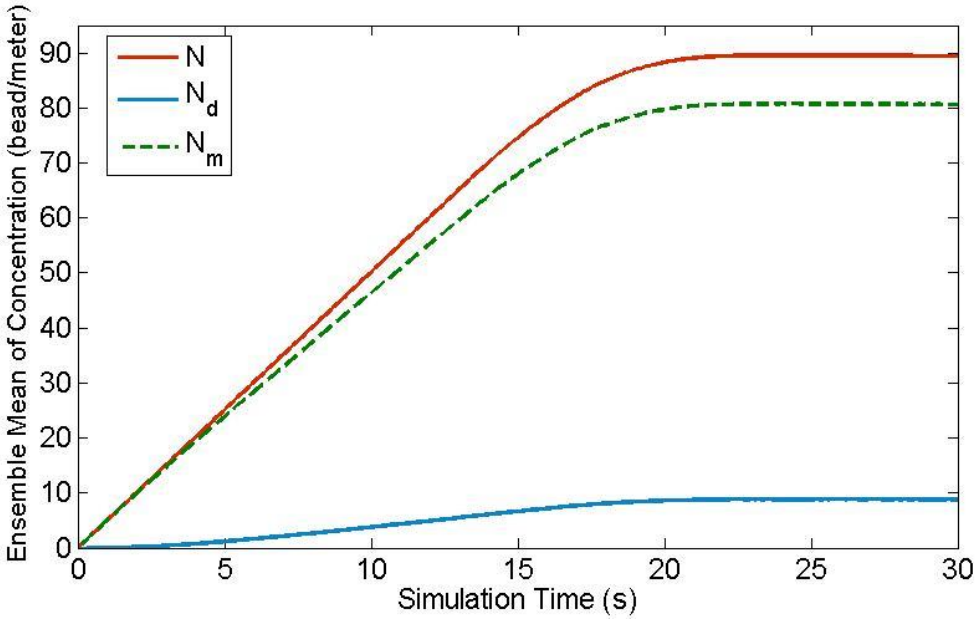

Figure 41. Ensemble mean of concentration (bead/meter). (RA-2D)

The ensemble means of concentrations N, N_d, N_m are shown in Figure 41. Concentrations increased at the beginning of the simulations. The increase can be attributable to the initial condition when the control volume was empty before the simulation. Therefore after the particles started to be released into the control volume, the concentrations would increase. As the particles started to deposit shown in Figure 44, the number of deposition particles started to grow. While the depart rate plus the deposition rate were equal to the arrival rate plus the resuspension rate, that is the time for the system to become steady. According to the simulation results, the time to equilibrium was 23 second in the simulation.

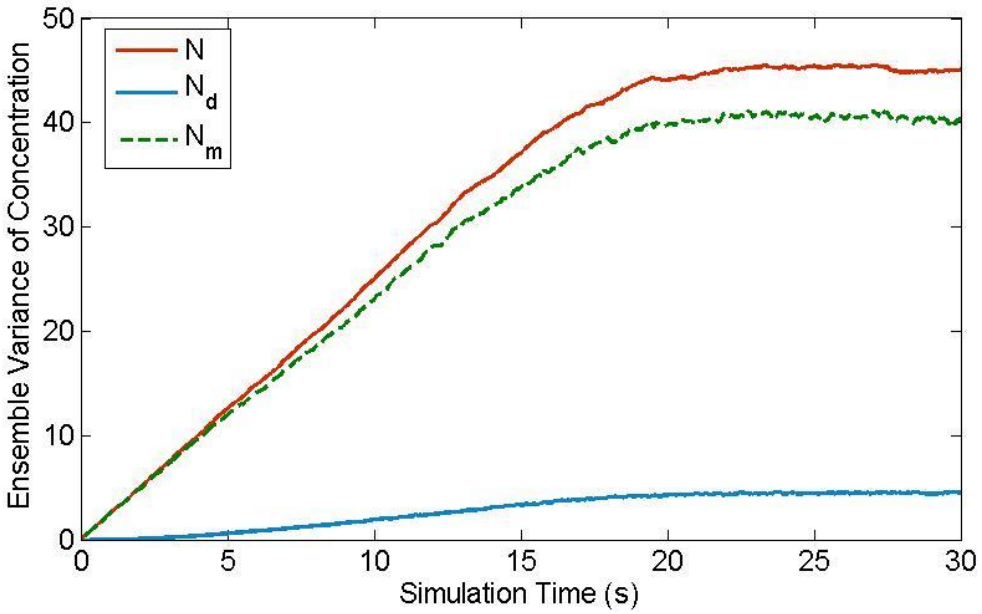

Figure 42. Ensemble variance of concentration (bead/meter). (RA-2D)

The Ensemble variances of concentration $\mathrm{N}, \mathrm{N_d}, N_m$ are presented in Figure 42. The ensemble variances show that the variations of the scenario results would grow along with the simulation time until the system became steady, then the variances became nearly constants for $\mathrm{N}, \mathrm{N_d}, \mathrm{N_m}$. The number of small fluctuations might become fewer when the number of scenarios in one simulation increase.

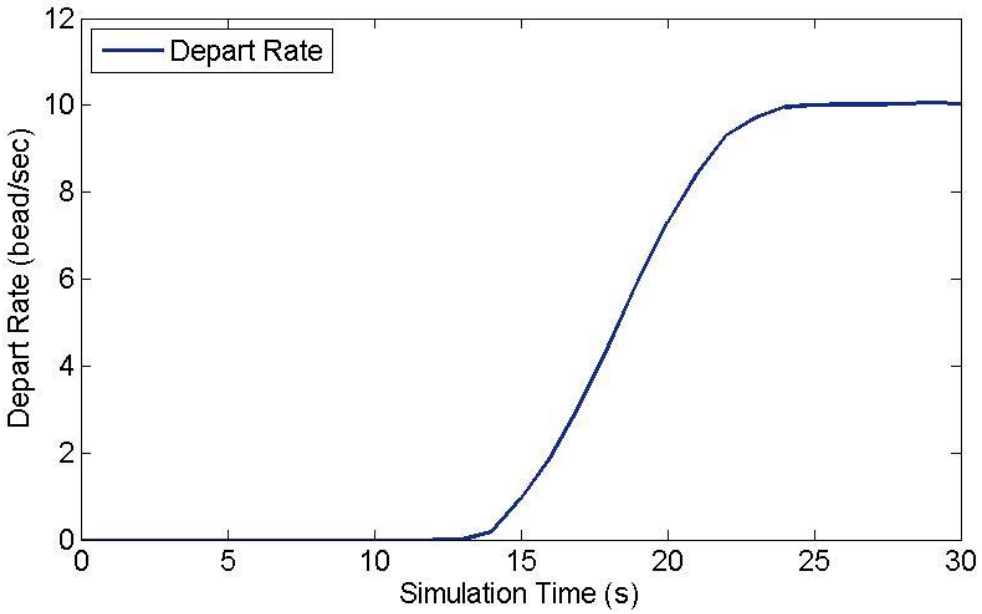

Figure 43. Depart rate of particles (bead/sec). (RA-2D)

Depart rates of particles along with simulation time were shown in Figure 43. The average time for particles transport through the control volume results in the zero values at the beginning of simulation. The ensemble mean of particle velocity was 0.153 m/s. A lack of taking the correlation between particles into consideration might result in larger particle velocity compared with experimental data (0.143 m/s) proposed by Kaftori et al. (1995). The depart rates were almost equal to arrival rates when the system became equilibrium.

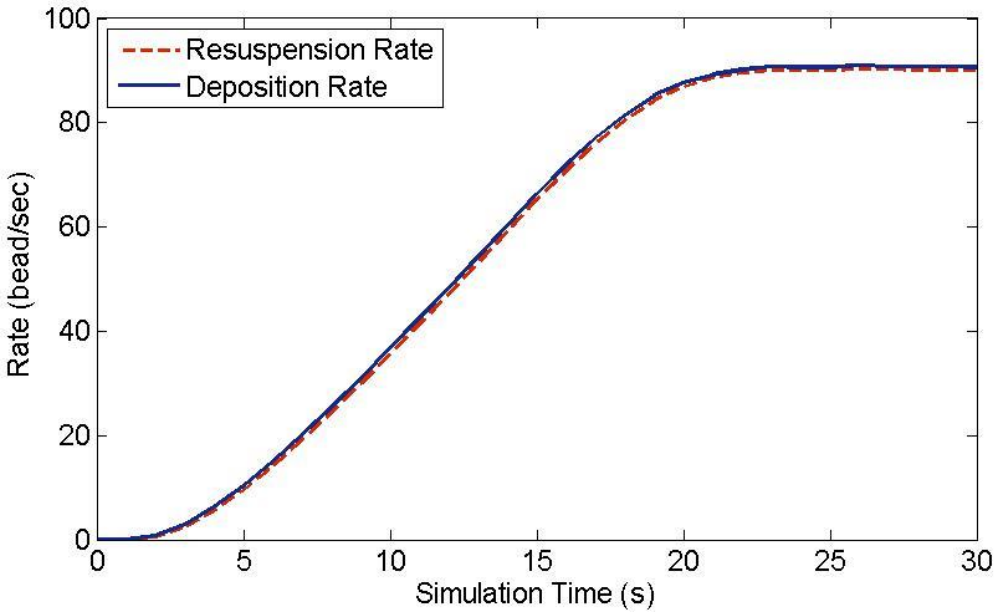

Figure 44. Deposition and resuspension rate of sediment particles (bead/sec). (RA-2D)

The curves of deposition and resuspension rates are given in Figure 44. The deposition rates are always a little higher than the resuspension rates along with simulation time. It might be due to the fact that there must be a deposition first before the suspension can occur. In the simulation, there were no particles on the bed before the simulation. The particles that had just deposited on the bed might resuspend or stay stationary on the bed for a short period of time. As a result, the resuspension rates would be smaller than the deposition rates. (Particle density applied in the simulation was 1050 kg m^{-3}, which was light and could easily respond to flow. Results showed that particles would resuspend in a short period of time after it had deposited on the reference height.)

Comparison RA-2D with RM-2D

In this section, simulation results of random magnitude (RM-2D) and random arrival case (RA-2D) were compared. For the random magnitude case, in each time step, there was one event (arrival) consisting of random particles according to a binominal distribution B(100, 0.1). As to the random arrival case, particles arriving at the control volume randomly with a constant Poisson rate λ =10 events per second. There would be only one particle in each arrival (event). The flow conditions, particle parameters and the model parameters were the same for both simulations. The time step was 0.1 second. Table 22 lists the comparison ensemble results when the systems were both steady. For both two cases, there were ten particles arriving at the control volume in average. Table 22 shows that there is not much difference in the ensemble means of results between the random magnitude case and random arrival case when the mean arrival rate was the same (10 beads per second). However, refer to ensemble variances; the values of $\boldsymbol{\mu_d}$, $\boldsymbol{\lambda_s}$, $\boldsymbol{\mu}$, **N**, $\mathbf{N_d}$ of RA were all higher than those of RM (see Table 23). The results indicated that the random arrival case can bring more uncertainty compared to the random magnitude case.

Table 22. Comparison ensemble means between RA-2D and RM-2D.

Case	$\boldsymbol{\mu_d}$ (bead/sec)	$\boldsymbol{\lambda_s}$ (bead/sec)	$\boldsymbol{\mu}$ (bead/sec)	**N** (bead/meter)	$\mathbf{N_d}$ (bead/meter)
RM	90.68	90.09	10.00	89.54	8.80
RA	90.73	90.16	10.01	89.49	8.81

Table 23. Comparison ensemble variances between RA-2D and RM-2D.

Case	μ_d (bead/sec)	λ_s (bead/sec)	μ (bead/sec)	N (bead/meter)	N_d (bead/meter)
RM	172.92	172.21	9.99	44.69	4.41
RA	179.00	177.78	10.08	45.10	4.47

Summary

In this simulation, particles arriving at the control volume according to a constant Poisson rate λ =10 events per second. The experimental data proposed by Kaftori et al. (1995) were applied as the flow conditions and particles parameters. Particles in the control volume would transport based on the SD-PTM (Man and Tsai, 2007). If particles had deposited on the bed, they might resuspend or keep staying stationary on the bed depending on the pickup probability proposed by Wu and Lin (2002). The random variables in this case were the particle interarrival time, turbulence term in SD-PTM and the instantaneous velocities approaching on the particles. The same values of depart rate and arrival rate confirmed the equilibrium of the system inside the control volume, the resuspension rate and deposition rate were also close to each other. The cases of the random magnitude and random arrivals were compared. The comparison shows that while there is no significant difference between these two cases shown in ensemble means of transport rates (deposition rate, resuspension rate and depart rate) and concentrations (concentration of deposition particles and total number of particles in the control volume). However, the ensemble variances of these results demonstrated the differences of these two cases and showed the incoming mechanism of random arrivals could bring more uncertainty than random magnitude case.

Chapter 6 Random-sized Batch Arrivals Simulated by Batch Poisson Process

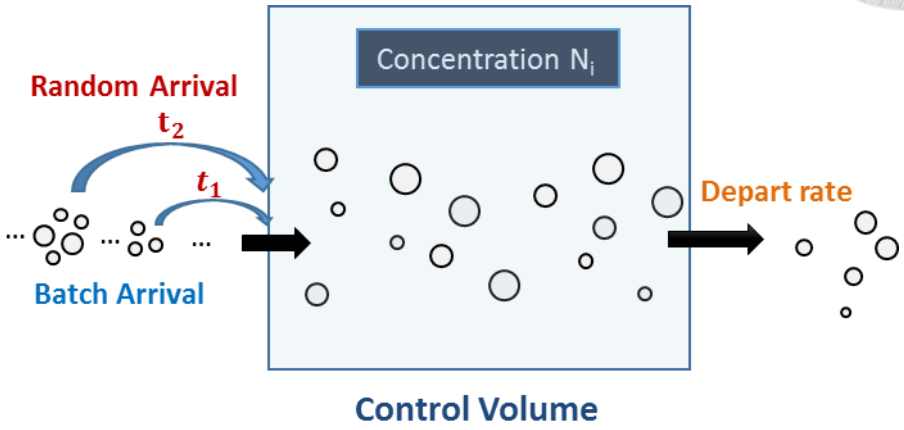

Figure 45. Illustration of random arrivals and random magnitude of incoming particles.

6.1 Introduction

In this chapter, sediment particles arrive at the control volume not only at random time but also with a random number of particles. In other words, both the random arrivals and random magnitude of incoming particles are taken into consideration in order to model the uncertain behaviors of incoming sediment particles. The case is actually the batch Poisson process in continuous time batch Markovian arrival process (Cordeiro and Kharoufeh, 2011). In BMAP, if the batch size is larger than one in the standard Poisson process with rate λ, it is a batch Poison process. Referred to Ross (2007), the arrivals occurring in accordance with a Poisson process and consisting a random number of customers are so called random-sized batch arrivals. In the study, we simply call them batch arrivals (BA). The arrivals of the sediment particles were defined as events. Based on the random arrivals, the numbers of the events were decided by Poisson process with a constant rate **λ**. The random number of sediment particles included in each event were generated by a binominal distribution **B**. Consequently, the mean total number of

incoming sediment particles was **λB**. In the perspective of BMAP, the phase process $J(t)$ was random variables of a binominal distribution and the counting process $N(t)$ was governed by the Poisson process. The theoretical mean of the batch Markovian arrival process $(N, J) \equiv \{N(t), J(t),\ t \geq 0\}$ was equal to **λB.**

The concentrations in the case are defined as the number of sediment particles divided by the length of the control volume. Moreover, the equilibrium of the system is defined as the situation that when the moving particles in the control volume become a constant. The depart rate, deposition rate and resuspension rate are calculated based on the condition listed in Table 17

6.2 Assumptions

In the simulation, the sediment particles are assumed to be no correlation between each other and fluid particles. The probabilistic characteristics of random arrivals and random numbers of incoming sediment particles could be simulated by the Poisson process and the binomial distribution respectively.

6.3 Procedure

(1). Apply Poisson process to generate a series of random numbers of the occurrences of events.

(2). Generate a series of random numbers of as the magnitude of the events according to the binomial distribution.

(3). Release different numbers of particles at different time according to the binomial distribution and Poisson process respectively.

(4). Track particle trajectories and calculate the concentrations and transport rates

(5). Repeat (1) to (4) and calculate the ensemble means and variances of particle concentrations and transport rates.

6.4 Simulations (BA-2D)

The aim of this simulation is to observe particle transport patterns while both the arrival times and the number of sediment particles are random. Figure 46 illustrates the number of events according to the random arrivals of sediment particles. The numbers of events in each time step was random variables of the Poisson distribution with $\lambda = 5$ events per second. Figure 47 shows the numbers of particles for each event along with simulation time. The random numbers of particles were generated by the binomial distribution B(100, 0.02). In average, one event would include two particles. After timing the numbers of events with the number of particles of events, one could have the numbers of particles that arrive at the control volume along with simulation time shown in Figure 48. Theoretically, the ensemble means of incoming rate of particles would be 10 beads per second.

Table 18 lists the setting of the simulation while the particles parameters and flow conditions are listed in Table 19. In this simulation, mechanics of particles included suspension, deposition and resuspension. The SD-PTM (Man and Tsai, 2007) was applied to simulate the suspension and deposition of particles in the control volume. The instantaneous velocities approaching on the particles deposited on the bed were assumed to be log-normally distributed (Wu and Lin, 2002). By comparing the lift force with the submerged weight of the particles, the resuspension threshold could be calculated to determine whether a particle would resuspend or not. Flow velocities were assumed to follow the logarithmic velocity profile, $\overline{U} = (u_*/\kappa) ln(z/z_0)$, and are shown in Figure 39. In the simulation, the time step was 0.1 second. Model parameters are listed in Table 20.

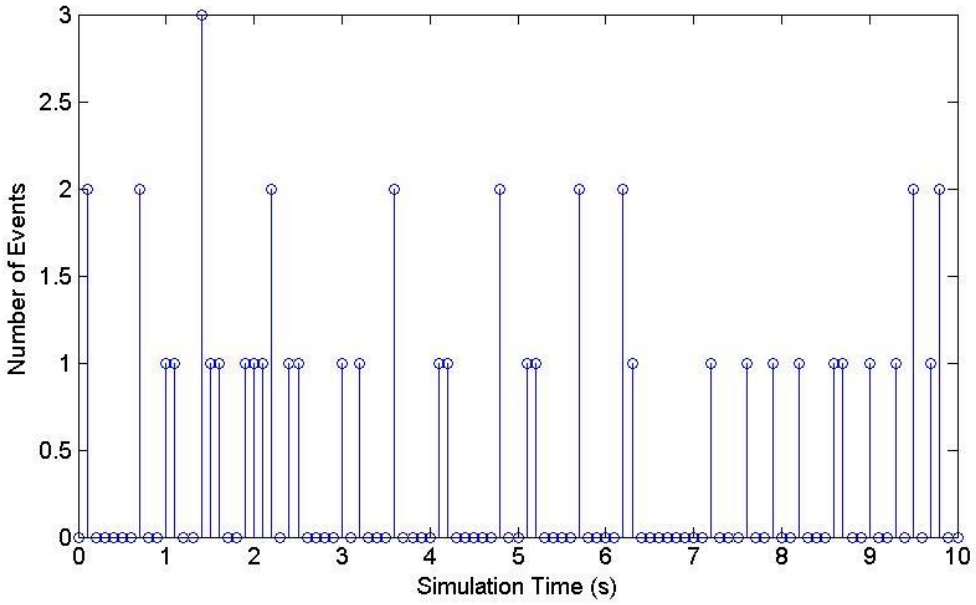

Figure 46. The number of events along with simulation time.

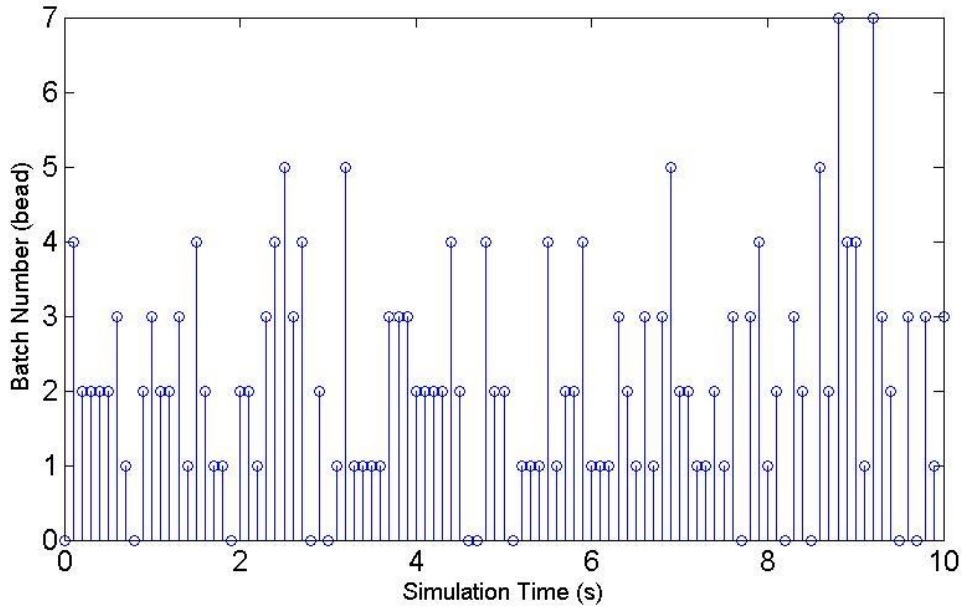

Figure 47. The amounts of particles of events along with time .

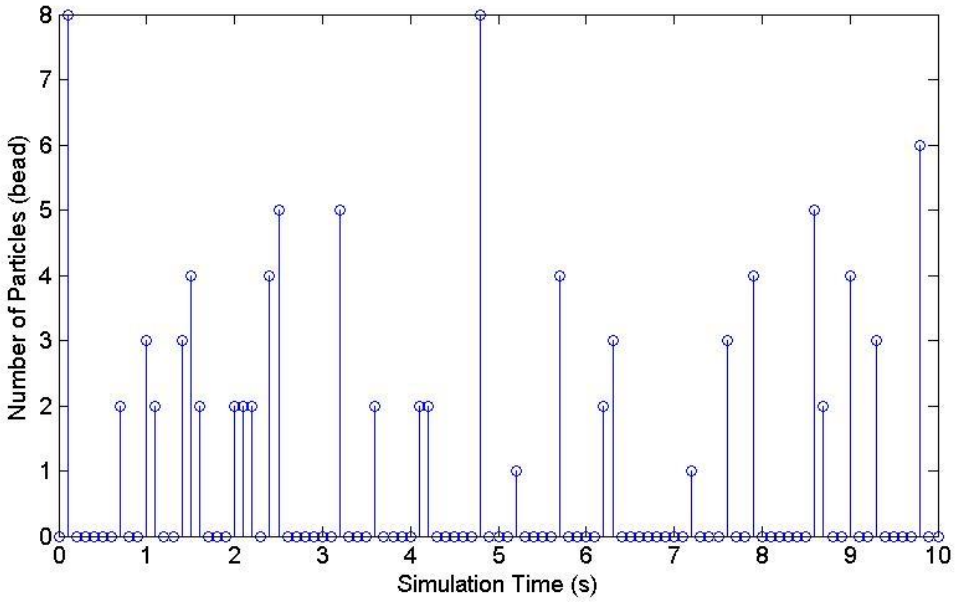

Figure 48. The number of particles arriveing at control volume versus simulation time.

Table 24. Comparison table of case BA-2D with queue

Queue	Case BA -2D
Store	Control volume
Customer	Particles with diameter 2.75 mm
Server	Suspension/**Deposition/Resuspension**
Service (Mechanics of sediment transport)	**Governing Equation** : **1. SD-PTM (Man and Tsai, 2007)** Mean drift + Brownian motion $\boldsymbol{X}_{n+1} = \boldsymbol{X}_n + u_*/\kappa \ \ln(\boldsymbol{Z_n}/\boldsymbol{Z}_0)$ $\boldsymbol{Z}_{n+1} = \boldsymbol{Z}_n + (\overline{W_n} - w_s + \kappa u_* - 2\kappa u_* \boldsymbol{Z_n}/H)\Delta t + \sqrt{2(\kappa u_* \boldsymbol{Z_n}(1 - \boldsymbol{Z_n}/H))}\Delta \boldsymbol{B}_t$ **2. Resuspension threshold (Wu and Lin, 2002)** $v_b \geq ln\left(\sqrt{4d(\rho_s - \rho)g/(3\rho C_L)}\right)$

Table 25. Flow conditions and particle parameters. (BA-2D)

Variables[2]	**value**	**units**
Particle diameter, **D**	**275**	**μm**
Particle density, $\boldsymbol{\rho_p}$	**1050**	**kg m^{-3}**
Flow density, $\boldsymbol{\rho_f}$	**1000**	**kg m^{-3}**
Settling velocity, $\mathbf{w_s}$	**0.0025**	**m/s**
Roughness height	**0.000550**	**m**
Reference height	**0.000275**	**m**
Von Karman constant, **κ**	**0.4**	
Shear velocity, $\mathbf{u_*}$	**0.0086**	**m/s**
Flow height, **H**	**0.0284**	**m**

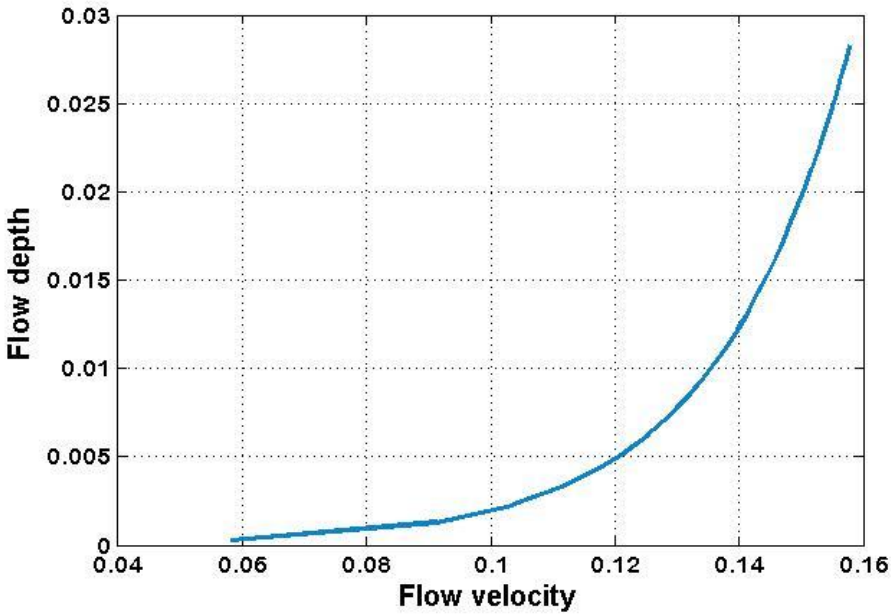

Figure 49. Flow velocity versus flow depth. (BA-2D)

[2] The flow conditions and particle parameters applied in this simulation were experimental data proposed by Kaftori et al. (1995).

Table 26. Model parameters (BA-2D)

Parameters	**value**	**units**
Time step, Δt	**0.1**	**s**
Simulation time **T**	**30**	**s**
Control volume size in X-direction	**2**	**m**
Runs	**10000**	

6.4.1 Simulation Results

The simulation results were calculated when the system was in an equilibrium and were listed in Table 27. Figure 50 depicts the transport rates in the control volume when the system reached the dynamic equilibrium. The sum of arrival rate and resuspension rate were almost equal to deposition rate plus the depart rate.

Table 27. Results. (BA-2D)

Results (at steady state)	**value**	**units**
Concentration N	**89.54**	**bead/meter**
Concentration N_m	**80.73**	**bead/meter**
Concentration N_d	**8.08**	**bead/meter**
Arrival rate, λ	**10.03**	**bead/sec**
Depart rate, μ	**10.01**	**bead/sec**
Deposition rate, μ_d	**90.70**	**bead/sec**
Resuspension rate, λ_s	**90.14**	**bead/sec**

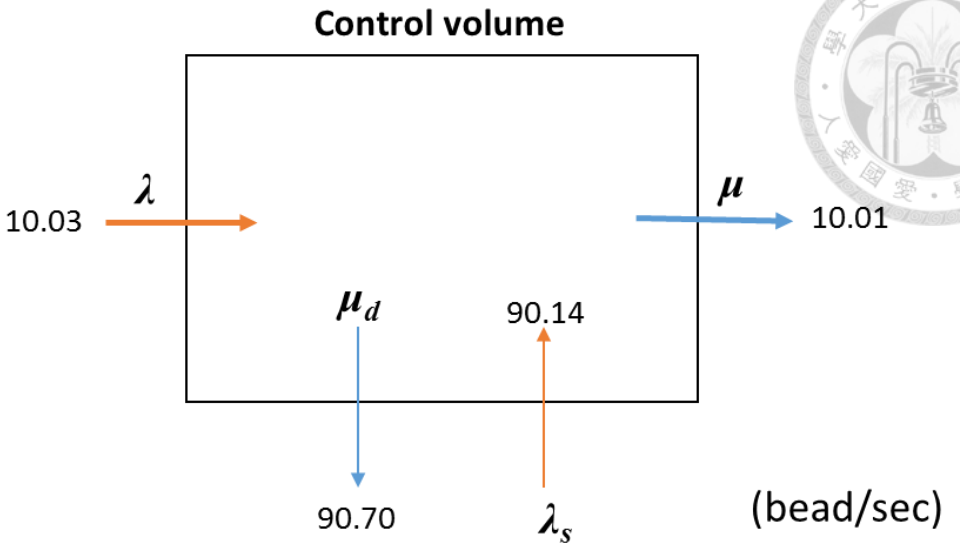

Figure 50. Simulation results. (BA-2D)

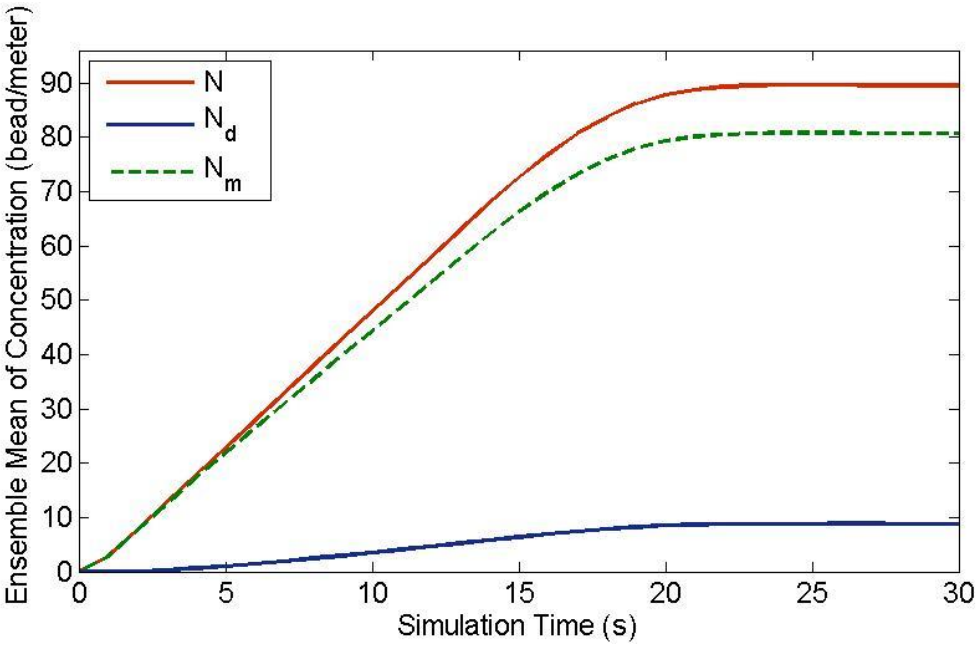

Figure 51. Ensemble mean of concentration (bead/meter). (BA-2D)

Figure 51 presents the ensemble means of concentrations N, N_d, N_m along with time. While N denotes the total number, N_d and N_m represent the deposition and moving particles in the control volume respectively. Control volume was empty before the simulation, thus when the simulation started and the particles were released along with

time, the ensemble means of concentrations would increase at the beginning of the simulation. The lines of ensemble means of concentrations in Figure 51 had the same tendency with RM-2D in Figure 29 and RA-2D in Figure 41. The concentrations would rise at the beginning of simulation and until the system became stable, concentrations would become constants. The time when the system reached the equilibrium was 22.6 seconds.

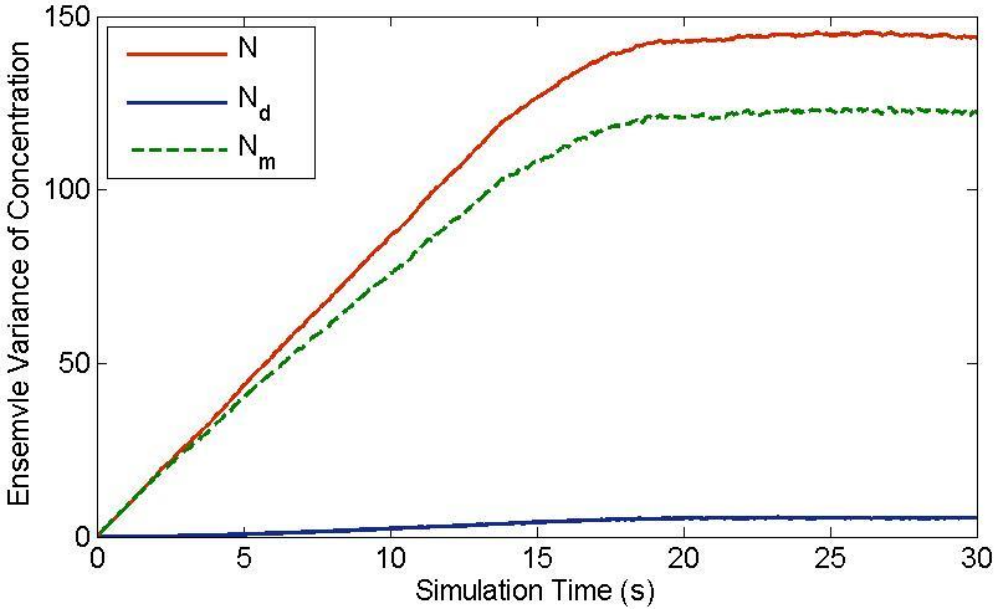

Figure 52. Ensemble variance of concentration. (BA-2D)

The ensemble variances of concentrations N, N_d, N_m were presented in Figure 52. The blue line representing the ensemble variances of deposition particles was smoother than others due to its relatively small value. As the simulation time went on, the variations of concentrations N, N_d, N_m would grow. As soon as the system became stable, the values of ensemble variances of concentrations would be close to constants in Figure 52.

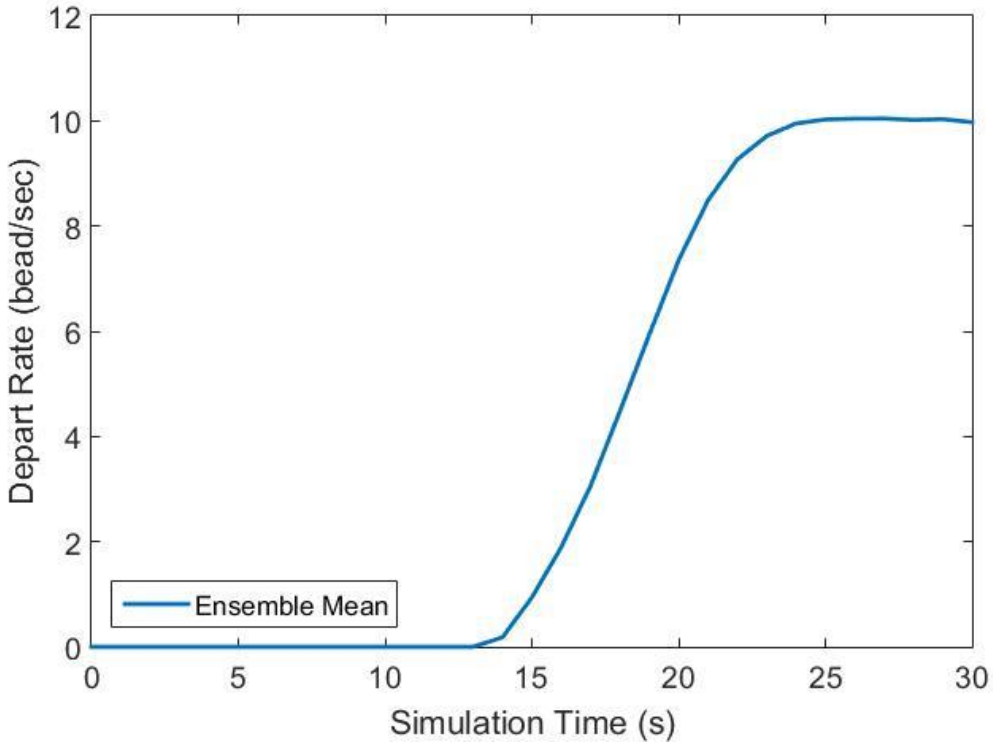

Figure 53. Ensemble mean of depart rate of particles (bead/sec). (BA-2D)

Figure 53 shows the ensemble means of depart rates along with simulation time. At first, it took the particles some time to transport through the control volume, which is reflected on the zero values at the beginning of the simulation. The zero values can be used as the representative mean time for particles to transport through the control volume. After particles started to leave the control volume, the depart rates started to climb up and asymptotically reached the incoming rates when the system became steady.

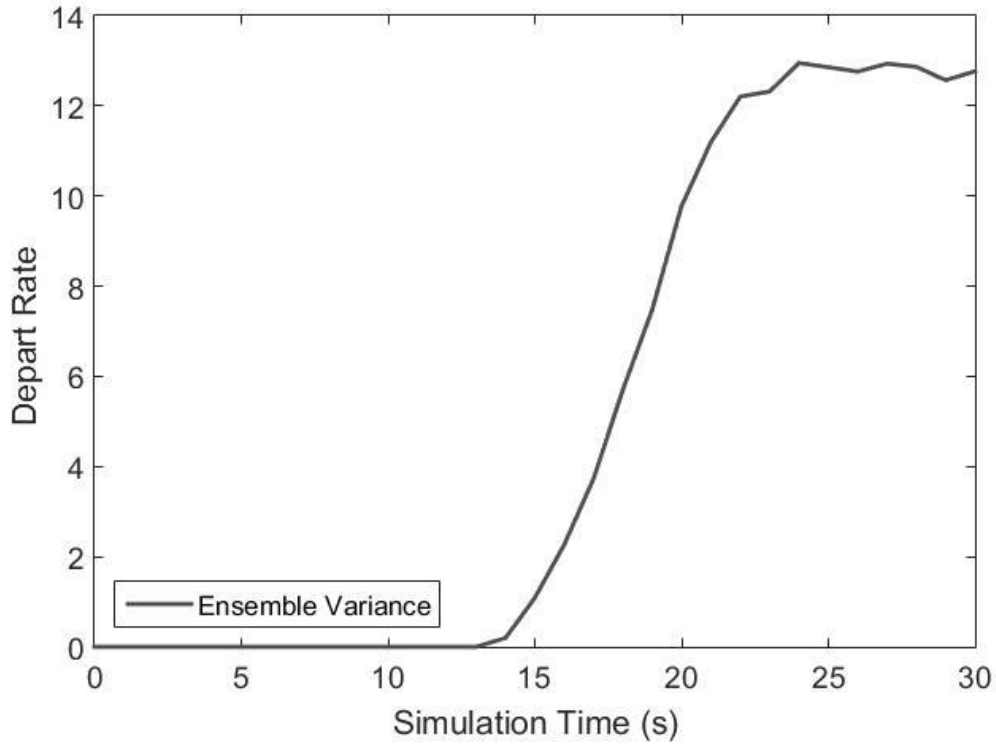

Figure 54. Ensemble variance of depart rate of particles (bead/sec). (BA-2D)

Ensemble variances of depart rates are presented in Figure 54. The trend of ensemble variances had the same tendency as ensemble means of depart rates. However, unlike ensemble means in Figure 53, when the system became stable, there were still small fluctuations in ensemble variances.

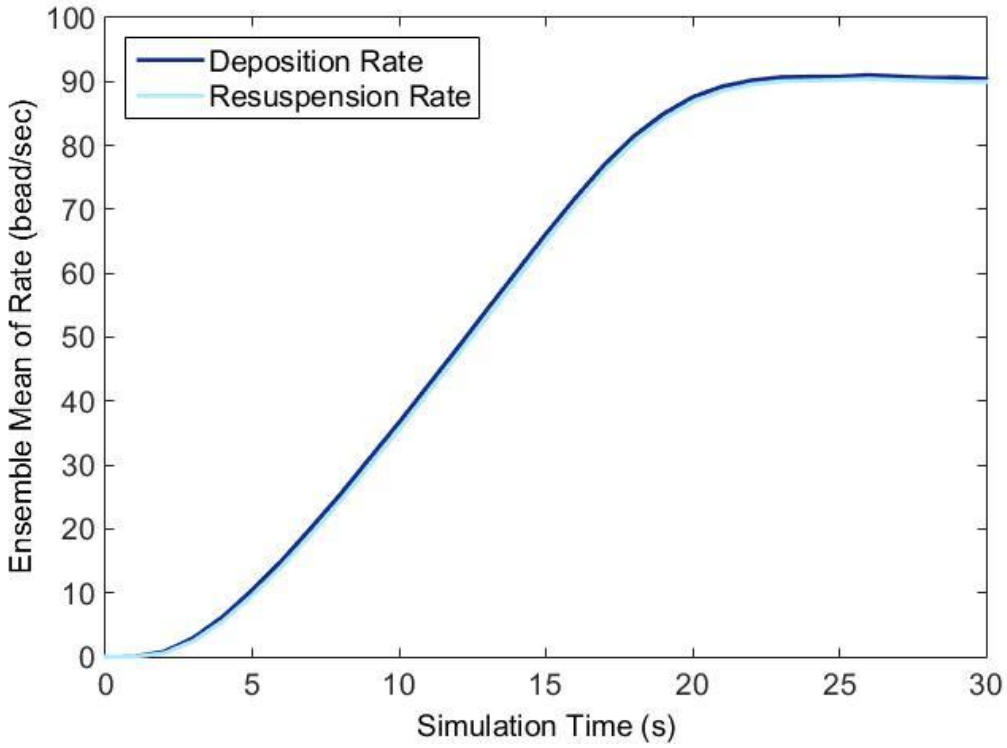

Figure 55. Ensemble means of deposition and resuspension rate (bead/sec). (BA-2D)

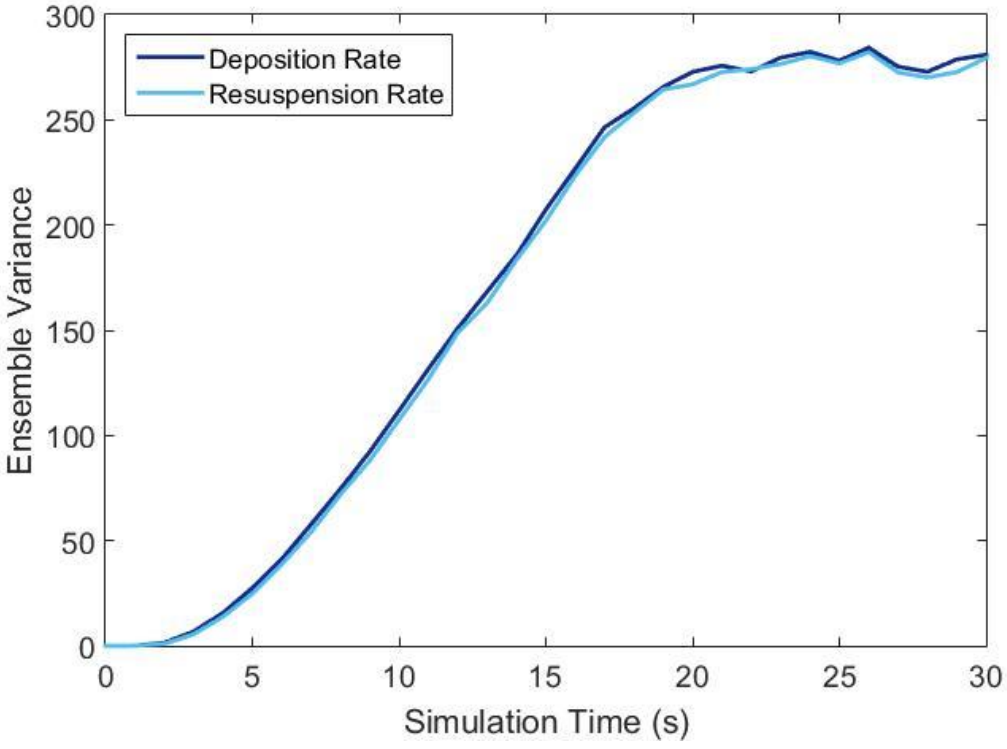

Figure 56. Ensemble variances of deposition and resuspension rate (bead/sec). (BA-2D)

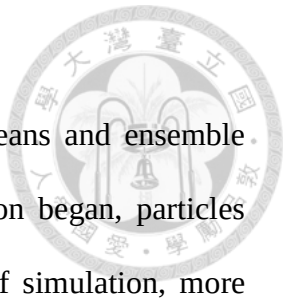

Figure 55 and Figure 56 schematize the curves of ensemble means and ensemble variances of deposition and resuspension rates. After the simulation began, particles started to be released into the control volume. At the beginning of simulation, more particles in the system means more depositions and resuspensions, therefore the curves would increase along with simulation time. As soon as the system reached equilibrium, the rates would become constants. The trends and the values were almost the same as each other in Figure 55. It indicated that when deposition happened, resuspension occurred. However, not all the deposited particles would resuspend, therefore the resuspension rates were always a little bit smaller than the deposition rates.

6.4.2 Model Validation

In the simulation, the flow conditions (flow velocity, shear velocity and flow height) and particle parameters (particle diameter and particle density) applied the experimental data proposed by Kaftori et al. (1995). The particle velocities were calculated in the simulation and compared with the particle velocity in experiments of Kaftori et al. (1995). The number of time steps for each particle spending to transport through the control volume was recorded and the mean of the numbers were the mean transport time. The mean particle velocity was obtained by dividing the length of the control volume by the mean transport time of particles transporting through the control volume which was 0.1527 meter per second. Comparison of particle velocities between simulation results and the experimental data is shown in Table 28. The particle velocities were at the same order. The lager value of simulation results might be due to a lack of considering the interaction between particles (one of the basic assumptions of the simulation was that there were no correlation between particles).

Table 28. Comparison between simulation results and experimental results of particle velocities. (BA-2D)

	Simulation Results	Experimental Results	unit
Particle Velocity	0.1527	0.143	m/s

6.4.3 Comparison between BA -2D cases

In this section, two cases with different input conditions were compared to highlight the difference of random occurrences and random magnitudes of the incoming particles. The flow conditions, particles characteristics and the model parameters were the same as values shown in Table 25 and Table 26 for case A and case B. Table 29 lists different particle arrival processes, namely case A and case B. In average, each arrival would consist of five particles, and there were two arrivals per second in case A; an arrival in case B would consist of two particles in average to the binomial distribution and there would be five arrivals in one second according to the mean Poisson rate. The overall incoming rates of particles were ten particles per second for both two cases. Figure 57, Figure 58, and Figure 59 present the ensemble means and ensemble variances of the concentration of N, N_d, N_m respectively. Figure 60, Figure 61 and Figure 62 illustrate the ensemble means and ensemble variances of transport rates including depart rate, deposition rate and resuspension rate.

The results of ensemble means did not show any difference between case A and case B. However, the results of ensemble variances (concentrations N, N_d, N_m and transport rates $\boldsymbol{\mu}$, $\boldsymbol{\mu_d}$, $\boldsymbol{\lambda_s}$) indicated that case A had more uncertainty than case B, thus the values of

the ensemble variances were always higher than that of case B. The low random occurrences plus the high random magnitude were important factors contributing to the higher values of ensemble variances. In other words, high occurrences with low magnitude of arrivals would be less uncertain than particles arriving with high magnitude and at low random occurrences when overall incoming numbers were the same (both were 10 bead per second).

Table 29. Conditions of case A and case B

Case	Random Occurrences (Poisson Process)	Random Magnitude Binominal Distribution
A	2	5
B	5	2
unit	event / sec	bead / event

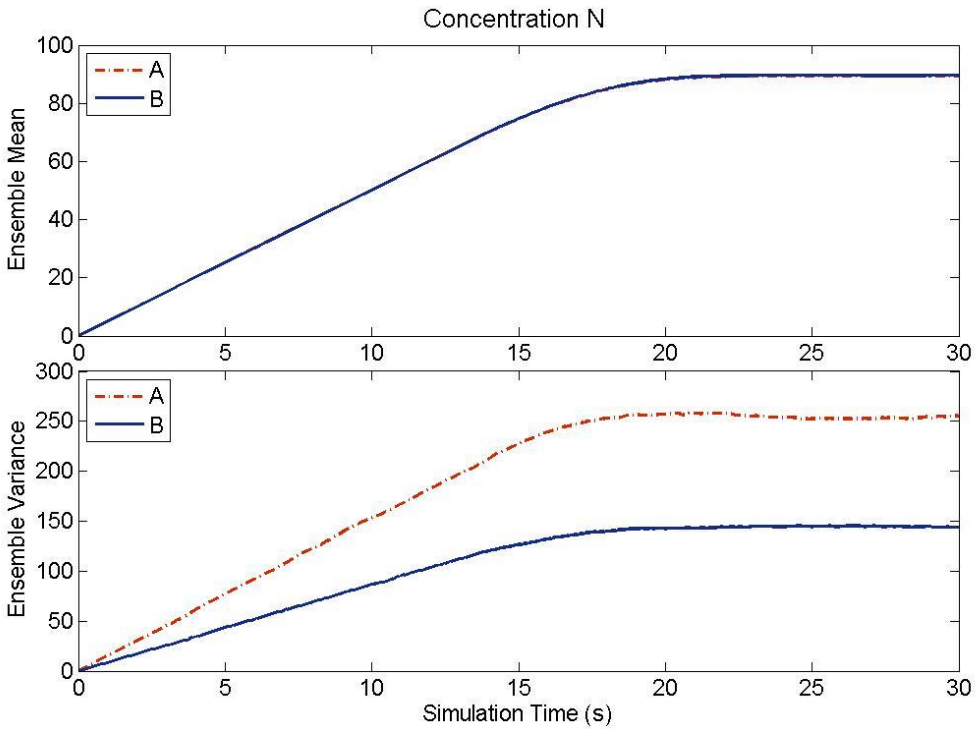

Figure 57. Ensemble mean and ensemble variance of concentration N.

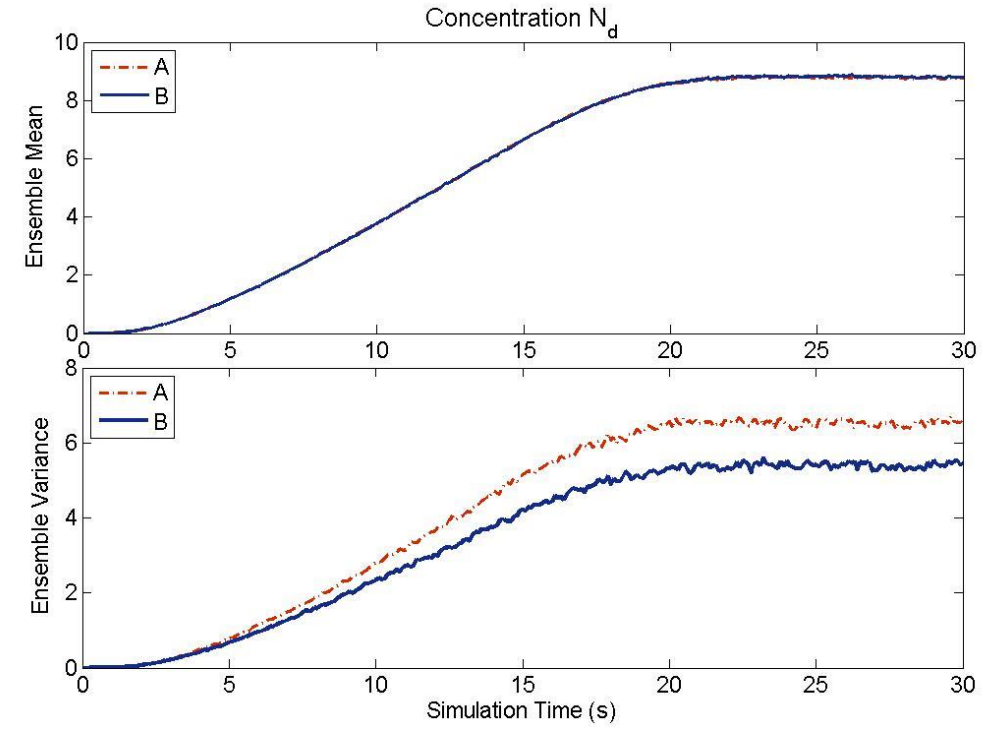

Figure 58. Ensemble mean and ensemble variance of concentration N_d.

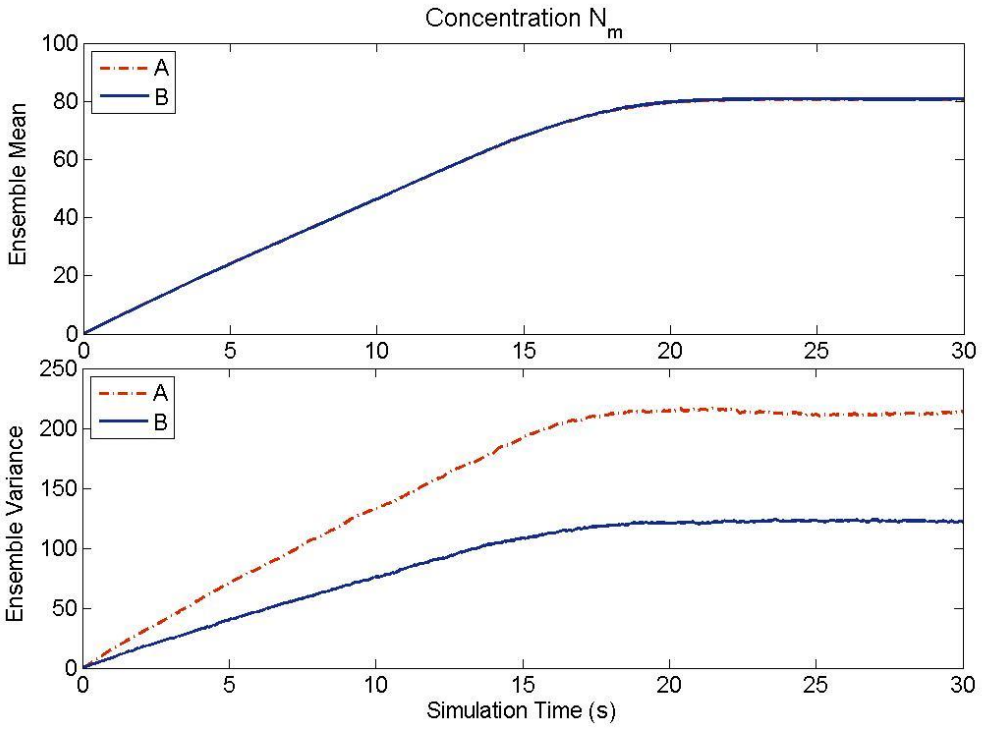

Figure 59. Ensemble mean and ensemble variance of concentration N_m.

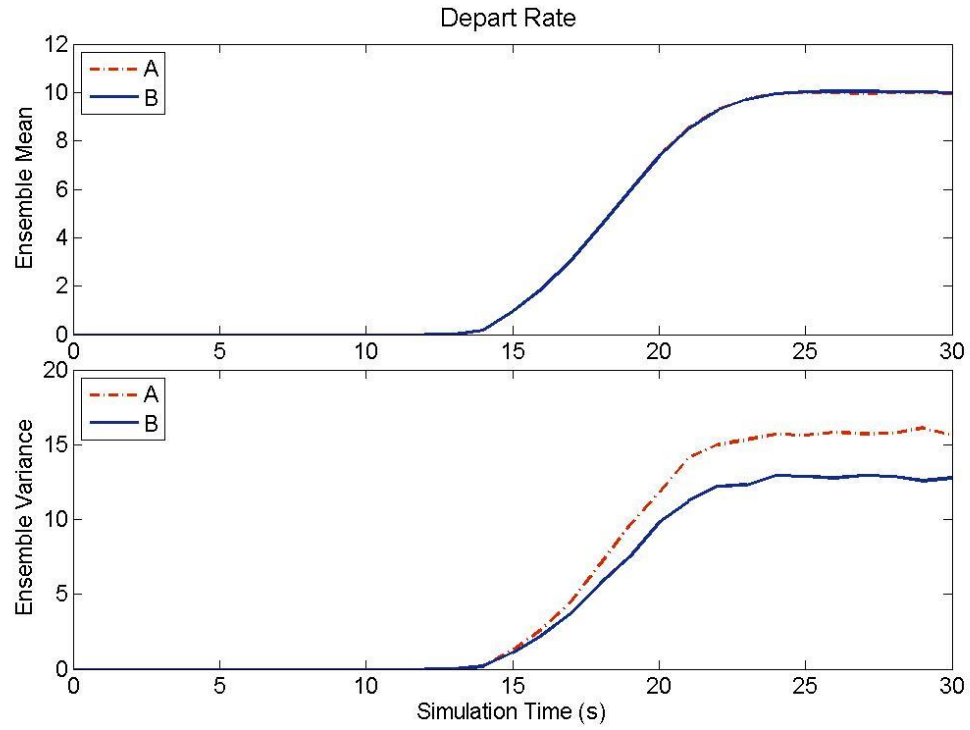

Figure 60. Ensemble mean and ensemble variance of depart rate $\boldsymbol{\mu}$.

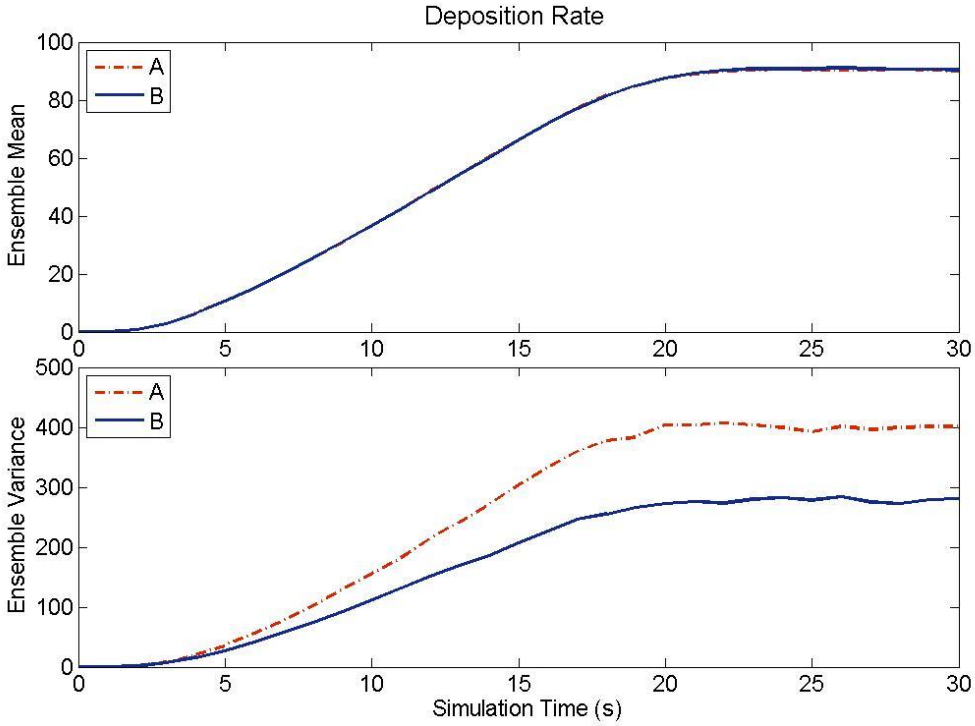

Figure 61. Ensemble mean and ensemble variance of deposition rate $\boldsymbol{\mu_d}$.

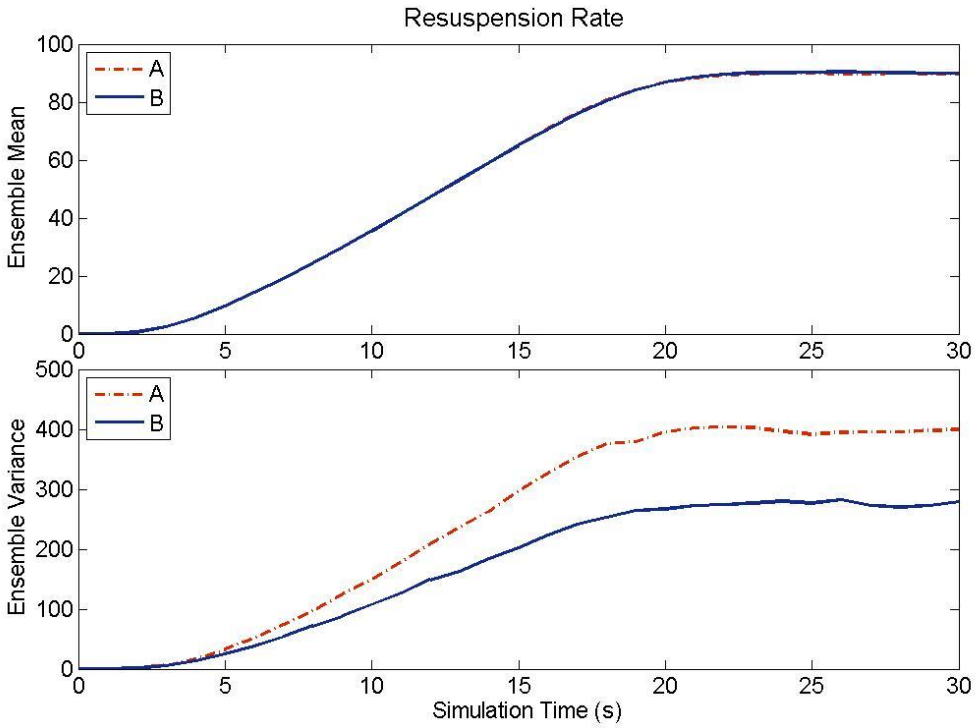

Figure 62. Ensemble mean and ensemble variance of resuspension rate λ_s.

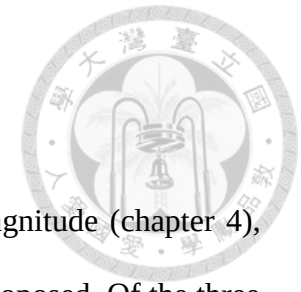

6.4.4 Comparison of RM, RA, and BA

In this section, comparisons of simulation results of random magnitude (chapter 4), random arrivals (chapter 5) and random-sized batch arrivals were proposed. Of the three cases, the flow conditions, particle characteristics and the model parameters applied the same experimental data proposed by Kaftori et al. (1995). Despite the incoming mechanisms were different, the theoretical means of incoming rates were the same which were all equal to 10 beads per second. Table 30 lists the results of transport rates μ, μ_d, λ_s and concentrations N, N_d, N_m of three cases when the systems became stable in the form of ensemble means and ensemble variances. As shown in Table 30, the ensemble means of simulation results almost had the same values in three cases. However, as to the ensemble variance results, the variances of random-sized batch arrivals were larger than those of random magnitude and random arrivals. Figure 63, Figure 64 and Figure 65 depict the ensemble variances of N, N_d, N_m of three simulations cases respectively. Based on Figure 63, Figure 64 and Figure 65, although random magnitude case and random arrivals case did not show a lot of differences, one could still find that the curves of random arrivals case were more fluctuant than that of the batch arrivals. It indicated that the random arrivals had more uncertainty than random magnitude. Still, the most obvious differences were the ensemble variances of this case (random-sized batch arrivals, BA). In Figure 63, Figure 64, Figure 65, Figure 66, Figure 67, and Figure 68, the greater values of ensemble variances in of transport rates and concentrations in random-sized batch arrivals (BA) can be attributed to different degrees of uncertainty, for this case, there was one more random variable compared with other two cases. These results faithfully presents the stochastic property that under same input parameters, while the ensemble mean results did not differ from each other, the ensemble variances, however,

would present the difference resulting from various incoming mechanisms among cases, i.e. random magnitude of the arrivals (RM), random arrivals (RA) and random-sized batch arrivals (BA).

Table 30. Comparison of ensemble means and ensemble variances results of three cases.

	RM	**RA**	**BA**
Ensemble Mean			
μ_d	90.68	90.79	90.70
λ_s	90.09	90.19	90.14
μ	9.98	10.01	10.01
N	89.54	89.49	89.82
$\mathbf{N_d}$	8.80	8.81	8.81
$\mathbf{N_m}$	80.74	80.68	81.01
Ensemble Variance			
μ_d	172.92	179.00	278.37
λ_s	172.21	177.78	275.65
μ	9.99	10.08	12.79
N	44.61	45.01	144.36
$\mathbf{N_d}$	4.41	4.47	5.38
$\mathbf{N_m}$	40.24	40.45	122.52

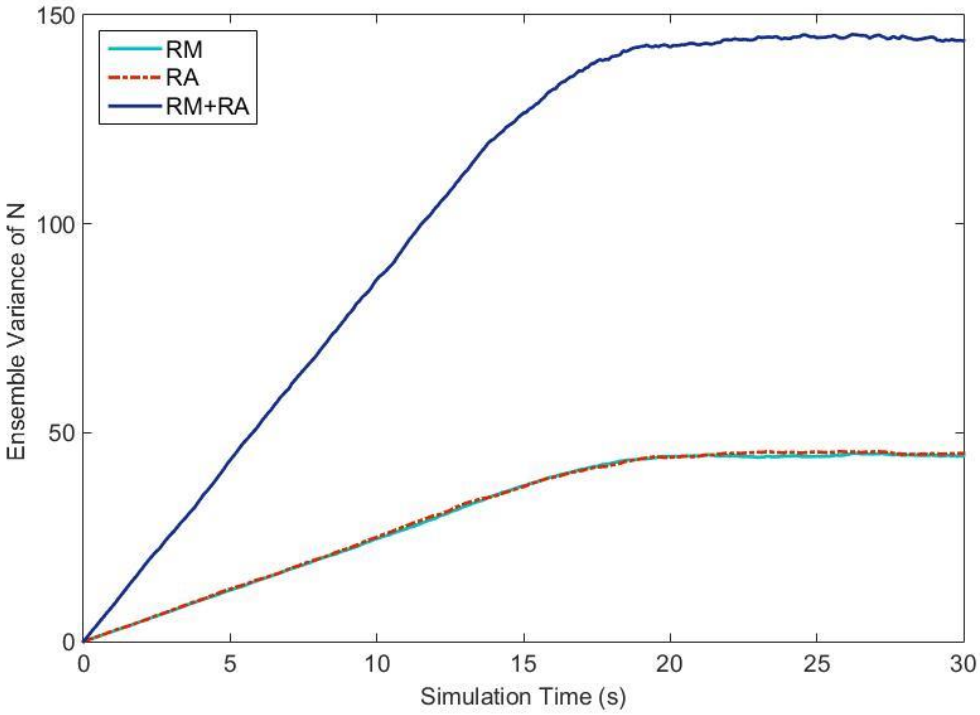

Figure 63. Comparison between ensemble variances of concentration N.

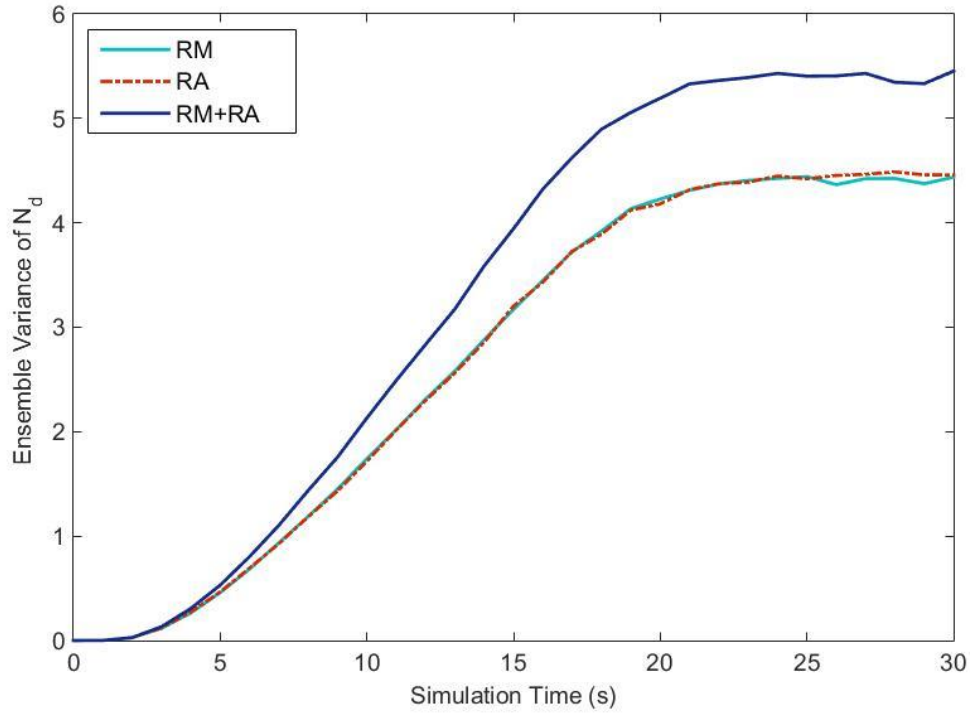

Figure 64. Comparison between ensemble variances of concentration N_d.

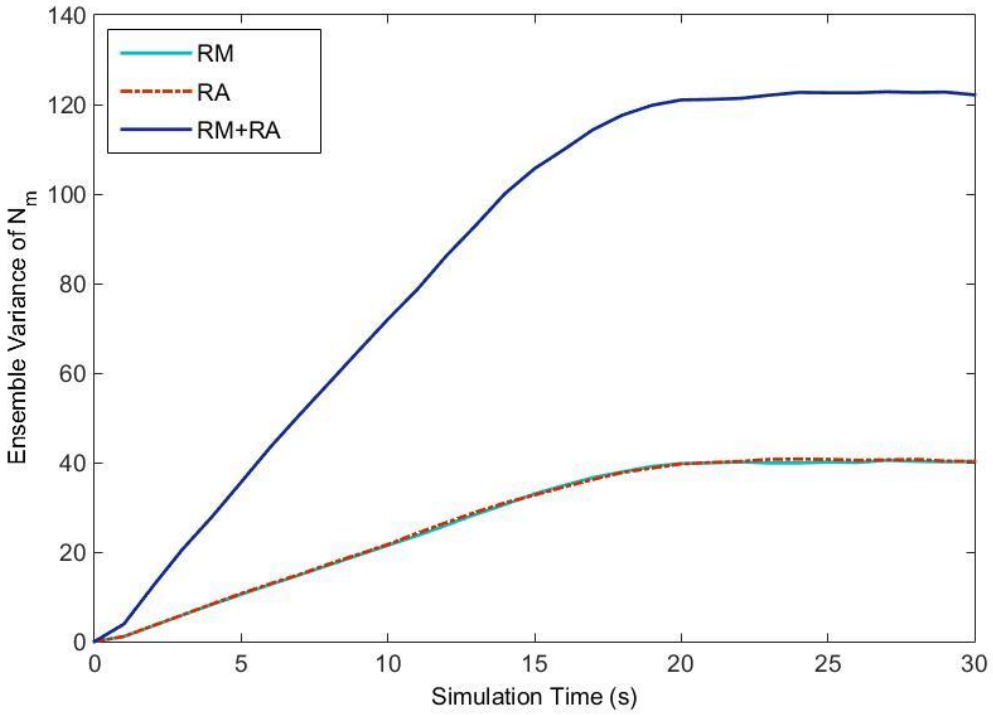

Figure 65. Comparison between ensemble variances of concentration N_m.

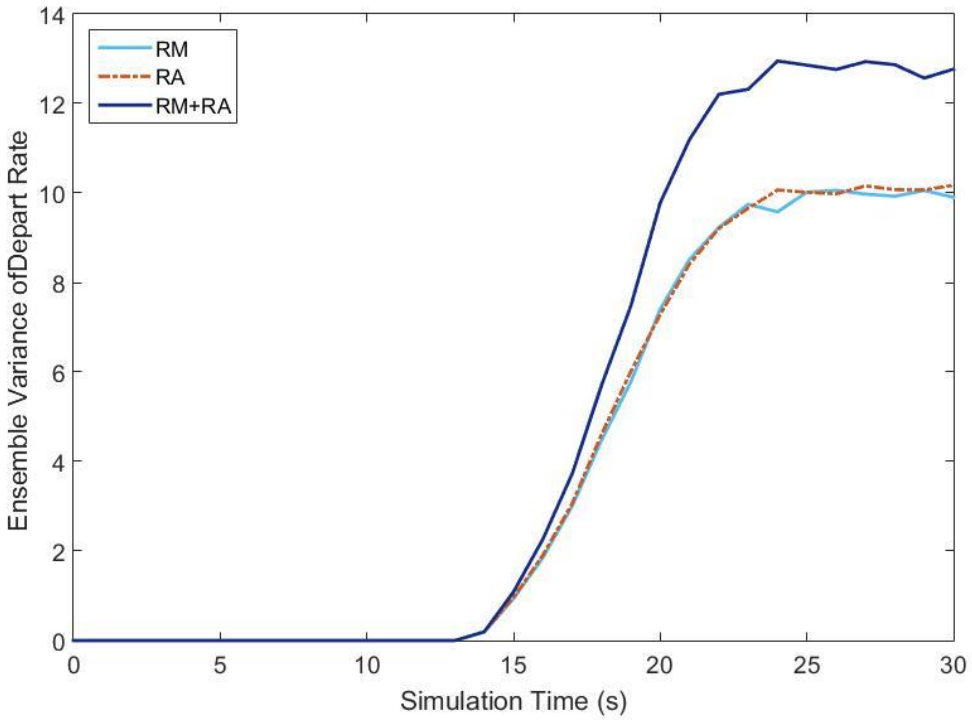

Figure 66. Comparison between ensemble variances of depart rate $\boldsymbol{\mu}$.

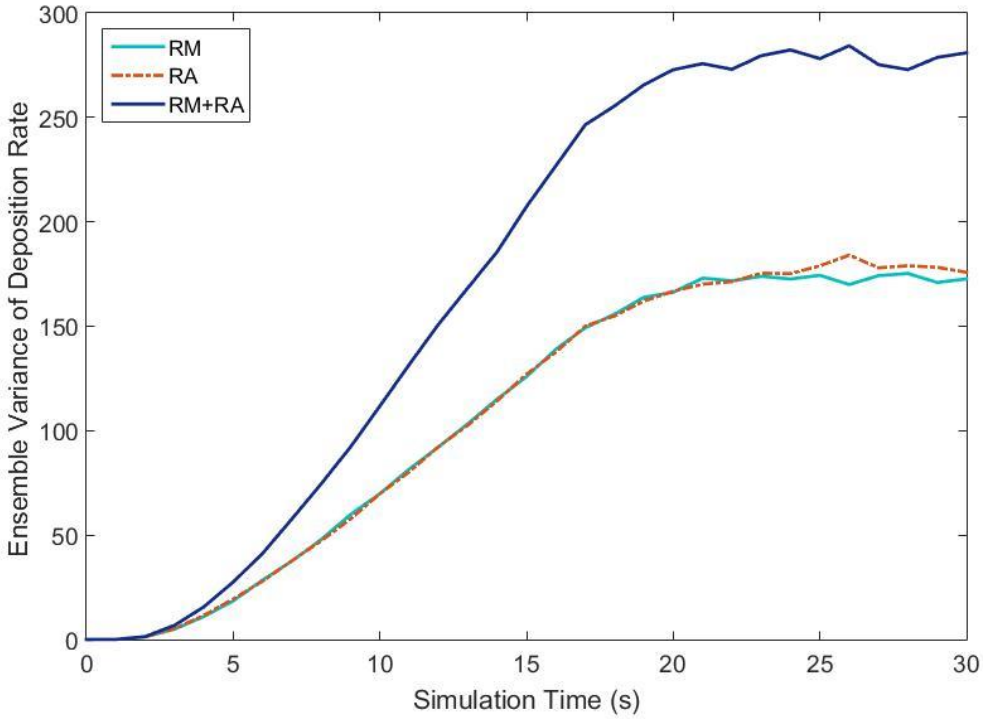

Figure 67. Comparison between ensemble variances of deposition rate μ_d.

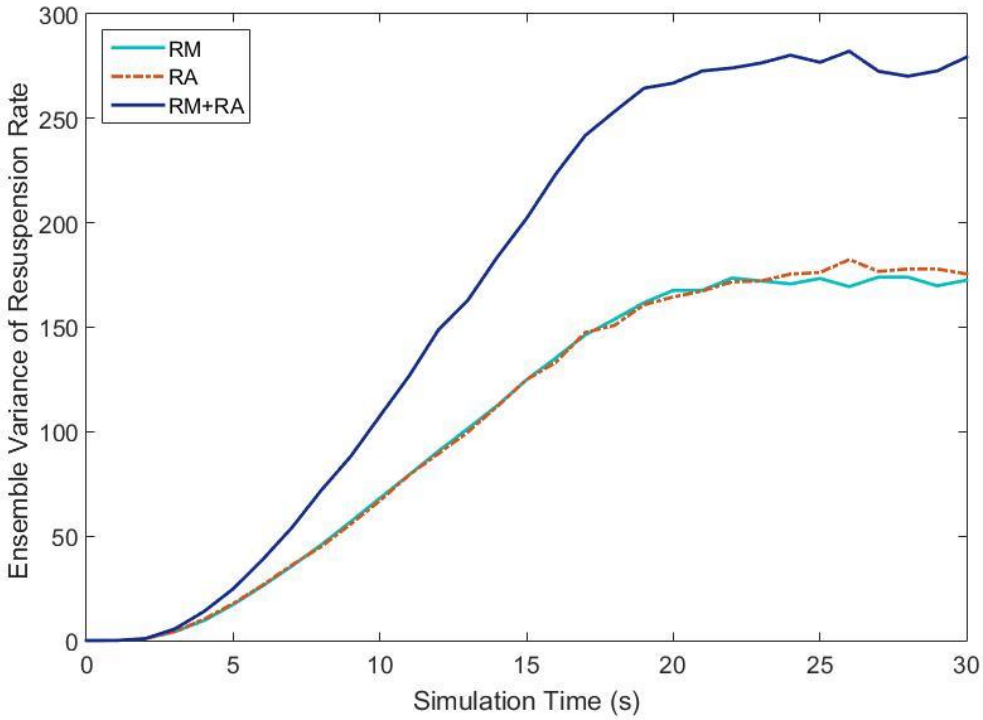

Figure 68. Comparison between ensemble variances of resuspension rate λ_s.

6.4.5 Summary

In the simulation, the random-sized batch arrivals were applied to simulate the uncertain property of the incoming sediment particles. Each arrival defined as an event included different numbers of particles based on the binomial distribution **B**(100, 0.02). The random number of events were generated by a Poisson process with a constant rate $\lambda = 5$ (event/second). There were four random variables in the simulation, the random arrival process, random numbers of incoming particles, turbulence term in SD-PTM and the log-normal distributed instantaneous velocity approaching on the deposited particles. The flow conditions and particles characteristics were from experimental data proposed by Kaftori et al. (1995). The transport equations included SD-PTM (Man and Tsai, 2007) and the particle resuspension (Wu and Lin, 2002). Ensemble means and variances of concentrations were displayed in Figure 51 and Figure 52. The transport rates were also calculated. The system was proved to reach equilibrium based on these results. The dynamic equilibrium results were drawn in Figure 40. Two random-sized batch arrivals simulations were compared. Results showed while under the same incoming rates, simulation of low occurrences with higher magnitude was more uncertain than the simulation case whose occurrences was higher and the magnitude of each arrival was lower.

Moreover, the comparison of results of random magnitude case (RM), random arrival case (RA) and the case in this chapter were presented. The flow conditions, particle characteristics and the model parameters were the same and the ensemble mean incoming rates of particles were all equal to 10 beads per second for the three simulations, theoretically. Under these conditions, while the ensemble mean results did not differ from each other, there exist discrepancies in the ensemble variances. The comparison shows that the variations of results including concentrations and transport rates in this case (BA-

2D) were much larger than that of the random magnitude and random arrivals cases while in average, the incoming rates were the same (all were 10 beads per seconds in three cases). In other words, ensemble variances of the results can reflect the uncertainty of the outcomes due to various incoming mechanisms (RM, RA, BA).

Chapter 7 Summary and Recommendations

7.1 Summary and Conclusion

In this study, a stochastic framework for the random input of sediment particles is proposed. The stochastic framework is the application to queueing theory, which treats the sediment particle, control volume, transport mechanics as customer, service facility and server, respectively, in analogy to queueing theory. The stochastic framework combines with the stochastic diffusion particle tracking model (SD-PTM) in order to observe the variation of sediment concentration in the control volume. In the study, three types of random input processes are examined. Chapter 4 presents the random magnitude of the arrivals. In the study, random magnitude case applies the binominal distribution to generate the random numbers of incoming sediment particles for the discrete property in the Binomial distribution. For one-dimensional simulations, the control volume is divided into segments. The ensemble means and ensemble variances of concentrations show the particle concentration values in the first segment would be more reliable when the size of time step was smaller. Different control volume sizes are also discussed in the 1-D case. The results point out that the larger the size of the control volume, the longer it takes for the system to become steady, and the smaller the variation of the concentration. As for the two 2-D cases, one simulation includes the resuspension of sediment particles while the other simulation does not. The curves in the results of the 2-D case without considering particle resuspension are more stiff and inflexible. The numbers of deposition and total sediment particles in the control volume will increase along with simulation time but the number of moving particles would become a constant. For another random magnitude 2-D case (including the resuspension of sediment particles), the curves of

ensemble means and ensemble variances are smoother. The balance of resuspension rate and deposition rate is discussed. Results show the size of a time step has a great impact on the values of deposition and resuspension rate. The concentrations of deposited particles bring out a shortcoming of SD-PTM. While the particles travel near the bed, the effect of the turbulence term in SD-PTM would affect the number of deposited particles. When the time step is too large, the number of deposited particles would become larger than what it should have been. After comparing three sizes of time steps, the appropriate time step for this study is suggested to be 0.1 seconds based on the balance between theoretical accuracy and the computational efficiency.

In Chapter 5, the random arrival process is described by Poisson process. The results of ensemble means and ensemble variances of transport rates confirm the dynamic equilibrium of the system. Comparison of random magnitude and random arrivals of incoming particles is discussed. The comparison shows that there is not much difference in terms of ensemble means between random magnitude case and random arrival case when the ensemble arrival rates of particles are the same (10 bead/second), however, the ensemble variances for the above two cases present apparent differences. The comparison of ensemble variances of particle concentrations and transport rates reveal that random arrivals has more uncertainty than random magnitude of particle arrivals.

Chapter 6 combines the random magnitude and random arrivals together as the random input process of particles. Results (ensemble means and ensemble variances of concentrations and transport rates) also reveal the dynamic equilibrium of the system under the condition that the flow was steady. Comparisons of simulation cases among chapter 4, 5 and 6 are made. The mechanisms of incoming processes of particles would show the differences in ensemble variances while the ensemble means of the concentrations and the transport rates were similar among three simulation cases under

the same incoming rates of particles (10 bead/second). The higher values of ensemble variances of simulation results of random-sized batch arrivals implicate that when taking both the random arrivals and random magnitude of incoming particles into consideration, there would exist a higher uncertainty in particle transport (i.e., concentrations, and transport rates)

Application of both the proposed stochastic framework of incoming particles and the stochastic particle tracking model (SPTM) could be a very helpful tool for decision makers. For instance, one of the applications could be used to model the pollutant propagation in a river. Imagine that there is a pollution source released by a factory in the river, and one might want to know the influence of pollution to the certain area at the downstream of river. By knowing the average number of pollutants released in a certain period of time, the mean magnitude and mean Poisson rate can be determined. As a result, not only the mean concentrations of pollution, including moving and deposited particles, but also the variations of the pollutant concentration could be obtained by our proposed model. Moreover, if there is a pre-established water quality standard, the excessive risk of water pollution can be estimated for decision makers.

7.2 Recommendation for Future Research

The proposed stochastic framework provides a probabilistic approach to simulate the random arrivals of sediment particles (including the random magnitude and random interarrival time). Up to this point, there are more deterministic sediment transport equations that have been developed to model mechanics of sediment transport quiet well. Therefore, the combination of these deterministic sediment transport models with proposed stochastic framework would be a great and useful application. Additionally, research focusing on the proposed stochastic framework can take various sediment particle sizes and densities into consideration. The stochastic framework can treat particles of different sizes as different kinds of customers in queueing theory. Then applying appropriate services needed for different customers, the store could offer different services in line with customer demands. In other words, one could adopt an appropriate sediment transport formulas for suspended load and bed load particles under the same flow conditions. Then, particles of various particle sizes and densities could be simulated in the same control volume at the same time. Moreover, the proposed model could be used to reflect variations of environment, such as climate change. Mean Poisson rate denotes the mean occurrences of events while the mean of random numbers of a binominal distribution represents the mean magnitude of the events. The Poisson rate and mean magnitude of events (arrivals) might vary due to environmental factors. And by adopting trend analysis models, such as the logistical regression or HHT, meaningful Poisson rates and the mean magnitude of events (arrivals) could be calculated and applied in the proposed framework. Then we can better understand the behavior of sediment transport under the random input process in the uncertain environment.

REFERENCE

[1] Dimou, K. N., & Adams,E. E. (1993). A random-walk, particle tracking model for well-mixed estuaries and coastal waters. Estuarine, Coastal and Shelf Science, 37(1), 99-110.

[2] Gorenflo, R., Mainardi, F., Moretti, D., & Paradisi, P. (2002). Time fractional diffusion: a discrete random walk approach. Nonlinear Dynamics, 29(1-4), 129-143.

[3] Ross, S. M. (2007). Introduction to probability models. Chapter 8. Academic press.

[4] Al Hanbali, A., & Boxma, O. (2010). Busy period analysis of the state dependent M/M/1/K queue. Operations Research Letters, 38(1), 1-6.

[5] Ancey, C., Davison, A. C., Böhm, T., Jodeau, M., & Frey, P. (2008). Entrainment and motion of coarse particles in a shallow water stream down a steep slope. Journal of Fluid Mechanics, 595, 83-114.

[6] Arnold, J. G., & Williams, J. R. (1988). HYDROLOGIC MODELING USING A SIMULATION LANGUAGE BASED ON QUEUEING THEORY1.

[7] Arunachalam, V., Gupta, V., & Dharmaraja, S. (2010). A fluid queue modulated by two independent birth-death processes. Computers & Mathematics with Applications, 60(8), 2433-2444.

[8] Batchelor, G. K. (1977). The effect of Brownian motion on the bulk stress in a suspension of spherical particles. Journal of Fluid Mechanics, 83(01), 97-117.

[9] Bridge, J. S. (1981). A discussion of Bagnold's (1956) bedload transport theory in relation to recent developments in bedload modelling. Earth surface processes and landforms, 6(2), 187-190.

[10] Cordeiro, J. D., & Kharoufeh, J. P. (2011). Batch Markovian arrival processes (bmap). Wiley Encyclopedia of Operations Research and Management Science.

[11] Dimou, K., 1989. Simulation of estuary mixing using a 2-dimensional random walk model, MS thesis, MIT.

[12] Gorenflo, R., & Mainardi, F. (1998). Random walk models for space-fractional diffusion processes. Fractional Calculus and Applied Analysis, 1(2), 167-191.

[13] Malhotra, R., Mandjes, M. R., Scheinhardt, W. R. W., & Van den Berg, J. L. (2009). A feedback fluid queue with two congestion control thresholds. Mathematical methods of operations research, 70(1), 149-169.

[14] Malmon, D. V., Dunne, T., & Reneau, S. L. (2003). Stochastic theory of particle trajectories through alluvial valley floors. The Journal of geology, 111(5), 525-542.

[15] Mitra, D. (1988). Stochastic theory of a fluid model of producers and consumers coupled by a buffer. Advances in Applied Probability, 646-676.

[16] Naden, P. (1987). Modelling gravel‐bed topography from sediment transport. Earth Surface Processes and Landforms, 12(4), 353-367.

[17] Oh, J. (2011). Stochastic particle tracking modeling for sediment transport in open channel flows. State University of New York at Buffalo.

[18] Oh, J., & Tsai, C. W. (2010). A stochastic jump diffusion particle‐tracking model (SJD‐PTM) for sediment transport in open channel flows. Water Resources Research, 46(10).

[19] Oh, J., & Tsai, C. W. (2014). A stochastic multivariate framework for modeling the movement of discrete sediment particles in open channel flows.

[20] Oh, J., & Tsai, C. W. (2014). A stochastic particle based model for suspended particle movement in surface flows.

[21] Pope, S. B. (1994). Lagrangian PDF methods for turbulent flows. Annual review of fluid mechanics, 26(1), 23-63.

[22] Schumer, R., Meerschaert, M. M., & Baeumer, B. (2009). Fractional advection–dispersion equations for modeling transport at the Earth surface. Journal of Geophysical Research: Earth Surface (2003–2012), 114(F4).

[23] Tsai, C. W., Hsu, Y., Lai, K. C., & Wu, N. K. (2014). Application of gambler's ruin model to sediment transport problems. Journal of Hydrology, 510, 197-207.